The Roles of Myosin II and Rap2 in Synaptic Structure and Function

by

Jubin Wonsun Ryu

B.S. Biology
B.A. English
Stanford University, 2001

SUBMITTED TO THE DEPARTMENT OF BIOLOGY IN PARTIAL FULFILLMENT OF THE REQUIREMENTS FOR THE DEGREE OF

DOCTOR OF PHILOSOPHY

AT THE
MASSACHUSETTS INSTITUTE OF TECHNOLOGY

JUNE 2008

Signature of author: _____
Department of Biology
March 18, 2008

Certified by: _____
Morgan Sheng
Professor of Biology
Thesis Supervisor

Accepted by: _____
Stephen P. Bell
Chair, Committee on Graduate Students
Department of Biology

The Roles of Myosin II and Rap2 in Synaptic Structure and Function

by

Jubin Ryu

Submitted to the Department of Biology on March 18, 2008
in Partial Fulfillment of the Requirements for the Degree of
Doctor of Philosophy in Biology

Abstract

Synapses, the connections between neurons, exhibit both structural and functional plasticity, and these changes could underlie learning and memory. Two synaptic phenomena that have been studied extensively are Hebbian plasticity and changes in dendritic spine morphology. Recent proteomics studies have uncovered many proteins that reside in the synapse and could play critical roles in these processes. Among these are the molecular motor myosin II and the Ras family GTPase Rap2. Myosin II can move and contract actin filaments in non-neuronal cells, and it represents a novel way to alter spine structure, which is classically thought to occur through actin polymerization and depolymerization. Rap GTPases are the closest relatives to Ras, which is well established as a positive regulator of spines and synaptic transmission. In vitro evidence indicates that Raps could act antagonistically to Ras in neurons, inhibiting spine growth and synaptic strength.

To study myosin II's role in dendritic spine morphology and synaptic function, we inhibited myosin II function either pharmacologically or genetically in dissociated hippocampal neurons. Knockdown of myosin II by RNA interference resulted in loss of mature mushroom-shaped spines, and an increase in thin, filopodia-like structures. Treatment with blebbistatin, a chemical inhibitor of myosin II, phenocopied this result. Live imaging revealed that mature spines unravel into filopodia within tens of minutes of myosin II inhibition by blebbistatin. Furthermore, blebbistatin treatment led to decreases in levels of the glutamatergic alpha-amino-3-hydroxy-5-methyl-4-isoxazolepropionic acid receptor (AMPAR), as well as impairment of synaptic transmission.

To study Rap2 neuronal function *in vivo*, we created transgenic mice that expressed constitutively active Rap2 (Rap2V12) in postnatal forebrain. Consistent with an inhibitory role for Rap at synapses, Rap2V12 mice exhibited reduced levels of phospho-ERK (pERK) and a reduction in spine density and length. Behaviorally these mice were hyperactive and showed impairments in spatial learning. In addition, Rap2V12 mice showed normal acquisition of fear memories, but were defective in the extinction of contextual fear. Fear extinction has been associated with several psychiatric disorders, including posttraumatic stress disorder (PTSD), and Rap2V12 mice might offer a potential therapeutic model for such diseases.

Thesis Supervisor: Morgan Hwa-Tze Sheng
Title: Menicon Professor of Neuroscience

Acknowledgments

I thank my parents for their unfailing love and patience. All my life, they have listened and tended to my concerns while quietly setting aside their own. They will always be my standard. I'm so lucky to have my younger brother Justin; no one could replace what he means or gives to me. And I thank Chen-Tsen, who is not related to me by blood but knows me as if she was.

I thank my friends – Richard, David, Jen, Michael, Young, Nancy, Alaka, Jason, and many others – for giving me refuge when work and school grew hard. I was always uplifted by our conversations, Chinatown runs, and late-night video and board games. I will especially remember Ben, my college roommate with whom I arrived to Boston for grad school; I'm not sure I will have another friendship as rich and rooted as ours.

I chose the Sheng lab in large part because I was drawn to the people and the culture, and that feeling has been validated. I'm grateful and better for having met people of such varied backgrounds, personalities, talents, and scientific styles. In particular, I want to thank Kenny Futai and Mónica Feliú-Mójer for their invaluable help during the Rap2 project. Thanks also to Albert, who broke me into the lab and has given me valued advice ever since, and to Daniel, my older bruder who showed me the way.

Lastly, I send my deepest respect and thanks to Morgan, a truly insightful, honest, and kind mentor.

TABLE OF CONTENTS

Chapter One

Introduction

Jubin Ryu

Composed of billions of neurons, the brain is able to acquire and modify information based on experience. This plasticity is thought to be mediated largely through the structural and functional modification of synapses, the connections between brain cells. In this chapter, we introduce two types of synaptic changes that have been correlated with learning and memory: Hebbian plasticity and changes in dendritic spine structure. We then review the molecular mechanisms thought to underlie these phenomena and conclude by highlighting two proteins – the molecular motor myosin II and the small GTPase Rap2 – that have recently been identified at synapses and may play key roles in these processes.

General Structure and Function of Synapses

Synapses may be either electrical or chemical, depending on whether the electrical stimulus travels directly from cell to cell or is converted into a chemical intermediate (Cowan et al., 2001). In chemical synapses – the focus of this chapter – specialized regions of two cells' plasma membranes align 20-40 nm from each other. Most often, the presynaptic compartment is located on axons and the postsynaptic side on dendrites, although exceptions exist to this rule. Both pre and postsynaptic compartments are distinguished by ultrastructural hallmarks and protein compositions that reflect their function in synaptic transmission.

Presynaptic Compartment

The presynaptic compartment rapidly translates an incoming electrical signal (the action potential) to a chemical one (neurotransmitter) that is sent to the postsynaptic

neuron. On average, each CNS neuron sends out ~500 presynaptic terminals to its neighbors (Sudhof, 2004). Two prominent ultrastructural features of this space are synaptic vesicles and the active zone. Synaptic vesicles are electron-lucent organelles 35-50 nm in diameter that store nonpeptide neurotransmitters, including acetylcholine, glutamate, GABA, and glycine (Palay and Palade, 1955; Whittaker, 1968; Katz, 1969). These organelles are estimated to house ~200 proteins, which fall into one of two classes: transport proteins involved in neurotransmitter uptake and membrane trafficking proteins involved in endocytosis, exocytosis, and vesicle recycling (Sudhof, 2004). Synaptic vesicles exist in pools of about 200-500 at the axon terminal (Harris and Sultan, 1995). Of this pool, only 5-10 are actually docked to the presynaptic membrane at the active zone, an electron-dense, disc-shaped thickening that is situated directly opposite the synaptic cleft (Harris et al., 1992; Schikorski and Stevens, 2001). At the active zone, synaptic vesicles are primed for Ca^{2+}-dependent fusion pore opening, and upon Ca^{2+} influx, the vesicles release their contents into the synaptic cleft (Sudhof, 2004).

Postsynaptic Compartment

The postsynaptic compartment is specialized to bind the incoming neurotransmitter and transmit the resulting signal to the rest of the neuron. At most excitatory synapses within the mammalian CNS, the postsynaptic space is located on outgrowths of dendritic branches called spines, with each spine typically harboring a single synapse (Harris and Kater, 1994). Dendritic spines range in volume from 0.01 mm^3 to 0.8 mm^3 and are classically mushroom-shaped, although their morphology can

vary greatly. Ultrastructurally, spines are characterized by a disc-shaped thickening directly beneath the membrane that measures 200-500 nm in diameter and 30-60 nm in thickness (Gray, 1959; Sheng and Hoogenraad, 2007). This structure has been termed the postsynaptic density (PSD) and contains hundreds of distinct proteins, including glutamate receptors, signaling enzymes, scaffold proteins, and cytoskeletal proteins. The PSD is highly modifiable, changing its protein composition and arrangement in response to specific types of synaptic activity.

Synaptic Cleft

The pre- and postsynaptic membranes are linked together tightly, and the space between them measures 20-40 nm across. The molecular basis of this adhesion resides in homo and heterophilic interactions between presynaptic and postsynaptic transmembrane proteins. To date, the best studied synaptically localized cell adhesion molecules (SAMs) include the neurexins and neuroligins, EphBs and ephrin-Bs, the cadherins, and members of the Ig superfamily (Dalva et al., 2007). These molecules not only mediate adhesion extracellularly but can bind to signaling and scaffold proteins intracellularly, situating them to initiate and regulate processes such as synaptogenesis and modulation of mature synapses.

Functional and Structural Plasticity of Synapses

Hebbian Plasticity

In 1949, D.O. Hebb proposed that learning is caused by the selective strengthening of synapses between cells that are simultaneously active (Hebb, 1949).

Figure 1

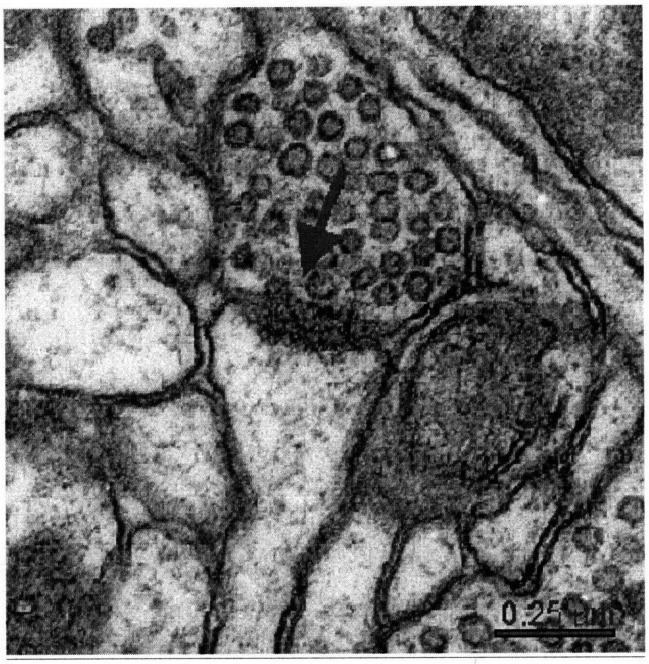

Figure 1. Ultrastructure of a CNS chemical synapse. Arrow points to the synapse from the presynaptic side, which is characterized by synaptic vesicles and an electron-dense thickening (active zone). The postsynaptic compartment of excitatory synapses is often located within dendritic spines, and is marked by the postsynaptic density (PSD) (reproduced from http://synapse-web.org/anatomy/chemical/type1h.htm).

The first experimental evidence for such "Hebbian" plasticity came in 1973, when Bliss and Lomo discovered that brief, high-frequency stimulation (HFS) of the synapses between entorhinal perforant path fibers and hippocampal dentate granule cells led to a sustained enhancement of synaptic transmission (Bliss and Lomo, 1973). This effect was termed long term potentiation (LTP), and it has since been observed in the three major monosynaptic excitatory pathways in the hippocampus (perforant pathway, mossy fiber pathway, and Schaffer collateral pathway), as well as in multiple other regions of the brain and at different stages in development (Malenka and Bear, 2004). Furthermore, different forms of LTP appear to utilize distinct molecular mechanisms to increase synaptic strength. Later studies showed that previously potentiated CA3-CA1 synapses could be weakened, or "depotentiated," by low frequency stimulation (LFS) (Barrionuevo et al., 1980; Staubli and Lynch, 1990; Fujii et al., 1991). Dudek and Bear used this LFS protocol on naïve CA3-CA1 synapses to reliably induce a weakening of synaptic transmission, or long-term depression (LTD) (Dudek and Bear, 1993). Like LTP, both LTD and depotentiation have been found to occur at multiple sites and developmental stages, with varying mechanisms depending on the particular type.

Do LTP, LTD, and depotentiation actually mediate learning and memory? Although it is difficult to prove this directly, several studies have correlated behavioral or sensory experiences with these forms of synaptic plasticity. Heynen *et al.* reported that brief monocular deprivation (MD) causes molecular changes in visual cortex that mimic the changes observed after LFS-induced LTD (Heynen et al., 2003). In addition, further LTD was occluded in visual cortex following MD, suggesting that MD and LTD share a common molecular mechanism. Similarly, Whitlock *et al.* have shown that

Figure 2.

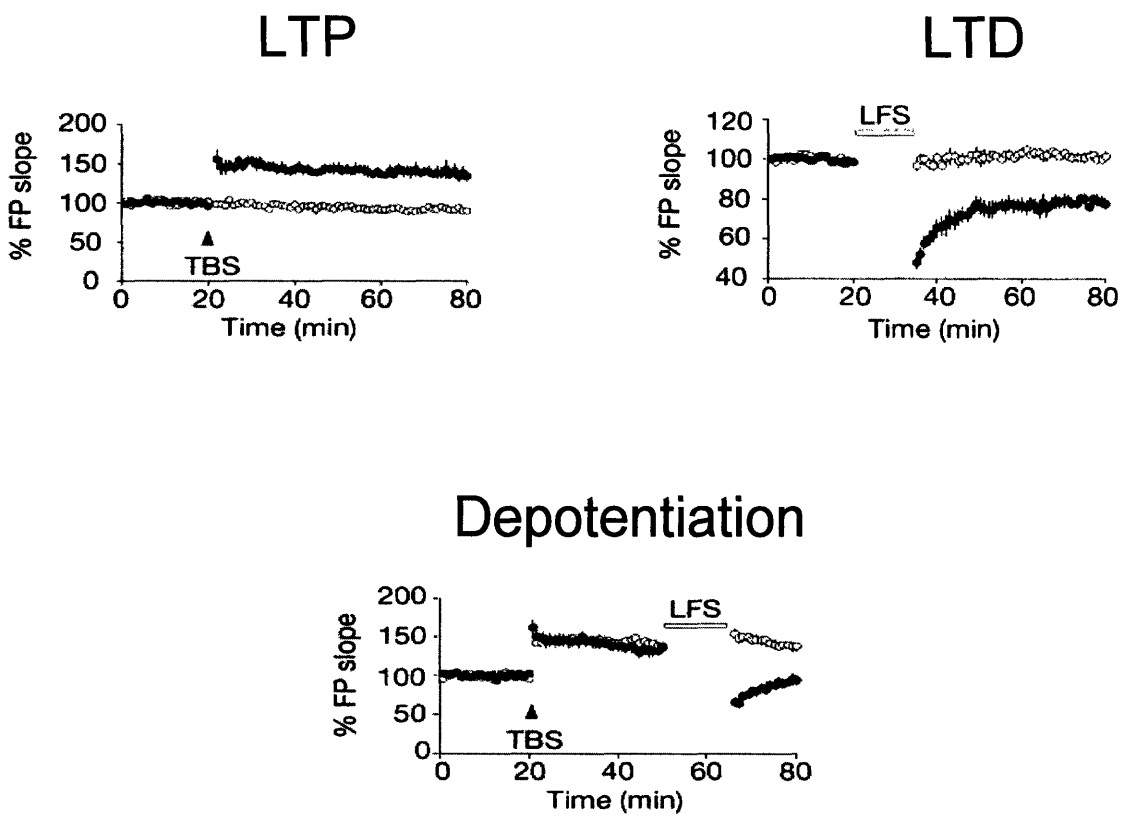

Figure 2. Types of Hebbian plasticity. Long-term potentiation (LTP) is an increase in synaptic strength following certain patterns of activity. Long-term depression (LTD) is a decrease in synaptic strength at naïve synapses, and depotentation is a decrease in synaptic strength in previously potentiated synapses. All three types of plasticity are input-specific. Filled circles represent recordings from synapses that have undergone patterns of correlated activity [eg. Theta burst stimulation (TBS) or low frequency stimulation (LFS)]. Unfilled circles represent unpaired pathways (reproduced from Lee et al., 2000).

inhibitory avoidance learning in rats can cause the same molecular changes as HFS induced LTP, and that this training occludes further LTP in hippocampal slices (Whitlock et al., 2006).

Changes in Spine Morphology and Motility

First discovered more than a century ago by Golgi staining, dendritic spines house the postsynaptic terminals of most excitatory synapses in the mammalian CNS. There is great heterogeneity in the shape and size of spines, which can be roughly categorized as thin, stubby, mushroom-shaped, or branched (Segal, 2005; Tada and Sheng, 2006). In addition, each spine may be rapidly motile, changing its morphology over seconds. Fischer *et al.* transfected GFP-actin into dissociated neurons and found that it localized to spines and was highly dynamic (Fischer et al., 1998). Dunaevsky *et al.* biolistically transfected cultured hippocampal slices with GFP and also observed an array of rapid morphological changes in spines: elongation and retraction, growth of filopodial extensions from spine heads, "kissing" of neighboring spines, and amorphous morphing of spine heads (Dunaevsky et al., 1999). In recent years, many studies have tested the physiological significance of changes in spine structure and explored the molecular mechanisms underlying these phenomena.

What is the functional significance of spine shape and size? Using two-photon uncaging of glutamate to stimulate individual spines, two groups discovered a positive correlation between both postsynaptic excitatory currents and size of the spine head (Matsuzaki et al., 2001; Noguchi et al., 2005). Spines can also act as distinct Ca^{2+} compartments, and the geometry of the spine may influence the kinetics and amplitude of

the postsynaptic Ca^{2+} signal. Some spines primarily use active transport to pump Ca^{2+} out of the cell ("pumpers"), while other spines rely more on passive diffusion into the parent dendrite ("diffusers") (Majewska et al., 2000). Noguchi *et al.* reported that pumpers are primarily spines with thin necks and low Ca^{2+} conductances, while diffusers are large spines with wider necks and higher Ca^{2+} conductances (Noguchi et al., 2005). Peak Ca^{2+} amplitude was higher in smaller spines, presumably because of the reduced rate of passive diffusion. Therefore, changing the shape and size of a spine may be one way of regulating Ca^{2+}, which will be discussed later in this chapter as a key signaling component in synaptic plasticity.

The development of time-lapse fluorescent microscopy and two-photon uncaging of glutamate have yielded insights into the relationship between spine morphology and synaptic plasticity (Lang et al., 2004; Matsuzaki et al., 2004; Okamoto et al., 2004; Otmakhov et al., 2004; Segal, 2005). Using two-photon microscopy, Maletic-Savetic *et al.* observed formation of new filopodia on CA1 neurons of the hippocampus following local stimulation (Maletic-Savatic et al., 1999). Engert and Bonhoeffer reported similar results following an LTP-inducing stimulus (Engert and Bonhoeffer, 1999). These changes occurred slowly, about 30-60 minutes after tetanic stimulation. More recently, several groups have found that LTP is associated with increased size of individually stimulated spines, and conversely, that LTD is correlated with decreased spine size. Matsuzaki *et al.* reported the largest and most rapid effects – a threefold increase within 2-4 minutes of stimulation, which subsequently decreased to a 20-30% increase after 20-40 minutes (Matsuzaki et al., 2004). In addition, this group found that smaller spines were more likely to increase in size than larger spines, suggesting that smaller spines are

more plastic and larger spines more stable. Zhou *et al.* reported a slower and smaller increase after high-frequency stimulation – a 16-33% increase over 20-60 minutes – and for the first time showed that LTD could cause the opposite result, a shrinkage of spines (Zhou et al., 2004). Okamato *et al* used fluorescence resonance energy transfer (FRET) to measure the ratio of filamentous actin (F-actin) to globular actin (G-actin) before and after LTP and LTD (Okamoto et al., 2004). They found that the F-actin/G-actin ratio increased after LTP and decreased after LTD. They also tracked spine morphology using inert Alexa dyes and found changes consistent with their FRET data.

Thanks to the generation of transgenic animals expressing fluorescent proteins in a sparse, neuron-specific manner, recent studies have been able to track spines in vivo and over development (Alvarez and Sabatini, 2007). A window can be cut into the skulls of these mice, and two-photon laser scanning microscopy can be used to image neurons and spines over weeks to months. Several groups have observed the persistence of cortical layer 5 pyramidal neurons in different brain regions and ages. In the somatosensory cortex, 55% of spines were stable in young adult mice (1-2 months old) and 70% were persistent in mature adult mice (4-5 months old) (Trachtenberg et al., 2002; Holtmaat et al., 2005). In visual cortex, 75% of spines were stable in young adults and 90% in mature adults (Grutzendler et al., 2002; Majewska and Sur, 2003). Thus, there is a progressive stabilization of spines over development, and this seems to be achieved in part through a decreased elimination of spines; although spine formation holds steady at about 5-15% throughout the first five months of life, spine elimination declines over adulthood.

Several groups have shown that spine number and morphology can be regulated by learning or sensory input. Eastern marsh wrens that were taught a larger repertoire of songs averaged 37% more spines in certain brain nuclei than control wrens (Airey et al., 2000). In other bird studies, behavioral imprinting led to an increase in spine density after one day (Lowndes and Stewart, 1994) Similarly, rats have shown increased spine density in specific brain regions following learning tasks such as olfactory discrimination and trace eye blink conditioning (Leuner et al., 2003; Knafo et al., 2004). Also in rodents, trimming or removal of whiskers has been used to study plasticity of circuits within the barrel cortex. 3-4 days after whisker trimming, layer 5 pyramidal neurons in the somatosensory cortex showed an increase in transient spines and a decrease in stable spines (Trachtenberg et al., 2002). Similarly, in rodent visual cortex, Majewska and Sur found that binocular deprivation increased spine motility (Majewska and Sur, 2003). In both the somatosensory and visual cortices, these structural changes were correlated in time with changes in synaptic function and preceded higher-order rearrangements in connectivity.

Molecular Mechanisms

Mechanisms Underlying Hebbian Plasticity

There has been significant interest in uncovering the molecular mechanisms behind LTP, LTD, and depotentiation. To date, these studies have focused most on types of plasticity that are dependent on the glutamatergic N-methyl-D-aspartate receptor (NMDAR), and this chapter will be limited primarily to these data. By definition, NMDAR antagonists reproducibly and completely block induction of NMDAR-

dependent LTP, while having little effect on baseline synaptic transmission (Collingridge et al., 1983; Malenka and Bear, 2004). In addition, multiple lines of evidence suggest Ca^{2+} is required for LTP. Ca^{2+} levels increase in dendritic spines after NMDAR activation, Ca^{2+} chelators block LTP, and photolysis of caged Ca^{2+} can mimic LTP (Lynch et al., 1983; Malenka et al., 1988; Regehr and Tank, 1990). The period of Ca^{2+} influx required for LTP has been estimated at less than 2-3 seconds after stimulation (Malenka et al., 1992). These data have led to a model in which depolarization of the postsynaptic cell relieves the voltage-sensitive Mg^{2+} block present in NMDARs, allowing Ca^{2+} to enter the cell and initiate the necessary signaling events.

Downstream of Ca^{2+} influx through NMDARs, a large body of pharmacological and genetic evidence points to calcium/calmodulin dependent protein kinase II (CaMKII) as a necessary and sufficient mediator of LTP. CaMKII is one of the most abundant proteins in the PSD, and inhibition of CaMKII activity abolishes LTP in hippocampal slices (Malenka et al., 1989; Malinow et al., 1989; Ito et al., 1991; Silva et al., 1992; Otmakhov et al., 1997; Cheng et al., 2006). Consistent with these in vitro results, α-CaMKII knockout mice exhibit reduced LTP (Silva et al., 1992). Conversely, expression of constitutively active CaMKII strengthens synaptic transmission and can occlude LTP, suggesting that active CaMKII initiates the same molecular mechanisms employed in LTP (Pettit et al., 1994; Lledo et al., 1995). Phosphorylation at residue Thr286 of CaMKII appears to be critical for its role in LTP. This modification is necessary for preventing CaMKII autoinhibition and also renders CaMKII independent of Ca^{2+} (Hanson et al., 1994; Mukherji and Soderling, 1994). Increased phosphorylation at this

site has been observed after LTP induction, and knock-in mice expressing a T286A substitution exhibit impaired LTP (Fukunaga et al., 1995; Giese et al., 1998).

The actual strengthening of transmission seen in LTP is thought to result from the modification of and increase in number of alpha-amino-3-hydroxy-5-methyl-4-isoxazolepropionic acid receptors (AMPARs), which bind glutamate and mediate most of the fast excitatory transmission at central synapses. (Sheng and Lee, 2001; Malinow and Malenka, 2002; Bredt and Nicoll, 2003; Malenka and Bear, 2004). Studies using recombinant AMPAR subunits with an electrophysiological signature showed that either LTP or constitutively active CaMKII can drive the AMPAR subunit GluR1 into synapses, and that this insertion requires the PDZ binding sequence of GluR1 (Shi et al., 1999; Hayashi et al., 2000). GluR1 can also be phosphorylated at two unique sites on its intracellular carboxy-terminal tail: Ser831, which is a PKC and CaMKII substrate, and Ser845, which is phosphorylated by PKA (Barria et al., 1997a). After LTP induction, increased phosphorylation at Ser831 has been observed (Barria et al., 1997b; Lee et al., 2000). Phosphorylation at Ser831 increases the open channel conductance of GluR1, and this mechanism might therefore contribute to LTP (Derkach et al., 1999).

Ras-MAP kinase (MAPK) signaling appears to be a critical link between CaMKII and GluR1 insertion during LTP. Increased phosphorylation of the MAPK extracellular signal-regulated kinase (ERK) is observed following LTP induction, and MAPK inhibitors can block LTP (English and Sweatt, 1996, 1997). Ras GTPases, which lie upstream of MAPKs, have been shown to be necessary and sufficient for LTP (Zhu et al., 2002). Constitutively active Ras mutants enhance basal synaptic transmission and occlude further LTP, while dominant negative mutants depress basal transmission and

block LTP. Increased ERK phosphorylation is observed following expression of constitutively active CaMKII in hippocampal slices. In addition, both pharmacological MEK inhibition and dominant negative Ras block the synaptic potentiation usually caused by constitutively active CaMKII. Like active CaMKII, constitutively active Ras mutants can drive recombinant GluR1 subunits into synapses.

Like LTP, LTD at CA3-CA1 synapses has been found to be NMDAR and Ca^{2+} dependent (Mulkey and Malenka, 1992; Dudek and Bear, 1993; Malenka and Bear, 2004). Thus the molecular models for LTP and LTD induction are similar, and how LTP and LTD can both be mediated by Ca^{2+} entry through activated NMDARs remains unknown. One explanation is that different NMDAR subtypes and their associated signaling complexes mediate LTP and LTD. This theory is supported by the observation that antagonists with specificities for different NMDAR subtypes affect LTP and LTD distinctly (Kirkwood and Bear, 1994; Hrabetova et al., 2000; Liu et al., 2004).

Downstream of NMDARs and Ca^{2+}, protein phosphatase 1 (PP1) and calcineurin (PP2B) are necessary for induction of LTD (Mulkey et al., 1993; Kirkwood and Bear, 1994; Mulkey et al., 1994). In addition, PKA and PKC substrates are dephosphorylated after LTD induction, while CaMKII substrates remain unchanged (Kameyama et al., 1998; Lee et al., 1998; Hrabetova and Sacktor, 2001). Postsynaptic inhibition of PKA reduces baseline synaptic transmission and occludes LTD, and conversely, postsynaptic activation of PKA can reverse LTD (Kameyama et al., 1998).

LTD is expressed primarily by a reduction in AMPARs at the synapse and by modification of channel properties (Sheng and Lee, 2001; Bredt and Nicoll, 2003; Malenka and Bear, 2004). The number of synaptic AMPAR puncta decreases after LTD,

and inhibitors of clathrin-dependent endocytosis block LTD (Carroll et al., 1999; Luscher et al., 1999). The GluR2 AMPAR subunit can interact with several different proteins via its C-terminus, and these interactions appear to be regulated during LTD to remove surface AMPARs. Two proteins, NSF and AP2, bind to GluR2 at overlapping sites. To examine the function of each, Lee *et al.* used peptides that could specifically inhibit either NSF or AP2 binding to GluR2 (Lee et al., 2002). When the NSF-GluR2 interaction was disrupted, baseline synaptic transmission was depressed, but LTD remained unaffected. Conversely, inhibition of AP2 binding left synaptic transmission intact but prevented LTD. These results suggest that NSF-GluR2 binding is required for maintenance of baseline synaptic strength, and that AP2 is necessary to remove AMPARs during LTD. GluR2 can also bind to the PDZ-containing proteins, GRIP/ABP and PICK1. Phosphorylation at Ser880 of GluR2 disrupts its interaction with GRIP/ABP but has no effect on PICK1 binding (Matsuda et al., 1999; Chung et al., 2000). Increased Ser880 phosphorylation has been detected following LTD, suggesting that the balance between GluR2-GRIP/ABP and GluR2-PICK1 binding is altered during LTD (Matsuda et al., 2000). In addition to this regulation of GluR2, GluR1 is also dephosphorylated at Ser845 following LTD (Lee et al., 2000). Ser845 phosphorylation leads to increased open channel conductance of GluR1, and LTD might therefore be expressed in part because of decreased current through GluR1 channels.

While Ras is necessary and sufficient for LTP, its closely related homologue Rap1 plays an analogous role in LTD (Zhu et al., 2002). In cultured hippocampal slices, dominant negative Rap1 mutants cause higher baseline synaptic transmission and impaired LTD. Constitutively active Rap1 reduces baseline transmission, occludes LTD,

and decreases surface expression of the GluR2 subunit. Calcineurin inhibitors can prevent the effects of active Rap1, suggesting that Rap1 signals upstream of calcineurin. Inhibition of the MAPK p38 also blocks Rap1-mediated depression, while MEK inhibitors have no effect. Therefore, Rap1-p38 signaling appears to be necessary and sufficient for LTD, just as Ras-ERK1/2 signaling is necessary and sufficient for LTP.

Relative to LTP and LTD, little is known about the molecular mechanisms behind depotentiation. After depotentiation, dephosphorylation is seen at Ser831 rather than at Ser845, as it is in LTD (Lee et al., 2000). Therefore, depotentiation may employ different signaling pathways than LTD to dampen synaptic transmission. A study by Zhu *et al.* supports this idea, showing that Rap2, rather than Ras or Rap1, is required for depotentiation in hippocampal slices (Zhu et al., 2005). Rap2 dominant negative mutants prevent depotentiation after LTP induction, while constitutively active mutants prevent LTP. In addition, Rap2 was found to signal through the MAPK Jun N-terminal kinase (JNK) to reduce surface levels of GluR1 subunit. Therefore, several lines of evidence indicate that LTP, LTD, and depotentiation employ three different Ras GTPases – Ras, Rap1, and Rap2, respectively – that signal through distinct MAP kinases.

Mechanisms Underyling Dendritic Spine Structure

Actin is highly enriched in dendritic spines, and several lines of evidence suggest that actin polymerization and depolymerization is a primary way to control spine shape. As mentioned earlier, LTP is correlated with a higher F-actin/G-actin ratio, while LTD is associated with the inverse (Okamoto et al., 2004) . Rhodamine-phalloidin labeling of stimulated neurons has also revealed similar activity-induced actin polymerization (Lin et

al., 2005). In cultured neurons, bath application of cytochalasin-D, an inhibitor of actin polymerization, prevents motility of overexpressed GFP-actin (Fischer et al., 1998; Dunaevsky et al., 1999).

In addition to actin itself, there are a number of actin-binding proteins that are enriched in spines and have been functionally correlated with changes in spine shape and/or density (Tada and Sheng, 2006). α-actinin links NMDARs to actin, and when overexpressed in dissociated hippocampal neurons, it causes an increase in length and density of dendritic protrusions (Nakagawa et al., 2004). Cortactin activates the Arp2/3 actin nucleation complex and can also bind to the postsynaptic scaffold Shank. RNAi knockdown of cortactin causes fewer spines, while overexpression causes elongation. In addition, NMDAR activation causes targeting of cortactin to dendritic spines, suggesting that cortactin can regulate spine morphology in response to activity (Hering and Sheng, 2003). Similarly, profilin is also recruited to spines by NMDAR activation (Ackermann and Matus, 2003). Profilin promotes actin filament assembly, and preventing profilin targeting to synapses leads to spine destabilization. Actin depolymerizing factor (ADF)/cofilin causes severing of actin filaments and can be inhibited by phosphorylation on its Ser3 residue (Agnew et al., 1995). Fukazawa *et al.* observed increased ADF/cofilin phosphorylation and F-actin content following LTP-inducing stimuli, and also found that peptides inhibiting phosphorylation of endogenous ADF/cofilin could prevent LTP (Fukazawa et al., 2003).

What are the signaling pathways that act upstream of actin and its direct binding partners? Recent evidence has suggested a significant role for the Ras and Rho/Rac/Cdc42 families of small GTPases. Ras appears to have a positive role in spine

growth. Transgenic mice expressing constitutively active Ha-Ras show increased spine density in cortical pyramidal neurons, and mice lacking SynGAP, a negative regulator of Ras, exhibit accelerated spine development and larger spines (Vazquez et al., 2004; Gartner et al., 2005). Like Ras, Rac1 appears to promote spine formation, while RhoA seems to prevent it. In cultured slices, overexpressed constitutively active RhoA reduces spine density, and constitutively active Rac1 increases spine density (Luo et al., 1996; Nakayama et al., 2000; Tashiro et al., 2000). RhoA and Rac1 have also been associated with two different kinds of motility. RhoA seems to control "head morphing," in which the spine head changes shape in an amorphous, non-vectorial manner. Rac1 regulates "protrusive motility," where filopodia shoot rapidly in and out of the spine head.

The protein tyrosine kinase-linked EphB receptors seem to be a major upstream signaling component of the Rho/Rac/Cdc42 GTPases. Cultured hippocampal neurons from EphB1/B2/B3 triple knockout mice fail to form dendritic spines, and their neurons do not form postsynaptic specializations and show reduced levels of NMDARs and AMPARs (Henkemeyer et al., 2003). One link between EphB receptors and Rac1 is the RacGEF kalirin-7. Kalirin-7 is enriched in the PSD, and EphB receptor activation using the clustered ligand ephrin B1 causes tyrosine phosphorylation and activation of kalirin-7 (Penzes et al., 2003). In addition, dominant negative kalirin-7 or dominant negative Rac1 both block EphB mediated formation of spines. In addition to kalirin-7, there are a number of known Rho/Rac/Cdc42 GAPs and GEFs that have been shown to affect spine morphology. αPIX and TIAM1 are both RacGEFs that play a role in dendrite and spine development (Tolias et al., 2005; Zhang et al., 2005). GEFT is another Rho family GEF that promotes neurite outgrowth and spine enlargement (Bryan et al., 2004). Lfc is a

Figure 3

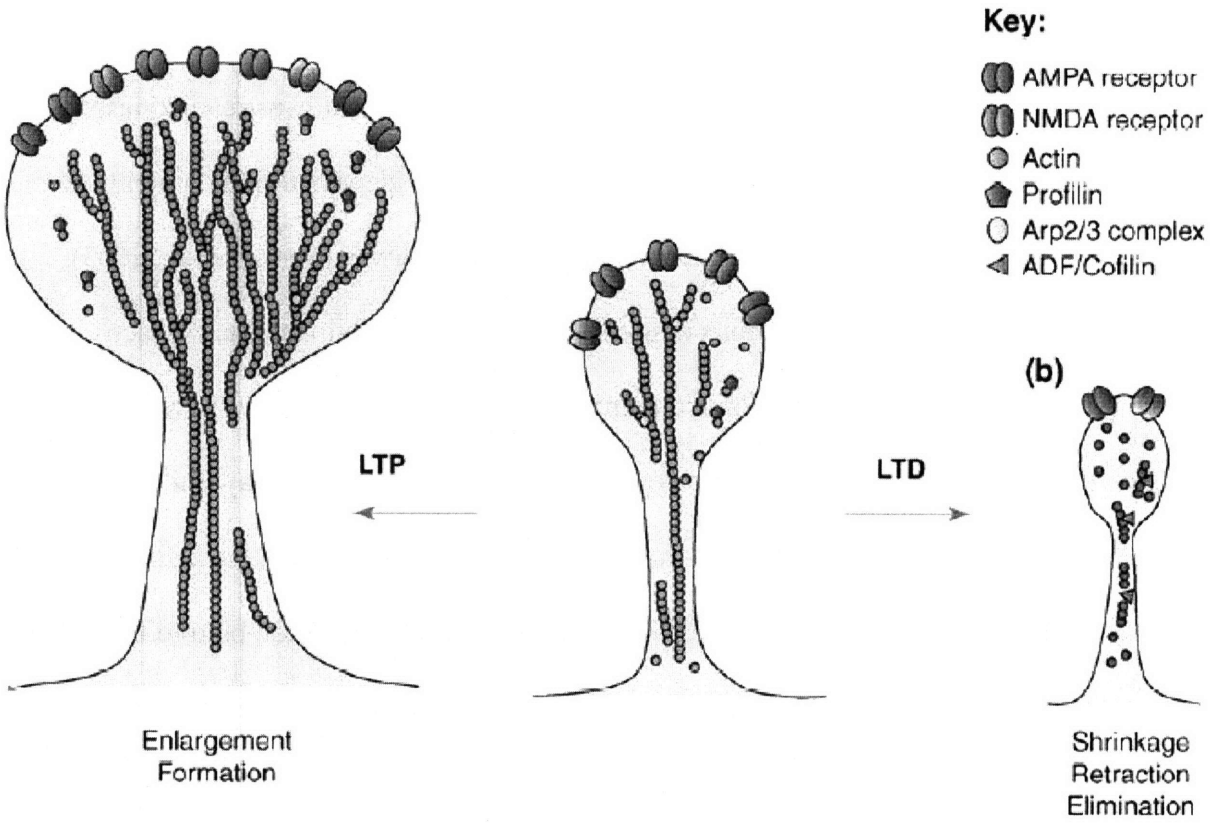

Figure 3. Actin polymerization/depolymerization drives structural plasticity of dendritic spines. Increases in spine size (i.e. after LTP induction) have been associated with increased actin polymerization, and decreases in spine size (i.e. following LTD induction) have been correlated with increased actin depolymerization. In addition, many regulators of actin stability have been implicated in dendritic spine morphogenesis (reproduced from Tada and Sheng, 2006).

Rho-specific GEF that translocates to spines after depolarization and reduces spine size when overexpressed (Bryan et al., 2004).

Once activated, Rho/Rac/Cdc42 GTPases can activate downstream kinases to transduce signals to the actin cytoskeleton. Penzes *et al.* identified PAK proteins as major effectors of the EphB-kalirin-7-Rac1 signaling pathway (Penzes et al., 2003). PAK1 dominant negative mutants diminished the spine formation caused by activation of EphB receptors. In addition, PAK dominant negative transgenic mice showed altered cortical spine morphology and impaired consolidation of memory (Hayashi et al., 2004). A potential link between the EphB-kalirin-7-Rac1-PAK cascade and the actin cytoskeleton is the serine/threonine kinase LIMK1. Active PAK can bind to LIMK1 and activate it by phosphorylating Thr508 in its catalytic domain (Edwards et al., 1999). Active LIMK1, in turn, can phosphorylate and inhibit ADF/cofilin, ultimately promoting actin polymerization.

Potential Roles for Myosins and Rap GTPases at Synapses

Recently, attempts to define the molecular mechanisms behind synaptic plasticity and structure have been greatly aided by proteomic analyses of biochemically purified PSDs or synaptic protein complexes. High sensitivity mass spectrometry methods such as matrix-assisted laser desorption/ionization time-of-flight (MALDI-TOF) and liquid chromatography/tandem MS have allowed a more global view of synaptic proteins (Husi et al., 2000; Walikonis et al., 2000; Husi and Grant, 2001; Jordan et al., 2004; Peng et al., 2004). Though these methods are subject to both false positives and negatives, they have yielded the identities of many more PSD proteins, as well as knowledge of post-

translational modifications. In addition, there has been a push to describe the PSD more quantitatively through quantitative MS, EM combined with quantitative immunoblotting, or GFP-based quantitative fluorescent calibration (Chen et al., 2005; Sugiyama et al., 2005; Cheng et al., 2006).

Two interesting classes of proteins that have been identified in many of these studies are myosins and Rap GTPases. Myosins make up a large superfamily of proteins that can bind to and move along actin filaments using ATP hydrolysis (Sellers, 2000). Typically, they possess three domains: 1) the motor domain, which can bind actin and ATP, 2) the neck domain, which binds myosin light chains and calmodulin, and 3) the tail domain, which is the most variable in sequence and length. Currently, 15 classes of myosins have been designated based on sequence similarity of the motor domain. Of these, the class II myosins, or "conventional myosins," were the first discovered and are the best studied to date. In the slime mold *Dictyostelium discoideum*, loss of the single myosin II gene causes an inability to undergo cytokinesis when cells are grown in suspension or on a hydrophobic surface (De Lozanne and Spudich, 1987). *Dictyostelium* myosin II null cells also cannot cap surface receptors and have reduced cortical tension (Pasternak et al., 1989). In the yeast *Saccharomyces cerevisiae*, loss of the single myosin II gene also caused cytokinesis defects, and in the fruit fly *Drosophila melanogaster*, loss of the single non-muscle myosin II gene is embryonic lethal due to failed completion of dorsal closure (Watts et al., 1987; Young et al., 1993).

Vertebrates have three non-muscle myosin II heavy chain genes: myosin IIA, IIB, and IIC (Simons et al., 1991). Knockout of myosin IIA in mice causes early embryonic death (E7) (Conti et al., 2004). Myosin IIB knockout mice also die in utero and show

profound hydrocephalus and heart defects (Tullio et al., 1997; Tullio et al., 2001). In neurons, multiple lines of evidence suggest that myosin II plays an important role in growth cone motility and axonal outgrowth. Antisense oligodeoxyribonucleotides against myosin IIB cause decreased neurite outgrowth in neuroblastoma cells (Wylie et al., 1998). Growth cones from myosin IIB knockout mice were smaller and showed decreased rates of outgrowth, increased retrograde flow rates, and altered actin organization (Bridgman et al., 2001; Tullio et al., 2001). In addition to exploration, myosin II has been shown to play a role in the adhesion and tension generation steps of neurite outgrowth as well. Antisense RNA targeted for myosin IIA causes a decrease in focal adhesions, and a loss of paxillin and vinculin targeting to adhesion sites (Wylie and Chantler, 2001). Growth cones from myosin IIB KO mice exhibit reduced traction force relative to wildtype growth cones (Bridgman et al., 2001).

In contrast to its role in axonal outgrowth, little is known about myosin II's function at synapses. Based on negative results using the myosin II inhibitor 2,3 butanedione-monoxime (BDM), a role for myosin II in dendritic spine morphogenesis was ruled out, and actin polymerization/depolymerization became established as the primary mechanism for changing dendritic spine shape and size (Fischer et al., 1998). However, BDM was later found to have poor affinity for myosin II, and thus it is still an open question whether myosins might represent a way to alter the spine cytoskeleton that is distinct from actin polymerization (Ostap, 2002).

Like myosin II, the Rap GTPases, Rap1 and Rap2, have been identified in purified PSD fractions or NMDAR complexes (Husi et al., 2000; Jordan et al., 2004; Peng et al., 2004). Rap1 and Rap2, share ~50% amino acid identity with Ras (Pizon et

Figure 4

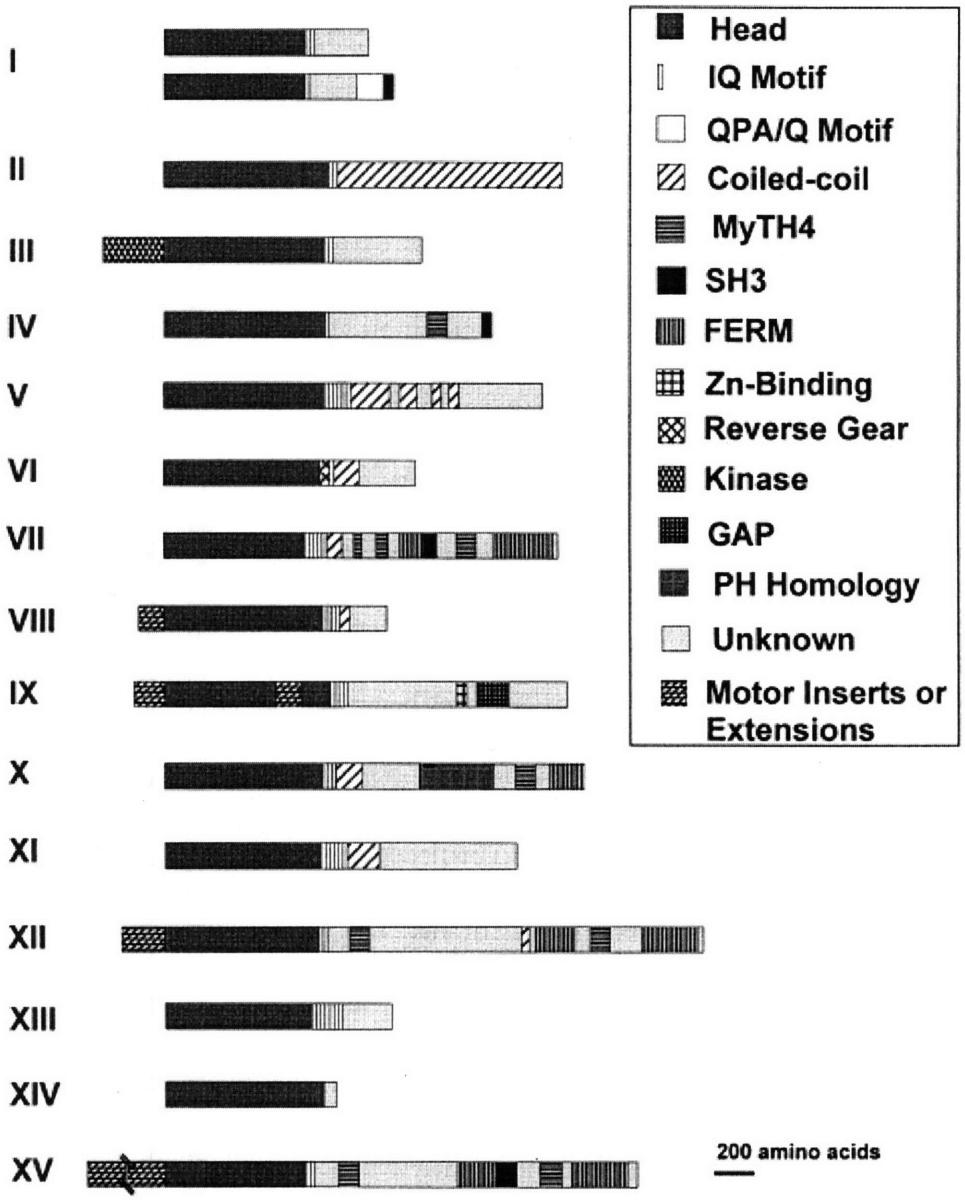

Figure 4. Myosin families. Phylogenetic analysis has identified 15 classes of myosins. All myosins contain three domains: 1) the motor or head domain that interacts with actin and binds ATP, 2) the neck domain which contains variable numbers of IQ motifs that bind light chains and calmodulin, and 3) the tail domain, which is the most diverse.

al., 1988). Rap1's effector domain is identical to that of Ras, while Rap2's effector domain differs by only a single amino acid. This observation led to the hypothesis that Rap GTPases might antagonize Ras signaling by competing for downstream effectors. Consistent with this idea, Rap1 was identified in a genetic screen for suppressors of Ras transforming activity in NIH 3T3 fibroblasts (Kitayama et al., 1989). Unlike Rap1, Rap2 cannot revert Ras-transformed cells, but it can inhibit Ras-dependent activation of the transcription factor Elk-1 (Ohba et al., 2000). In addition to modulating Ras signaling, the Rap GTPases have also been shown to regulate cell adhesion molecules, namely integrins and cadherins. Rap1 has been shown to regulate inside-out signaling to several integrin heterodimers, including α4β1, α5β1, αLβ2, αMβ2, and αIIbβ3 (Caron, 2003). In addition, loss of Rap1 or several of its GEFs has been shown to disrupt cadherin localization and formation of adherens junctions. Although less well characterized in cell adhesion, Rap2 has recently been shown to be necessary for integrin-dependent adhesion in B lymphocytes (Christian et al., 2003; McLeod et al., 2004).

In neurons, several lines of in vitro evidence suggest that the Rap GTPases might oppose Ras function at synapses and dampen synaptic development and strength. Overexpression of Spine-associated RapGAP (SPAR) in dissociated hippocampal neurons causes a prominent increase in spine size and density (Pak et al., 2001). Serum-inducible protein kinase (SNK), a polo-box kinase that primes SPAR for degradation, causes decreased spine density (Pak and Sheng, 2003). Overexpression of both Rap1 and Rap2 can reduce spine density, as well as cause loss of surface GluR2 receptors; Rap2 overexpression can cause dramatic shortening of dendrites and axons as well (Fu et al., 2007). In another study, Xie et al. showed that overexpressed constitutively active Rap1

causes thinning and elongation of spines, while dominant negative Rap1 causes spine enlargement (Xie et al., 2005). As mentioned earlier in this chapter, both Rap1 and Rap2 appear to play a role in Hebbian synaptic plasticity. Rap1 mediates LTD by signaling through the MAPK p38, while Rap2 is necessary for depotentiation by activating JNK.

Conclusion: Eludicating the roles of myosin II and Rap2 in synaptic structure and function

Myosin II and Rap2 have both been identified in the PSD, and they represent potentially novel ways of regulating synaptic structure and function. While actin polymerization and depolymerization is classically thought to drive morphological changes in spines, the role for myosins – which can contract and relax actin filaments – has never been fully explored. Similarly, though Ras is well established as a regulator of synaptic structure and function, less is known about its relatives. In addition, while the molecular mechanisms behind LTP and LTD have been extensively studied, the proteins and signaling pathways behind depotentation are less well understood.

Here, we describe experiments aimed to further elucidate the roles of myosin II and Rap2 at synapses. We used a combination of pharmacological and genetic inhibition of endogenous myosin II in cultured neurons to show that this protein is necessary for normal spine morphology, spine motility, and synaptic transmission. These results indicate that spine structure may be regulated not only by polymerization/depolymerization of actin, but by myosin-directed movement of actin as well. For Rap2, we sought to explore its *in vivo* function in neurons using transgenic mice that expressed either dominant negative or constitutively active Rap2 in postnatal

forebrain. Constitutively active Rap2 mice showed fewer and smaller dendritic spines and reduced ERK activation, consistent with an inhibitory role for Rap2 at synapses. In addition, they were hyperactive and exhibited defects in spatial learning and the extinction of fear; this latter defect makes them potential therapeutic models for psychiatric diseases in which fear extinction is disrupted, including anxiety disorders and posttraumatic stress disorder (PTSD).

Figure 5

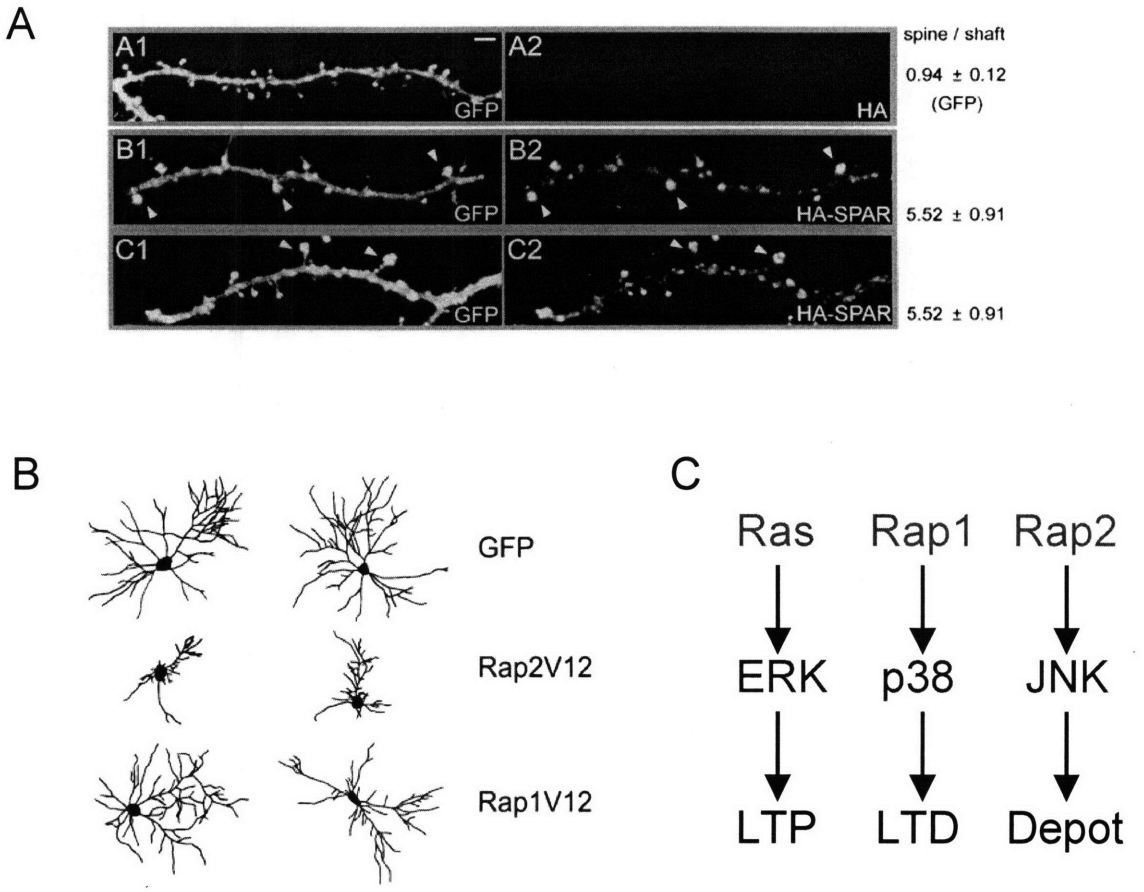

Figure 5. Rap GTPases are potential inhibitors of synapse growth and function. Several lines of evidence in cultured dissociated neurons or slices suggest that Rap2 can suppress neuronal development and synaptic transmission. (A) SPAR, a RapGAP, causes increases in spine size. (B) Active Rap2 dramatically reduces dendritic and axonal arborization, as well as synapse number. (C) Rap1 and Rap2 are necessary for LTD and depotentiation, respectively, while Ras is required for LTP.

References

Ackermann M, Matus A (2003) Activity-induced targeting of profilin and stabilization of dendritic spine morphology. Nat Neurosci 6:1194-1200.

Agnew BJ, Minamide LS, Bamburg JR (1995) Reactivation of phosphorylated actin depolymerizing factor and identification of the regulatory site. J Biol Chem 270:17582-17587.

Airey DC, Kroodsma DE, DeVoogd TJ (2000) Differences in the complexity of song tutoring cause differences in the amount learned and in dendritic spine density in a songbird telencephalic song control nucleus. Neurobiol Learn Mem 73:274-281.

Alvarez VA, Sabatini BL (2007) Anatomical and physiological plasticity of dendritic spines. Annu Rev Neurosci 30:79-97.

Barria A, Derkach V, Soderling T (1997a) Identification of the Ca2+/calmodulin-dependent protein kinase II regulatory phosphorylation site in the alpha-amino-3-hydroxyl-5-methyl-4-isoxazole-propionate-type glutamate receptor. J Biol Chem 272:32727-32730.

Barria A, Muller D, Derkach V, Griffith LC, Soderling TR (1997b) Regulatory phosphorylation of AMPA-type glutamate receptors by CaM-KII during long-term potentiation. Science 276:2042-2045.

Barrionuevo G, Schottler F, Lynch G (1980) The effects of repetitive low frequency stimulation on control and "potentiated" synaptic responses in the hippocampus. Life Sci 27:2385-2391.

Bliss TV, Lomo T (1973) Long-lasting potentiation of synaptic transmission in the dentate area of the anaesthetized rabbit following stimulation of the perforant path. J Physiol 232:331-356.

Bredt DS, Nicoll RA (2003) AMPA receptor trafficking at excitatory synapses. Neuron 40:361-379.

Bridgman PC, Dave S, Asnes CF, Tullio AN, Adelstein RS (2001) Myosin IIB is required for growth cone motility. J Neurosci 21:6159-6169.

Bryan B, Kumar V, Stafford LJ, Cai Y, Wu G, Liu M (2004) GEFT, a Rho family guanine nucleotide exchange factor, regulates neurite outgrowth and dendritic spine formation. J Biol Chem 279:45824-45832.

Caron E (2003) Cellular functions of the Rap1 GTP-binding protein: a pattern emerges. J Cell Sci 116:435-440.

Carroll RC, Lissin DV, von Zastrow M, Nicoll RA, Malenka RC (1999) Rapid redistribution of glutamate receptors contributes to long-term depression in hippocampal cultures. Nat Neurosci 2:454-460.

Chen X, Vinade L, Leapman RD, Petersen JD, Nakagawa T, Phillips TM, Sheng M, Reese TS (2005) Mass of the postsynaptic density and enumeration of three key molecules. Proc Natl Acad Sci U S A 102:11551-11556.

Cheng D, Hoogenraad CC, Rush J, Ramm E, Schlager MA, Duong DM, Xu P, Wijayawardana SR, Hanfelt J, Nakagawa T, Sheng M, Peng J (2006) Relative and absolute quantification of postsynaptic density proteome isolated from rat forebrain and cerebellum. Mol Cell Proteomics 5:1158-1170.

Christian SL, Lee RL, McLeod SJ, Burgess AE, Li AH, Dang-Lawson M, Lin KB, Gold MR (2003) Activation of the Rap GTPases in B lymphocytes modulates B cell

antigen receptor-induced activation of Akt but has no effect on MAPK activation. J Biol Chem 278:41756-41767.
Chung HJ, Xia J, Scannevin RH, Zhang X, Huganir RL (2000) Phosphorylation of the AMPA receptor subunit GluR2 differentially regulates its interaction with PDZ domain-containing proteins. J Neurosci 20:7258-7267.
Collingridge GL, Kehl SJ, McLennan H (1983) Excitatory amino acids in synaptic transmission in the Schaffer collateral-commissural pathway of the rat hippocampus. J Physiol 334:33-46.
Conti MA, Even-Ram S, Liu C, Yamada KM, Adelstein RS (2004) Defects in cell adhesion and the visceral endoderm following ablation of nonmuscle myosin heavy chain II-A in mice. J Biol Chem 279:41263-41266.
Cowan WM, Südhof TC, Stevens CF, eds (2001) Synapses. Baltimore: Johns Hopkins University Press.
Dalva MB, McClelland AC, Kayser MS (2007) Cell adhesion molecules: signalling functions at the synapse. Nat Rev Neurosci 8:206-220.
De Lozanne A, Spudich JA (1987) Disruption of the Dictyostelium myosin heavy chain gene by homologous recombination. Science 236:1086-1091.
Derkach V, Barria A, Soderling TR (1999) Ca2+/calmodulin-kinase II enhances channel conductance of alpha-amino-3-hydroxy-5-methyl-4-isoxazolepropionate type glutamate receptors. Proc Natl Acad Sci U S A 96:3269-3274.
Dudek SM, Bear MF (1993) Bidirectional long-term modification of synaptic effectiveness in the adult and immature hippocampus. J Neurosci 13:2910-2918.
Dunaevsky A, Tashiro A, Majewska A, Mason C, Yuste R (1999) Developmental regulation of spine motility in the mammalian central nervous system. Proc Natl Acad Sci U S A 96:13438-13443.
Edwards DC, Sanders LC, Bokoch GM, Gill GN (1999) Activation of LIM-kinase by Pak1 couples Rac/Cdc42 GTPase signalling to actin cytoskeletal dynamics. Nat Cell Biol 1:253-259.
Engert F, Bonhoeffer T (1999) Dendritic spine changes associated with hippocampal long-term synaptic plasticity. Nature 399:66-70.
English JD, Sweatt JD (1996) Activation of p42 mitogen-activated protein kinase in hippocampal long term potentiation. J Biol Chem 271:24329-24332.
English JD, Sweatt JD (1997) A requirement for the mitogen-activated protein kinase cascade in hippocampal long term potentiation. J Biol Chem 272:19103-19106.
Fischer M, Kaech S, Knutti D, Matus A (1998) Rapid actin-based plasticity in dendritic spines. Neuron 20:847-854.
Fu Z, Lee SH, Simonetta A, Hansen J, Sheng M, Pak DT (2007) Differential roles of Rap1 and Rap2 small GTPases in neurite retraction and synapse elimination in hippocampal spiny neurons. J Neurochem 100:118-131.
Fujii S, Saito K, Miyakawa H, Ito K, Kato H (1991) Reversal of long-term potentiation (depotentiation) induced by tetanus stimulation of the input to CA1 neurons of guinea pig hippocampal slices. Brain Res 555:112-122.
Fukazawa Y, Saitoh Y, Ozawa F, Ohta Y, Mizuno K, Inokuchi K (2003) Hippocampal LTP is accompanied by enhanced F-actin content within the dendritic spine that is essential for late LTP maintenance in vivo. Neuron 38:447-460.

Fukunaga K, Muller D, Miyamoto E (1995) Increased phosphorylation of Ca2+/calmodulin-dependent protein kinase II and its endogenous substrates in the induction of long-term potentiation. J Biol Chem 270:6119-6124.

Gartner U, Alpar A, Behrbohm J, Heumann R, Arendt T (2005) Enhanced Ras activity promotes spine formation in synRas mice neocortex. Neuroreport 16:149-152.

Giese KP, Fedorov NB, Filipkowski RK, Silva AJ (1998) Autophosphorylation at Thr286 of the alpha calcium-calmodulin kinase II in LTP and learning. Science 279:870-873.

Gray EG (1959) Axo-somatic and axo-dendritic synapses of the cerebral cortex: an electron microscope study. J Anat 93:420-433.

Grutzendler J, Kasthuri N, Gan WB (2002) Long-term dendritic spine stability in the adult cortex. Nature 420:812-816.

Hanson PI, Meyer T, Stryer L, Schulman H (1994) Dual role of calmodulin in autophosphorylation of multifunctional CaM kinase may underlie decoding of calcium signals. Neuron 12:943-956.

Harris KM, Kater SB (1994) Dendritic spines: cellular specializations imparting both stability and flexibility to synaptic function. Annu Rev Neurosci 17:341-371.

Harris KM, Sultan P (1995) Variation in the number, location and size of synaptic vesicles provides an anatomical basis for the nonuniform probability of release at hippocampal CA1 synapses. Neuropharmacology 34:1387-1395.

Harris KM, Jensen FE, Tsao B (1992) Three-dimensional structure of dendritic spines and synapses in rat hippocampus (CA1) at postnatal day 15 and adult ages: implications for the maturation of synaptic physiology and long-term potentiation. J Neurosci 12:2685-2705.

Hayashi ML, Choi SY, Rao BS, Jung HY, Lee HK, Zhang D, Chattarji S, Kirkwood A, Tonegawa S (2004) Altered cortical synaptic morphology and impaired memory consolidation in forebrain- specific dominant-negative PAK transgenic mice. Neuron 42:773-787.

Hayashi Y, Shi SH, Esteban JA, Piccini A, Poncer JC, Malinow R (2000) Driving AMPA receptors into synapses by LTP and CaMKII: requirement for GluR1 and PDZ domain interaction. Science 287:2262-2267.

Hebb DO (1949) The organization of behavior; a neuropsychological theory. New York,: Wiley.

Henkemeyer M, Itkis OS, Ngo M, Hickmott PW, Ethell IM (2003) Multiple EphB receptor tyrosine kinases shape dendritic spines in the hippocampus. J Cell Biol 163:1313-1326.

Hering H, Sheng M (2003) Activity-dependent redistribution and essential role of cortactin in dendritic spine morphogenesis. J Neurosci 23:11759-11769.

Heynen AJ, Yoon BJ, Liu CH, Chung HJ, Huganir RL, Bear MF (2003) Molecular mechanism for loss of visual cortical responsiveness following brief monocular deprivation. Nat Neurosci 6:854-862.

Holtmaat AJ, Trachtenberg JT, Wilbrecht L, Shepherd GM, Zhang X, Knott GW, Svoboda K (2005) Transient and persistent dendritic spines in the neocortex in vivo. Neuron 45:279-291.

Hrabetova S, Sacktor TC (2001) Transient translocation of conventional protein kinase C isoforms and persistent downregulation of atypical protein kinase Mzeta in long-term depression. Brain Res Mol Brain Res 95:146-152.
Hrabetova S, Serrano P, Blace N, Tse HW, Skifter DA, Jane DE, Monaghan DT, Sacktor TC (2000) Distinct NMDA receptor subpopulations contribute to long-term potentiation and long-term depression induction. J Neurosci 20:RC81.
Husi H, Grant SG (2001) Isolation of 2000-kDa complexes of N-methyl-D-aspartate receptor and postsynaptic density 95 from mouse brain. J Neurochem 77:281-291.
Husi H, Ward MA, Choudhary JS, Blackstock WP, Grant SG (2000) Proteomic analysis of NMDA receptor-adhesion protein signaling complexes. Nat Neurosci 3:661-669.
Ito I, Hidaka H, Sugiyama H (1991) Effects of KN-62, a specific inhibitor of calcium/calmodulin-dependent protein kinase II, on long-term potentiation in the rat hippocampus. Neurosci Lett 121:119-121.
Jordan BA, Fernholz BD, Boussac M, Xu C, Grigorean G, Ziff EB, Neubert TA (2004) Identification and verification of novel rodent postsynaptic density proteins. Mol Cell Proteomics 3:857-871.
Kameyama K, Lee HK, Bear MF, Huganir RL (1998) Involvement of a postsynaptic protein kinase A substrate in the expression of homosynaptic long-term depression. Neuron 21:1163-1175.
Katz SB (1969) The release of neural transmitter substances. Springfield, Ill.,: Thomas.
Kirkwood A, Bear MF (1994) Homosynaptic long-term depression in the visual cortex. J Neurosci 14:3404-3412.
Kitayama H, Sugimoto Y, Matsuzaki T, Ikawa Y, Noda M (1989) A ras-related gene with transformation suppressor activity. Cell 56:77-84.
Knafo S, Ariav G, Barkai E, Libersat F (2004) Olfactory learning-induced increase in spine density along the apical dendrites of CA1 hippocampal neurons. Hippocampus 14:819-825.
Lang C, Barco A, Zablow L, Kandel ER, Siegelbaum SA, Zakharenko SS (2004) Transient expansion of synaptically connected dendritic spines upon induction of hippocampal long-term potentiation. Proc Natl Acad Sci U S A 101:16665-16670.
Lee HK, Kameyama K, Huganir RL, Bear MF (1998) NMDA induces long-term synaptic depression and dephosphorylation of the GluR1 subunit of AMPA receptors in hippocampus. Neuron 21:1151-1162.
Lee HK, Barbarosie M, Kameyama K, Bear MF, Huganir RL (2000) Regulation of distinct AMPA receptor phosphorylation sites during bidirectional synaptic plasticity. Nature 405:955-959.
Lee SH, Liu L, Wang YT, Sheng M (2002) Clathrin adaptor AP2 and NSF interact with overlapping sites of GluR2 and play distinct roles in AMPA receptor trafficking and hippocampal LTD. Neuron 36:661-674.
Leuner B, Falduto J, Shors TJ (2003) Associative memory formation increases the observation of dendritic spines in the hippocampus. J Neurosci 23:659-665.
Lin B, Kramar EA, Bi X, Brucher FA, Gall CM, Lynch G (2005) Theta stimulation polymerizes actin in dendritic spines of hippocampus. J Neurosci 25:2062-2069.

Liu L, Wong TP, Pozza MF, Lingenhoehl K, Wang Y, Sheng M, Auberson YP, Wang YT (2004) Role of NMDA receptor subtypes in governing the direction of hippocampal synaptic plasticity. Science 304:1021-1024.

Lledo PM, Hjelmstad GO, Mukherji S, Soderling TR, Malenka RC, Nicoll RA (1995) Calcium/calmodulin-dependent kinase II and long-term potentiation enhance synaptic transmission by the same mechanism. Proc Natl Acad Sci U S A 92:11175-11179.

Lowndes M, Stewart MG (1994) Dendritic spine density in the lobus parolfactorius of the domestic chick is increased 24 h after one-trial passive avoidance training. Brain Res 654:129-136.

Luo L, Hensch TK, Ackerman L, Barbel S, Jan LY, Jan YN (1996) Differential effects of the Rac GTPase on Purkinje cell axons and dendritic trunks and spines. Nature 379:837-840.

Luscher C, Xia H, Beattie EC, Carroll RC, von Zastrow M, Malenka RC, Nicoll RA (1999) Role of AMPA receptor cycling in synaptic transmission and plasticity. Neuron 24:649-658.

Lynch G, Larson J, Kelso S, Barrionuevo G, Schottler F (1983) Intracellular injections of EGTA block induction of hippocampal long-term potentiation. Nature 305:719-721.

Majewska A, Sur M (2003) Motility of dendritic spines in visual cortex in vivo: changes during the critical period and effects of visual deprivation. Proc Natl Acad Sci U S A 100:16024-16029.

Majewska A, Brown E, Ross J, Yuste R (2000) Mechanisms of calcium decay kinetics in hippocampal spines: role of spine calcium pumps and calcium diffusion through the spine neck in biochemical compartmentalization. J Neurosci 20:1722-1734.

Malenka RC, Bear MF (2004) LTP and LTD: an embarrassment of riches. Neuron 44:5-21.

Malenka RC, Lancaster B, Zucker RS (1992) Temporal limits on the rise in postsynaptic calcium required for the induction of long-term potentiation. Neuron 9:121-128.

Malenka RC, Kauer JA, Zucker RS, Nicoll RA (1988) Postsynaptic calcium is sufficient for potentiation of hippocampal synaptic transmission. Science 242:81-84.

Malenka RC, Kauer JA, Perkel DJ, Mauk MD, Kelly PT, Nicoll RA, Waxham MN (1989) An essential role for postsynaptic calmodulin and protein kinase activity in long-term potentiation. Nature 340:554-557.

Maletic-Savatic M, Malinow R, Svoboda K (1999) Rapid dendritic morphogenesis in CA1 hippocampal dendrites induced by synaptic activity. Science 283:1923-1927.

Malinow R, Malenka RC (2002) AMPA receptor trafficking and synaptic plasticity. Annu Rev Neurosci 25:103-126.

Malinow R, Schulman H, Tsien RW (1989) Inhibition of postsynaptic PKC or CaMKII blocks induction but not expression of LTP. Science 245:862-866.

Matsuda S, Mikawa S, Hirai H (1999) Phosphorylation of serine-880 in GluR2 by protein kinase C prevents its C terminus from binding with glutamate receptor-interacting protein. J Neurochem 73:1765-1768.

Matsuda S, Launey T, Mikawa S, Hirai H (2000) Disruption of AMPA receptor GluR2 clusters following long-term depression induction in cerebellar Purkinje neurons. Embo J 19:2765-2774.

Matsuzaki M, Honkura N, Ellis-Davies GC, Kasai H (2004) Structural basis of long-term potentiation in single dendritic spines. Nature 429:761-766.
Matsuzaki M, Ellis-Davies GC, Nemoto T, Miyashita Y, Iino M, Kasai H (2001) Dendritic spine geometry is critical for AMPA receptor expression in hippocampal CA1 pyramidal neurons. Nat Neurosci 4:1086-1092.
McLeod SJ, Shum AJ, Lee RL, Takei F, Gold MR (2004) The Rap GTPases regulate integrin-mediated adhesion, cell spreading, actin polymerization, and Pyk2 tyrosine phosphorylation in B lymphocytes. J Biol Chem 279:12009-12019.
Mukherji S, Soderling TR (1994) Regulation of Ca2+/calmodulin-dependent protein kinase II by inter- and intrasubunit-catalyzed autophosphorylations. J Biol Chem 269:13744-13747.
Mulkey RM, Malenka RC (1992) Mechanisms underlying induction of homosynaptic long-term depression in area CA1 of the hippocampus. Neuron 9:967-975.
Mulkey RM, Herron CE, Malenka RC (1993) An essential role for protein phosphatases in hippocampal long-term depression. Science 261:1051-1055.
Mulkey RM, Endo S, Shenolikar S, Malenka RC (1994) Involvement of a calcineurin/inhibitor-1 phosphatase cascade in hippocampal long-term depression. Nature 369:486-488.
Nakagawa T, Engler JA, Sheng M (2004) The dynamic turnover and functional roles of alpha-actinin in dendritic spines. Neuropharmacology 47:734-745.
Nakayama AY, Harms MB, Luo L (2000) Small GTPases Rac and Rho in the maintenance of dendritic spines and branches in hippocampal pyramidal neurons. J Neurosci 20:5329-5338.
Noguchi J, Matsuzaki M, Ellis-Davies GC, Kasai H (2005) Spine-neck geometry determines NMDA receptor-dependent Ca2+ signaling in dendrites. Neuron 46:609-622.
Ohba Y, Mochizuki N, Matsuo K, Yamashita S, Nakaya M, Hashimoto Y, Hamaguchi M, Kurata T, Nagashima K, Matsuda M (2000) Rap2 as a slowly responding molecular switch in the Rap1 signaling cascade. Mol Cell Biol 20:6074-6083.
Okamoto K, Nagai T, Miyawaki A, Hayashi Y (2004) Rapid and persistent modulation of actin dynamics regulates postsynaptic reorganization underlying bidirectional plasticity. Nat Neurosci 7:1104-1112.
Ostap EM (2002) 2,3-Butanedione monoxime (BDM) as a myosin inhibitor. J Muscle Res Cell Motil 23:305-308.
Otmakhov N, Griffith LC, Lisman JE (1997) Postsynaptic inhibitors of calcium/calmodulin-dependent protein kinase type II block induction but not maintenance of pairing-induced long-term potentiation. J Neurosci 17:5357-5365.
Otmakhov N, Tao-Cheng JH, Carpenter S, Asrican B, Dosemeci A, Reese TS, Lisman J (2004) Persistent accumulation of calcium/calmodulin-dependent protein kinase II in dendritic spines after induction of NMDA receptor-dependent chemical long-term potentiation. J Neurosci 24:9324-9331.
Pak DT, Sheng M (2003) Targeted protein degradation and synapse remodeling by an inducible protein kinase. Science 302:1368-1373.
Pak DT, Yang S, Rudolph-Correia S, Kim E, Sheng M (2001) Regulation of dendritic spine morphology by SPAR, a PSD-95-associated RapGAP. Neuron 31:289-303.

Palay SL, Palade GE (1955) The fine structure of neurons. J Biophys Biochem Cytol 1:69-88.
Pasternak C, Spudich JA, Elson EL (1989) Capping of surface receptors and concomitant cortical tension are generated by conventional myosin. Nature 341:549-551.
Peng J, Kim MJ, Cheng D, Duong DM, Gygi SP, Sheng M (2004) Semiquantitative proteomic analysis of rat forebrain postsynaptic density fractions by mass spectrometry. J Biol Chem 279:21003-21011.
Penzes P, Beeser A, Chernoff J, Schiller MR, Eipper BA, Mains RE, Huganir RL (2003) Rapid induction of dendritic spine morphogenesis by trans-synaptic ephrinB-EphB receptor activation of the Rho-GEF kalirin. Neuron 37:263-274.
Pettit DL, Perlman S, Malinow R (1994) Potentiated transmission and prevention of further LTP by increased CaMKII activity in postsynaptic hippocampal slice neurons. Science 266:1881-1885.
Pizon V, Chardin P, Lerosey I, Olofsson B, Tavitian A (1988) Human cDNAs rap1 and rap2 homologous to the Drosophila gene Dras3 encode proteins closely related to ras in the 'effector' region. Oncogene 3:201-204.
Regehr WG, Tank DW (1990) Postsynaptic NMDA receptor-mediated calcium accumulation in hippocampal CA1 pyramidal cell dendrites. Nature 345:807-810.
Schikorski T, Stevens CF (2001) Morphological correlates of functionally defined synaptic vesicle populations. Nat Neurosci 4:391-395.
Segal M (2005) Dendritic spines and long-term plasticity. Nat Rev Neurosci 6:277-284.
Sellers JR (2000) Myosins: a diverse superfamily. Biochim Biophys Acta 1496:3-22.
Sheng M, Lee SH (2001) AMPA receptor trafficking and the control of synaptic transmission. Cell 105:825-828.
Sheng M, Hoogenraad CC (2007) The postsynaptic architecture of excitatory synapses: a more quantitative view. Annu Rev Biochem 76:823-847.
Shi SH, Hayashi Y, Petralia RS, Zaman SH, Wenthold RJ, Svoboda K, Malinow R (1999) Rapid spine delivery and redistribution of AMPA receptors after synaptic NMDA receptor activation. Science 284:1811-1816.
Silva AJ, Stevens CF, Tonegawa S, Wang Y (1992) Deficient hippocampal long-term potentiation in alpha-calcium-calmodulin kinase II mutant mice. Science 257:201-206.
Simons M, Wang M, McBride OW, Kawamoto S, Yamakawa K, Gdula D, Adelstein RS, Weir L (1991) Human nonmuscle myosin heavy chains are encoded by two genes located on different chromosomes. Circ Res 69:530-539.
Staubli U, Lynch G (1990) Stable depression of potentiated synaptic responses in the hippocampus with 1-5 Hz stimulation. Brain Res 513:113-118.
Sudhof TC (2004) The synaptic vesicle cycle. Annu Rev Neurosci 27:509-547.
Sugiyama Y, Kawabata I, Sobue K, Okabe S (2005) Determination of absolute protein numbers in single synapses by a GFP-based calibration technique. Nat Methods 2:677-684.
Tada T, Sheng M (2006) Molecular mechanisms of dendritic spine morphogenesis. Curr Opin Neurobiol 16:95-101.
Tashiro A, Minden A, Yuste R (2000) Regulation of dendritic spine morphology by the rho family of small GTPases: antagonistic roles of Rac and Rho. Cereb Cortex 10:927-938.

Tolias KF, Bikoff JB, Burette A, Paradis S, Harrar D, Tavazoie S, Weinberg RJ, Greenberg ME (2005) The Rac1-GEF Tiam1 couples the NMDA receptor to the activity-dependent development of dendritic arbors and spines. Neuron 45:525-538.

Trachtenberg JT, Chen BE, Knott GW, Feng G, Sanes JR, Welker E, Svoboda K (2002) Long-term in vivo imaging of experience-dependent synaptic plasticity in adult cortex. Nature 420:788-794.

Tullio AN, Bridgman PC, Tresser NJ, Chan CC, Conti MA, Adelstein RS, Hara Y (2001) Structural abnormalities develop in the brain after ablation of the gene encoding nonmuscle myosin II-B heavy chain. J Comp Neurol 433:62-74.

Tullio AN, Accili D, Ferrans VJ, Yu ZX, Takeda K, Grinberg A, Westphal H, Preston YA, Adelstein RS (1997) Nonmuscle myosin II-B is required for normal development of the mouse heart. Proc Natl Acad Sci U S A 94:12407-12412.

Vazquez LE, Chen HJ, Sokolova I, Knuesel I, Kennedy MB (2004) SynGAP regulates spine formation. J Neurosci 24:8862-8872.

Walikonis RS, Jensen ON, Mann M, Provance DW, Jr., Mercer JA, Kennedy MB (2000) Identification of proteins in the postsynaptic density fraction by mass spectrometry. J Neurosci 20:4069-4080.

Watts FZ, Shiels G, Orr E (1987) The yeast MYO1 gene encoding a myosin-like protein required for cell division. Embo J 6:3499-3505.

Whitlock JR, Heynen AJ, Shuler MG, Bear MF (2006) Learning induces long-term potentiation in the hippocampus. Science 313:1093-1097.

Whittaker VP (1968) The storage of transmitters in the central nervous system. Biochem J 109:20P-21P.

Wylie SR, Chantler PD (2001) Separate but linked functions of conventional myosins modulate adhesion and neurite outgrowth. Nat Cell Biol 3:88-92.

Wylie SR, Wu PJ, Patel H, Chantler PD (1998) A conventional myosin motor drives neurite outgrowth. Proc Natl Acad Sci U S A 95:12967-12972.

Xie Z, Huganir RL, Penzes P (2005) Activity-dependent dendritic spine structural plasticity is regulated by small GTPase Rap1 and its target AF-6. Neuron 48:605-618.

Young PE, Richman AM, Ketchum AS, Kiehart DP (1993) Morphogenesis in Drosophila requires nonmuscle myosin heavy chain function. Genes Dev 7:29-41.

Zhang H, Webb DJ, Asmussen H, Niu S, Horwitz AF (2005) A GIT1/PIX/Rac/PAK signaling module regulates spine morphogenesis and synapse formation through MLC. J Neurosci 25:3379-3388.

Zhou Q, Homma KJ, Poo MM (2004) Shrinkage of dendritic spines associated with long-term depression of hippocampal synapses. Neuron 44:749-757.

Zhu JJ, Qin Y, Zhao M, Van Aelst L, Malinow R (2002) Ras and Rap control AMPA receptor trafficking during synaptic plasticity. Cell 110:443-455.

Zhu Y, Pak D, Qin Y, McCormack SG, Kim MJ, Baumgart JP, Velamoor V, Auberson YP, Osten P, van Aelst L, Sheng M, Zhu JJ (2005) Rap2-JNK removes synaptic AMPA receptors during depotentiation. Neuron 46:905-916.

Chapter Two

A critical role for myosin II in dendritic spine morphology and synaptic function

Jubin Ryu[1], Lidong Liu[2], Tak Pan Wong[2], Dong Chuan Wu[2], Alain Burette[3], Richard Weinberg[3], Yu Tian Wang[2], Morgan Sheng[1]*

[1]Picower Institute for Learning and Memory, RIKEN-MIT Neuroscience Research Center, Howard Hughes Medical Institute, Massachusetts Institute of Technology, Cambridge, MA 02139, [2]Brain Research Centre, University of British Columbia, 2211 Wesbrook Mall, Vancouver, BC V6T 2B5, Canada, [3]Department of Cell and Developmental Biology, University of North Carolina, CB #7090, Chapel Hill, North Carolina 27599

The majority of the work described in this chapter was performed by Jubin Ryu. Lidong Liu, Tak Pan Wong, and Dong Chuan Wu performed the electrophysiological studies. Alain Burette performed the myosin II immunohistochemistry in fixed brain sections.

Abstract

Dendritic spines show rapid motility and plastic morphology, which may mediate information storage in the brain. It is presently believed that polymerization/ depolymerization of actin is the primary determinant of spine motility and morphogenesis. Here, we show that myosin II, a molecular motor that binds and contracts actin filaments, is essential for normal spine morphology and dynamics and represents a distinct biophysical pathway to control spine size and shape. Myosin II is enriched in the post-synaptic density (PSD) of neurons. Pharmacologic or genetic inhibition of myosin II alters protrusive motility of spines, destabilizes their classical mushroom-head morphology, and impairs excitatory synaptic transmission. Thus the structure and function of spines is regulated by an actin-based motor in addition to the polymerization state of actin.

Introduction

Dendritic spines are small protrusions that serve as the main site of excitatory synapses in the mammalian brain (Harris and Kater, 1994; Hering and Sheng, 2001). Spines exist in a variety of shapes and sizes, making them attractive structural candidates for learning and memory (Yuste and Bonhoeffer, 2001). In support of this idea, long-term potentiation (LTP) has been associated with increased spinogenesis and spine head growth, whereas long-term depression (LTD) has been associated with spine shrinkage and retraction (Engert and Bonhoeffer, 1999; Maletic-Savatic et al., 1999; Matsuzaki et al., 2001; Nagerl et al., 2004; Zhou et al., 2004, Matsuzaki et al., 2004).

In addition to their morphological plasticity, spines also display rapid motility, changing shape and size over seconds to minutes in dissociated culture, slice, and *in vivo* contexts (Fischer et al., 1998; Dunaevsky et al., 1999; Lendvai et al., 2000). These changes include the appearance and disappearance of filopodia, "amorphous" fluctuations of the spine head, elongation of the spine neck, emergence of filopodia from the spine head, and transient "kissing" of spine heads. These phenomena are thought to be important in synaptogenesis as well as in modulation of extant synapses (Bonhoeffer and Yuste, 2002).

It is widely believed that both the heterogeneous morphology and rapid motility of dendritic spines are determined by the polymerization and depolymerization of actin (Fischer et al., 1998; Hering and Sheng, 2001; Bonhoeffer and Yuste, 2002; Star et al., 2002; Ackermann and Matus, 2003; Okamoto et al., 2004). In other cell biological contexts, however, actin dynamics are also regulated via a distinct and equally prominent mechanism: myosin motors. The myosin superfamily is characterized by the ability to

bind actin and hydrolyze ATP in order to translocate and maintain tension in actin filaments (Sellers 2000). Myosin II, a canonical member of this family, is a hexameric polypeptide comprised of two heavy chains and two pairs of regulatory light chains. In vertebrates, myosin II is typically divided into two classes: sarcomeric myosin II from skeletal muscle and nonmuscle myosin II. Nonmuscle myosin II, in turn, exists in two isoforms, A and B. While most tissues express equal amounts of both isoforms, neuronal tissue and embryonic cardiomyocytes express predominantly the B isoform (Kawamoto et al., 1991).

Nonmuscle myosin IIB (hereafter referred to as myosin IIB) is required for cytokinesis and maintenance of cortical tension in *Dictyostelium*, dorsal closure in *D. melanogaster*, maintenance of embryonic polarity in *C. elegans*, and neuronal migration and growth cone motility in mice (DeLozanne et al., 1987; Young et al., 1993; Guo et al., 1996; Tullio et al., 1997). Recent studies have revealed additional unexpected roles for myosin IIB in mitotic spindle assembly and in cell intercalation during development of the *Drosophila* embryo (Rosenblatt et al., 2004; Bertet et al., 2004).

Proteomic analyses have uncovered the abundant presence of the heavy chain of myosin IIB (MHCIIB) in the postsynaptic density (PSD) fraction of rat brain (Jordan et al., 2004; Peng et al., 2004). In this study, we provide evidence that postsynaptic myosin IIB represents a means of regulating spine dynamics that is mechanistically distinct from actin polymerization/depolymerization. We report the subcellular distribution of myosin IIB in neurons and elucidate the function of myosin IIB by pharmacological inhibition and molecular genetic suppression with RNA interference (RNAi). Our data indicate a

critical role for myosin II in the morphological integrity of dendritic spines, and in the maintenance of synaptic transmission.

Materials and Methods

Antibodies and Drugs

The following antibodies have been described previously: rabbit NR2A (Sheng et al., 1994) and monoclonal PSD95 (Hering et al., 2003). The following antibodies were purchased commercially: MHCIIB (Covance, Berkeley, CA); β-galactosidase (Promega, Madison, WI); GluR1 (Calbiochem, Darmstadt, Germany); Bassoon (StressGen, Sidney, Canada). Blebbistatin was purchased from Tocris (Ellisville, MO).

DNA Constructs

The following oligonucleotides (targeted to nts 4362-4380 of rat MHCIIB) were annealed and cloned into pSuper vector to make the RNAi construct against MHCIIB: 5'-gatccccgaagccaagaagaaactgcttcaagagagcagtttcttcttggcttctttttggaaa-3' and 5'-agctttccaaaaagaagccaagaagaaactgctctcttgaagcagtttcttcttggcttcggg-3'. mRFP was cloned into pGWI vector. DsRed2 expression plasmid was from Clontech.

Subcellular and PSD Fractionation

2 adult rat forebrains were fractionated as described (Huttner et al., 1983). Forebrains were homogenized and spun at 1400g, and the supernatant (S1) was set aside. The pellet (P1) was homogenized and spun at 710g. The supernatant was pooled with S1and spun at 13,800g. The supernatant (S2) was set aside. The pellet (P2) was layered onto a discontinuous sucrose gradient and spun at 82,500g. The synaptosomal fraction was isolated from the 1.0/1.2M sucrose interface and spun at 32,800g, and the pellet (PSDI)

was resuspended. PSDII and III were obtained by Triton and Sarcosyl extractions of the PSDI pellet, respectively. These pellets were spun down at 201,800g. S2 was also spun down at this stage to produce S3 and P3.

Neuronal Culture, Immunostaining, Drug Treatment and Transfection

Hippocampal neurons were dissected from E20 Sprague-Dawley rat embryos, plated onto coated glass coverslips (30 μg/mL PDL and 2.5 μg/mL laminin), and cultured in Neurobasal medium (Invitrogen) with B27 (Invitrogen), 0.5 mM glutamine, and 12.5 μM glutamate.

For MHCIIB, PSD95, and Bassoon staining, neurons were fixed in 100% methanol 10' at -20°C. Neurons in the blebbistatin trials were fixed in 4% PFA/4% sucrose at RT 10'. RNAi transfected neurons were fixed in 4% PFA/4% sucrose 3' at RT, followed by 10' in 100% methanol at -20°C. For AMPAR staining, neurons were incubated in GluR1 antibody (diluted in DMEM) at 37°C for 10' and fixed in 4% PFA/4% sucrose 8' at RT. Immunostaining was performed as previously described (Sala et al., 2001). Blebbistatin was administered to neurons by diluting 50 mM stock 1:500 into conditioned neuron media, for a final concentration of 100 μM. All transfections were done using calcium phosphate (Sala et al., 2001). For the blebbistatin trials, neurons were transfected with 4 μg β-gal/well. For RNAi experiments, each well of neurons was co-transfected with 2.5 μg of β-gal and 7.5 μg of pSuper or MHCIIB RNAi.

Microscopy and Quantitation

Fixed neurons were imaged with an LSM510 confocal microscope system (Zeiss, Oberkochen, Germany) and an Axioplan microscope (Zeiss). A 63x oil immersion lens (N.A. 1.40) was used. Except for neurons co-stained for PSD95 and MHCIIB, each image consisted of a z-stack projected into one image. Live imaging was performed using Multi-time software (Zeiss) with a Pascal confocal system (Zeiss) and an Axiovert microscope (Zeiss), using a 100x oil immersion lens and ~3.5x digital zoom. Cells were treated with 10 mM HEPES, pH 7.4 and imaged at 37°C/5% CO_2.

Morphometric measurements were performed using MetaMorph Software (Universal Imaging, West Chester, PA). For colocalization quantification, the PSD95 and MHCIIB channels were parsed into separate images. A threshold level for each channel was manually set in order to exclude diffuse background staining, leaving only the puncta visible; the same threshold level was used for each neuron. The two thresholded images – each in a different color – were overlaid upon each other and the percentage of puncta overlapping with each other was manually counted. 10 neurons were used for this analysis.

In the blebbistatin experiments, 10-15 neurons were imaged for each of the 4 conditions. For each neuron, 5 50-70 μm dendritic segments were chosen for spine morphometric analysis. Protrusions were defined as being >0.5 micron in length. Protrusion length was defined as the distance from the base to the tip of the protrusion; width was defined as the maximum distance perpendicular to the long axis of the protrusion. For each neuron, all the spine length, width, and density values were averaged into a single value; each cell was represented by one spine length, width, and density. The values for all neurons

within a condition were then used to calculate a mean and SEM. For the RNAi experiments, 10-15 neurons were imaged for pSuper and MHCIIB RNAi transfected neurons. The cell soma was manually traced using the immunofluorescence of the transfected marker βgal; a projection constructed from a stack of confocal images was used for each neuron. Once the tracing was finished, the average intensity of the traced area was quantified in the MHCIIB channel. Cell body immunofluorescence was quantified by comparing the average intensity of the transfected neuron's cell soma to the soma of an untransfected neighbor in the same visual field. Spine morphometric analysis in the RNAi experiments was performed in the same manner as in the blebbistatin experiments. For AMPAR-mediated EPSC experiments, 6-12 neurons were used for each condition. For mEPSC experiments, 5-7 neurons were used for each condition.

Electrophysiology

Hippocampal slices were prepared from 19-23 day old Sprague-Dawley rats. 400 μm coronal brain slices were cut using a vibrating blade microtome in ice-cold ACSF containing (mM) 126 NaCl, 2.5 KCl, 1 $MgCl_2$, 1 $CaCl_2$, 1.25 KH_2PO_4, 26 $NaHCO_3$ and 20 glucose that was bubbled with 95%O_2/5%CO_2. Slices were recovered at 34°C for 1.5 hr and maintained at RT. Slices were perfused at RT with carbogenated ACSF during recording. Whole-cell recordings of CA1 neurons were performed with a MultiClamp 700A amplifier (Axon Instruments, Foster City, CA) at holding potential –60 mV. The recording pipettes (6-8 MΣ) were filled with pH 7.2 solution containing (mM) 132.5 Cs-gluconate, 17.5 CsCl, 2 $MgCl_2$, 0.5 EGTA, 10 HEPES, 4 ATP, and 5 QX-314. Cells were excluded if >20% change in the series or input resistance occurred. EPSCs were evoked

every 20s by stimulating the Schaffer collateral-commissural pathway via a constant current pulse (0.05 ms) delivered in the presence of bicuculline methiodide (10 μM) in ACSF.

For mEPSCs, DIV12-14 cultured neurons were perfused with ECS containing (mM) 140 NaCl, 5.4 KCl, 1 $MgCl_2$, 1.3 $CaCl_2$, 25 HEPES and 30 glucose (pH7.35), in addition to bicuculline (10 μM) and tetrodotoxin (0.5 μM). Whole-cell patch-clamp recordings were performed at a holding membrane potential of -60 mV with an AXOPATCH-1D amplifier (Axon). Recordings were low-pass filtered at 2 kHz, sampled at 10 kHz, and stored as data files using Clampex 8.0 (Axon). Recordings where the series resistance varied more than 10% were rejected.

Results

Myosin II is enriched at synapses

To determine if myosin IIB is enriched in the PSD, we surveyed its abundance in subcellular fractions of rat forebrain by immunoblotting (Fig 1A). Myosin IIB was significantly enriched in PSD fractions relative to crude synaptosomal fraction (P2), albeit to a lesser degree than the NMDA receptor subunit NR2A, an established PSD "marker" protein (Fig 1A). Like NR2A, myosin IIB was also abundant in P2 and P3 (light membrane) fractions, suggesting partial association with membranes.

To investigate the subcellular distribution of myosin IIB at the morphological level, we performed immunocytochemistry on rat hippocampal neurons in dissociated culture. In immature neurons (DIV8), myosin IIB immunoreactivity was present throughout the neuron but was more concentrated in the cell body and proximal dendrites (Fig 1B). In addition, myosin IIB staining was more intense at dendritic branch points and at the tips of dendrites and axons.

In more mature neurons (DIV18), myosin IIB diminished in the soma and localized primarily to dendrites, where it accumulated in a punctate pattern on top of a less intense diffuse staining (Fig 1C). Greater than 90% of myosin IIB dendritic puncta colocalized with the PSD marker PSD-95, consistent with a clustering of myosin IIB at synaptic sites. In addition, in roughly half of these co-localizations, the myosin IIB puncta was larger in size and extended past the PSD-95 margin towards the dendritic shaft (Fig 1C). Therefore, the zone of myosin IIB enrichment may extend past the spine head into the neck of the spine.

Figure 1

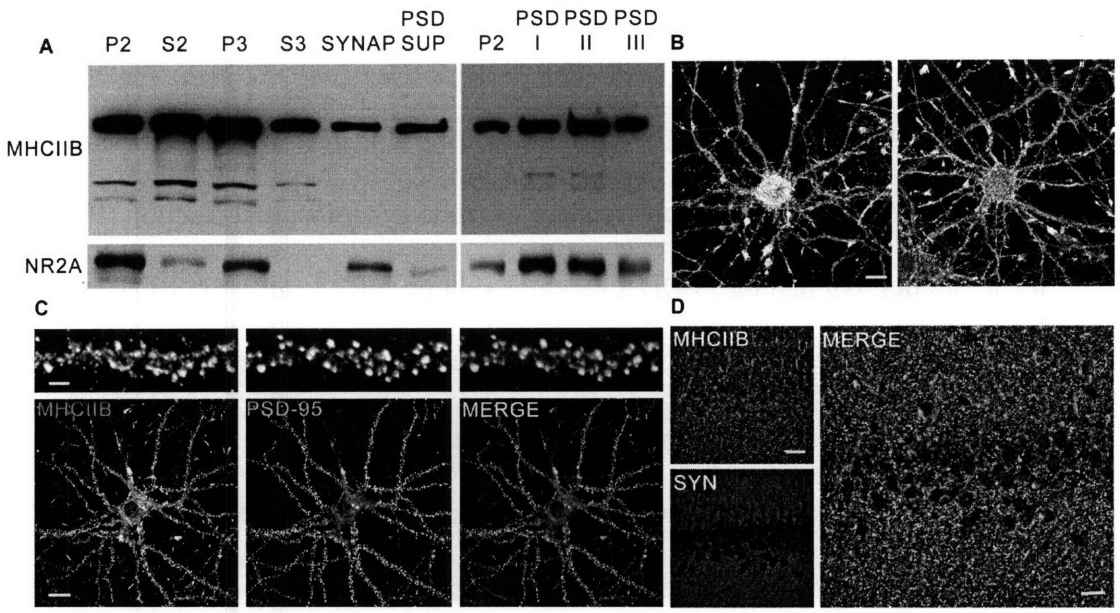
A
P2
S2
P3
S3
SYNAP
PSD SUP
P2
PSD I
PSD II
PSD III
MHCIIB
NR2A
B
C
MHCIIB
PSD-95
MERGE
D
MHCIIB
SYN
MERGE

Figure 1. Distribution of myosin IIB in neurons.

(A) Subcellular fractions from adult rat forebrain were immunoblotted for myosin heavy chain IIB (MHCIIB) or NMDA receptor NR2A subunit. 15 μg protein of P2, S2, P3, S3, total synaptosomes, and PSD sup were loaded. For MHCIIB immunoblot of PSD fractions (right), 5 μg of P2 and PSD I, II, and III were loaded. For the corresponding NR2A blot, 5 μg of P2 and 2 μg of PSD I, II, and III were loaded.

(B) Two examples of cultured dissociated rat hippocampal neurons (DIV8) immunostained for myosin IIB. Scale bar, 10 microns.

(C) DIV18 dissociated rat hippocampal neurons were double-labeled for myosin IIB (red) and PSD-95 (green). Individual channels shown in grayscale. Merge in color shows colocalization in yellow. Upper panels show high magnification views of dendrites. Scale bar, 10 microns (low magnification), 2 microns (high magnification image of dendrite).

(D) CA1 hippocampal sections from 90 day old rats were immunostained for myosin heavy chain IIB (green) and synaptophysin (red). Scale bars, 50 microns (single channels); 25 microns (merge).

To examine myosin IIB localization *in vivo*, we immunostained hippocampal sections from ~90 day old rats. Dense punctate labeling for myosin IIB filled the apical and basal dendritic fields of the CA1 region but was largely absent from the pyramidal cell soma (Fig 1D). The myosin IIB immunostaining showed extensive overlap with synaptophysin, a synaptic vesicle protein. Overall, the immunocytochemistry results are consistent with the biochemical fractionation data and support the idea that myosin IIB is enriched in but not exclusively localized to the postsynaptic compartment.

Blebbistatin induces loss of mushroom spines and formation of filopodia-like protrusions

What is the function of myosin II in neurons? To address this question, we utilized blebbistatin, a recently discovered small molecule inhibitor of myosin II (Straight et al., 2003; Kovacs et al., 2004; Limouze et al., 2004). Blebbistatin specifically inhibits the ATPase activity of myosin II, trapping it in an ADP-bound state that has low affinity for actin. At DIV17, control neurons treated for 30 min with nothing, DMSO, or the inactive (+) enantiomer of blebbistatin exhibited mostly mushroom-shaped spines (Fig 2A). Neurons treated with active blebbistatin (100 μM, 30 minutes) lost most of their mushroom-headed spines and instead displayed long, thin filopodia-like processes that lacked heads (Fig 2A). Accordingly, quantitative morphometry showed an increase in mean length and a reduction in mean width of dendritic protrusions (Fig 2B). The density of protrusions per length of dendrite was also increased by blebbistatin, relative to controls treated with nothing, DMSO or (+)blebbistatin (Fig 2B). In contrast to its effect on protrusion morphology, 100 μM blebbistatin did not alter cell soma circumference,

Figure 2

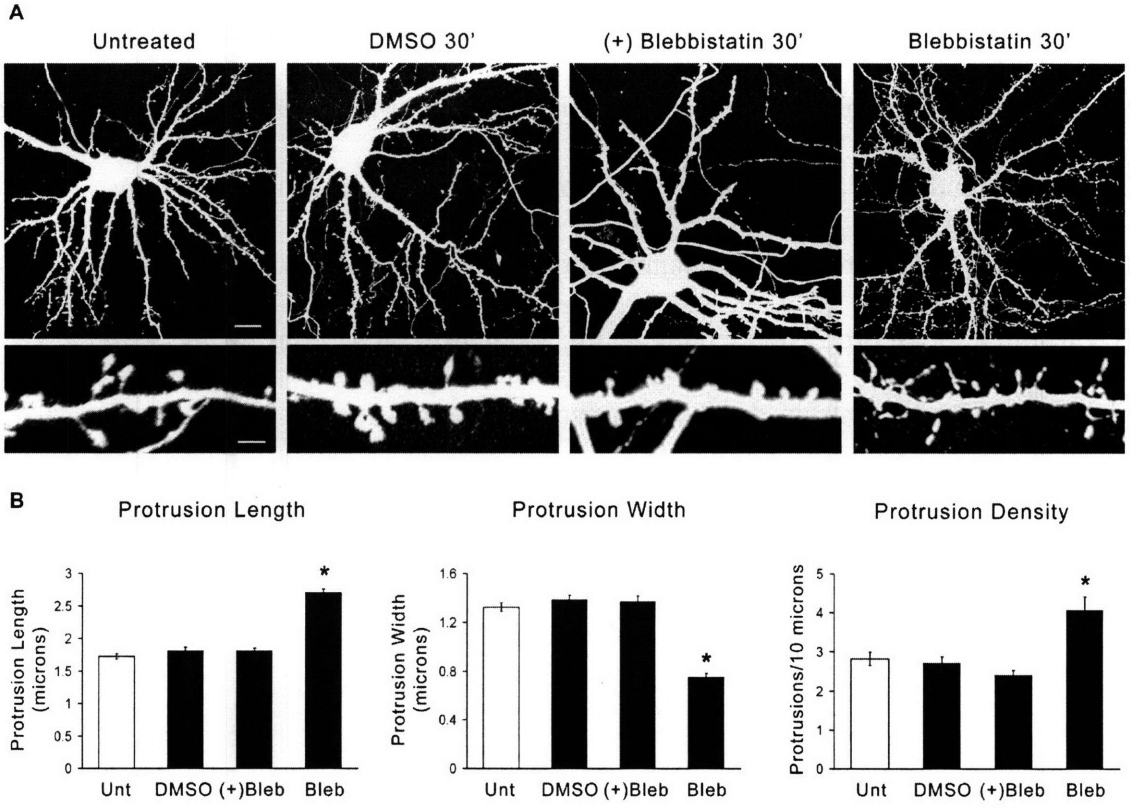
A
Untreated
DMSO 30'
(+) Blebbistatin 30'
Blebbistatin 30'
B
Protrusion Length
Protrusion Width
Protrusion Density
Protrusion Length (microns)
Protrusion Width (microns)
Protrusions/10 microns
Unt
DMSO
(+)Bleb
Bleb
*

Figure 2. Blebbistatin induces loss of mushroom spines and formation of filopodia-like protrusions.

(A) DIV10 rat hippocampal neurons were transfected with β-gal. Seven days later they were treated with nothing, DMSO, (+)blebbistatin (100 μM), or blebbistatin (100 μM) for 30 minutes, and fixed and immunostained for β-gal. Scale bar, 10 microns (low magnification); 2 microns (high magnification image of dendrite).

(B) Quantitation of protrusion length, width, and density in neurons treated with blebbistatin versus controls. *$p<0.001$ cf untreated neurons.

dendrite length, or dendrite width (data not shown). In summary, pharmacological inhibition suggests that myosin II function is required over the timeframe of minutes to maintain the proper morphology of mature spines.

RNAi knockdown of myosin II induces loss of mushroom spines and generation of filopodia-like protrusions

To confirm the veracity and specificity of the blebbistatin effect, we used a molecular genetic approach (RNAi) to suppress endogenous myosin IIB. Hippocampal neurons transfected at DIV14 for six days with a pSuper plasmid expressing small hairpin RNAs against rat myosin IIB showed loss of myosin IIB immunofluorescence (cell body intensity reduced to 30% of cell body intensity in neighboring untransfected cells; Fig 3A and B). There was little change in myosin IIB immunoreactivity in neurons transfected with empty pSuper vector.

Myosin IIB-RNAi resulted in a spine phenotype similar to that induced by 30 minute blebbistatin treatment – namely, a loss of mushroom-headed spines and a profusion of irregular filopodia-like protrusions (Fig 3A and B). Myosin IIB-RNAi caused an increase in mean length and a decrease in mean width of dendritic protrusions relative to control transfected neurons (Fig 3B). Unlike blebbistatin, however, RNAi-mediated inhibition of myosin IIB did not affect the density of protrusions significantly (Fig 3B). Myosin IIB RNAi did not alter cell soma circumference, dendrite length, or dendrite width (data not shown). The overall similarity of the pharmacological and RNAi findings supports a specific role for myosin IIB in the maintenance of mushroom-headed spines in cultured neurons.

Figure 3

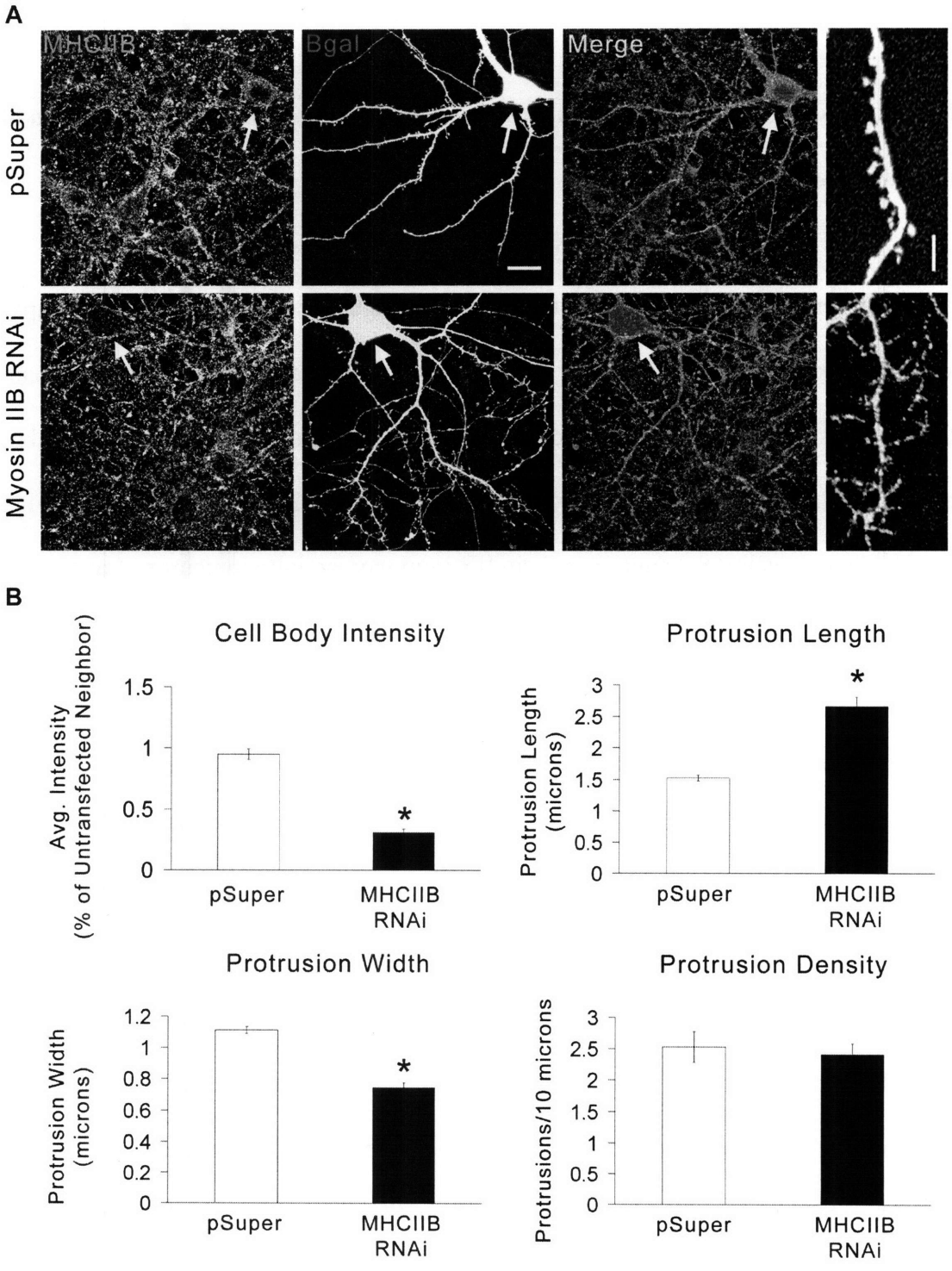
A
MHCIIB
Bgal
Merge
pSuper
Myosin IIB RNAi
B
Cell Body Intensity
Avg. Intensity
(% of Untransfected Neighbor)
1.5
1
0.5
0
*
pSuper
MHCIIB
RNAi
Protrusion Length
Protrusion Length
(microns)
3
2.5
2
1.5
1
0.5
0
*
pSuper
MHCIIB
RNAi
Protrusion Width
Protrusion Width
(microns)
1.2
1
0.8
0.6
0.4
0.2
0
*
pSuper
MHCIIB
RNAi
Protrusion Density
Protrusions/10 microns
3
2.5
2
1.5
1
0.5
0
pSuper
MHCIIB
RNAi

Figure 3. RNAi knockdown of myosin IIB induces loss of mushroom spines and generation of filopodia-like protrusions.

(A) DIV14 hippocampal neurons were transfected for 6 days with β-gal plus pSuper vector or myosin IIB-RNAi construct, as indicated, and stained for endogenous myosin IIB (green) and β-gal (red). Arrows indicate cell bodies of transfected cells. Rightmost panels show high magnification views of individual transfected dendrites. Scale bar, 10 microns (low magnification) and 2 microns (high magnification).

(B) Quantitation of myosin IIB immunofluorescence in the cell body, protrusion length, protrusion width, and protrusion density in transfected neurons. Myosin IIB staining intensity in the cell body was compared to untransfected neurons in the same field.

* $p<0.001$ cf pSuper transfected neurons.

Time lapse imaging reveals rapid changes in dendritic spine morphology and motility upon blebbistatin treatment

The above pharmacological and RNAi data imply that myosin IIB is required to maintain mushroom-headed spines while keeping filopodia in check, but this conclusion is based on examination of separate populations of fixed neurons. We therefore used time-lapse confocal imaging of live neurons to address the following question: Does blebbistatin inhibition of myosin II cause mushroom spines to directly transform into filopodia-like protrusions, or are mushroom spines lost and subsequently replaced by new filopodia?

Over a 70 min period (imaged once per minute), control spines treated with DMSO (added at the 11^{th} minute) showed dynamic movements, as previously described (Dailey and Smith, 1996; Dunaevsky et al., 1999; Bonhoeffer and Yuste, 2002). Two major forms of motility were observed (Figs 4A). First, most spines fluctuated in overall shape without any apparent directionality ("amorphous motility") (Fig 4A, arrows). Second, some spines repeatedly extended and retracted filopodia-like projections from their head ("protrusive" motility) (Fig 4A, arrowheads). Despite the constant flux of these two types of motility, there was a general maintenance of spine dimensions over a timeframe of tens of minutes. During amorphous motility, the overall size of the spine remained the same despite the rapid "morphing" of the head. Each filopodial extension was almost always followed by a retraction that reeled it back in. Thus, control spines appeared much the same at the end of 70 min as they did at the start (Figure 4A, bottom).

Blebbistatin caused marked changes in shape, size, and motility of dendritic spines. During the 10 minutes prior to drug application, spines displayed typical

Figure 4

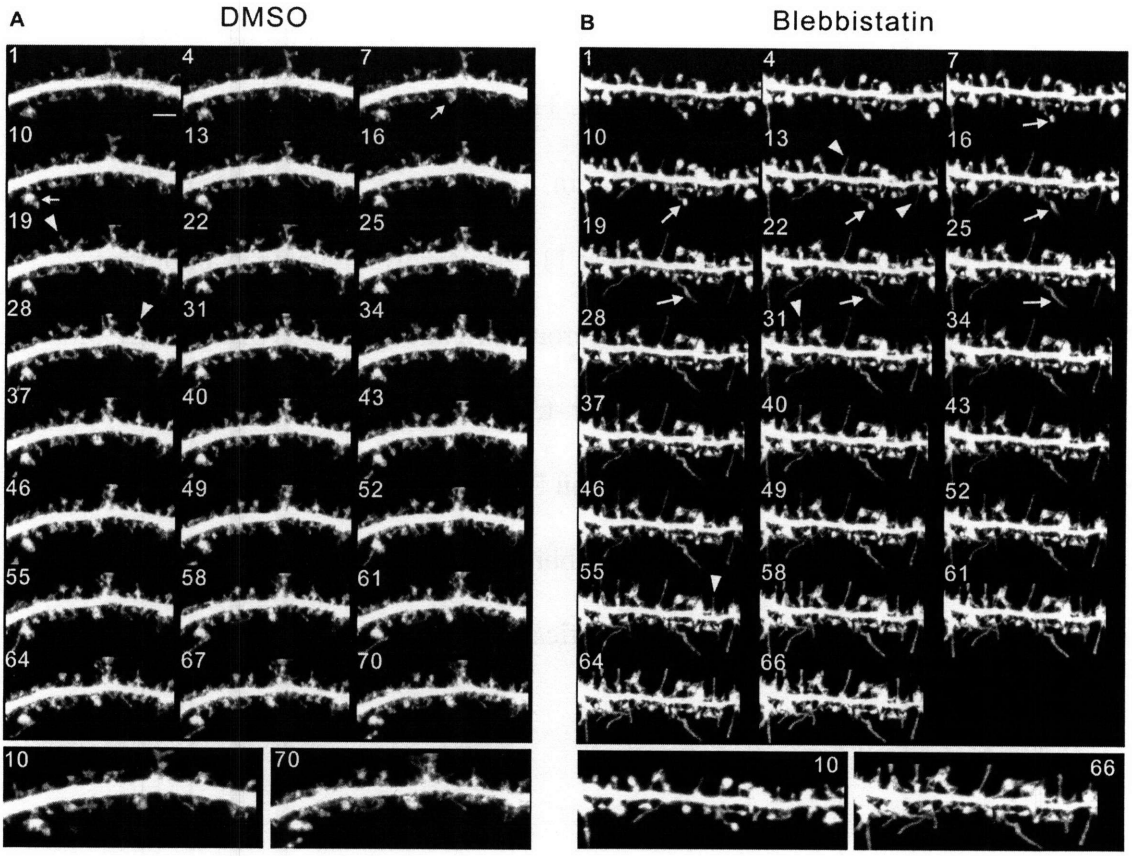
A
DMSO
B
Blebbistatin
1
4
7
10
13
16
19
22
25
28
31
34
37
40
43
46
49
52
55
58
61
64
67
70
66

Figure 4. Time-lapse imaging of blebbistatin effects on dendritic spines.

(A, B) DIV10 neurons were transfected with dsRed for 7 days and then imaged on DIV17. Images were captured every minute. Timestamp shows elapsed time in minutes (not all images are shown). In the first 10 min, neurons were left untreated. 100 μM blebbistatin (B) or DMSO (A) was added at 11 min. Arrows indicate examples of "amorphous" motility in DMSO-treated neurons (A), and examples of unfurling of dendritic spines into filopodia in blebbistatin-treated neurons (B). Arrowheads point to examples of filopodial extension/retraction in DMSO treated neurons (A), and to filopodial extension from spine heads in blebbistatin-treated neurons (B). Scale bar = 2 microns. Bottom panels show higher magnification views of early and late time-points (time stamp in min).

amorphous and protrusive motility and retained their overall mushroom-head morphologies (Fig 4B). Following blebbistatin (added at the 11th minute), spines adopted an altered protrusive motility. Rather than extend filopodial processes from their spine heads and then quickly retract them, blebbistatin-treated spines kept extending these projections without any retraction, resulting in long thin processes extending from the spine head (Fig 4B, arrowheads). Blebbistatin also caused a new behavior. Rather than "morphing" around a stable baseline size, many mushroom heads simply unfurled completely and transformed directly into a filopodium (Fig 4B, arrows). After 70 minutes of elapsed time, most of the original mushroom-shaped spines showed completely changed morphology, either with long filopodia-like protrusions extending from their heads or being transformed into a filopodium (Figure 4B, bottom). Time-lapse imaging revealed that filopodia arose directly from spines, rather than de novo.

Blebbistatin causes a decrease in AMPAR density

Given its role in the maintenance of dendritic spine morphology, myosin II might be important for the integrity of the synapse. We tested this by immunostaining for surface AMPA receptors in DIV17 dissociated hippocampal neurons after 30 minute treatment with 100 μM blebbistatin. Compared to control neurons treated with DMSO, blebbistatin-treated neurons showed a reduction in linear density of AMPAR puncta, and those puncta that remained were larger in size and irregularly shaped (Fig 5). Parallel immunostaining experiments showed no change in puncta density and size of the presynaptic marker Bassoon following blebbistatin treatment (30 min, 100 μM) (Fig 5).

These findings suggest that blebbistatin primarily affects synapse structure on the postsynaptic side.

Blebbistatin impairs excitatory synaptic transmission

To examine a potential role for myosin II in synaptic transmission, we tested the effects of blebbistatin on AMPA receptor-mediated EPSCs recorded from CA1 neurons in acute rat hippocampal slices in response to stimulation of Schaffer collateral inputs. In order to expose only postsynaptic cells to the drug, we applied blebbistatin (50 μM) to CA1 neurons intracellularly via the recording pipette. Starting ~10 min after "break-in," blebbistatin caused a progressive decrease in amplitude of EPSCs. Synaptic responses were depressed to ~60% of baseline after 60 minute exposure to the drug (Fig 6A and B). Control neurons exposed to normal intracellular solution, DMSO, or (+)blebbistatin in the recording pipette maintained their AMPA-EPSCs over the same timecourse (Fig 6A and B).

We also tested the effects of blebbistatin on mini-EPSC's in dissociated hippocampal neurons. Neurons filled intracellularly with 50 μM blebbistatin through the recording pipette displayed a 36% decrease in frequency and 27% decrease in amplitude of mini-EPSC's after 50 minutes (Fig 6C and D). Neurons treated with DMSO or (+)blebbistatin showed no change in frequency or amplitude of mini-EPSCs.

Figure 5

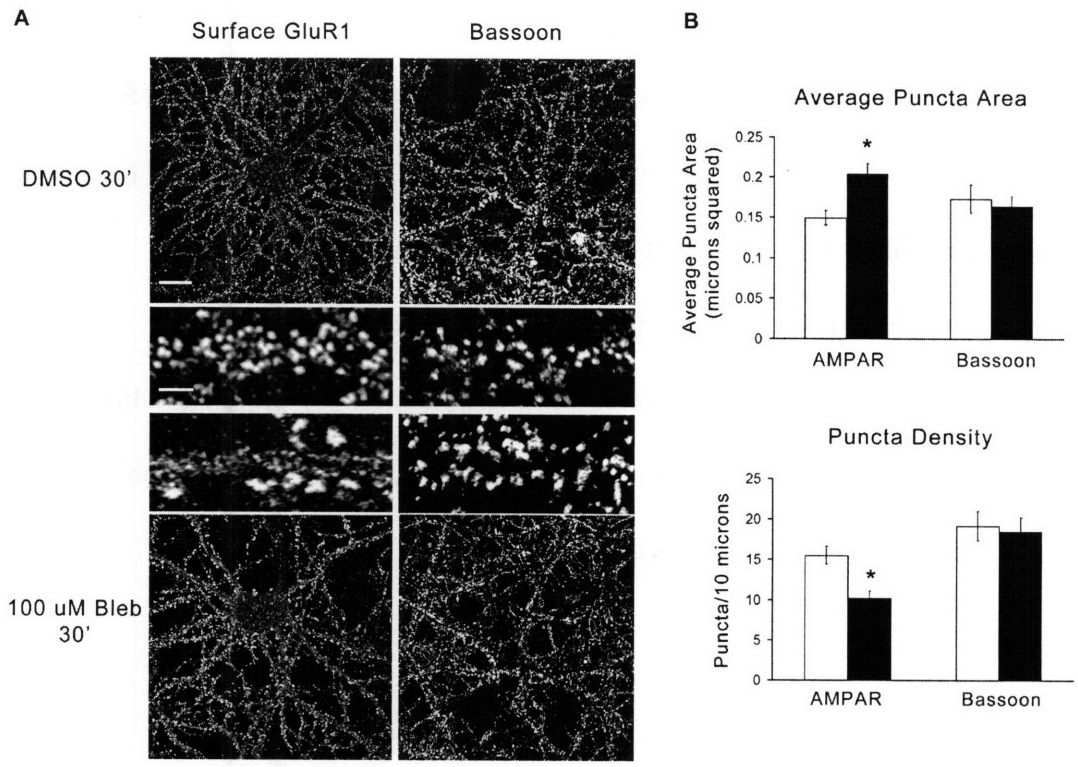
A
Surface GluR1
Bassoon
DMSO 30'
100 uM Bleb 30'
B
Average Puncta Area
Average Puncta Area (microns squared)
0.25
0.2
0.15
0.1
0.05
0
*
AMPAR
Bassoon
Puncta Density
Puncta/10 microns
25
20
15
10
5
0
*
AMPAR
Bassoon

Figure 5. Effects of blebbistatin on surface AMPA receptors and the pre-synaptic marker Bassoon.

(A) DIV17 hippocampal neurons were treated for 30 minutes with either DMSO or 100 μM blebbistatin, as indicated. They were then stained for surface GluR1 (left column) or the presynaptic marker Bassoon (right column). Scale bar, 10 microns (low magnification); 2 microns (high magnification image of dendrites).

(B) Quantitation of AMPAR and Bassoon mean puncta area (top graph) and linear puncta density (lower graph). White bars = DMSO-treated. Black bars = blebbistatin-treated. * $p<0.01$ cf DMSO-treated neurons.

Figure 6

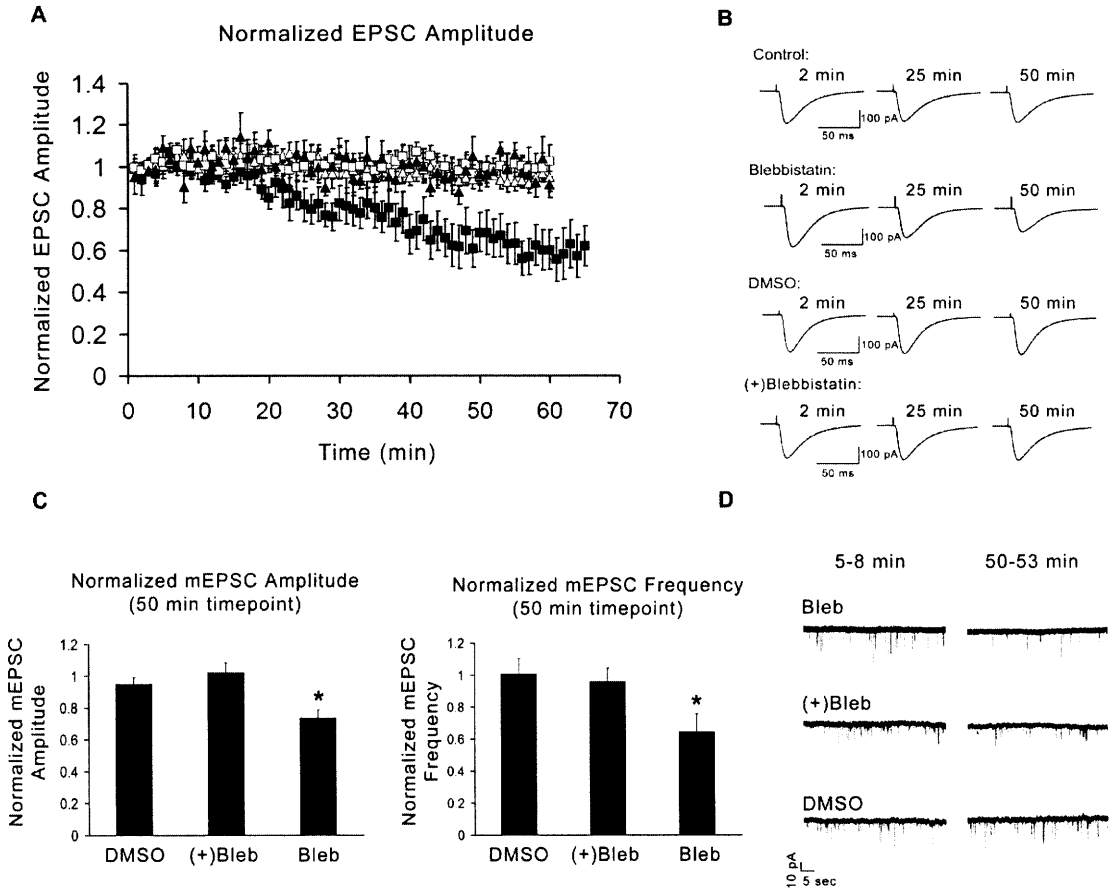
A
Normalized EPSC Amplitude
Normalized EPSC Amplitude
1.4
1.2
1
0.8
0.6
0.4
0.2
0
0
10
20
30
40
50
60
70
Time (min)
B
Control:
2 min
25 min
50 min
100 pA
50 ms
Blebbistatin:
2 min
25 min
50 min
100 pA
50 ms
DMSO:
2 min
25 min
50 min
100 pA
50 ms
(+)Blebbistatin:
2 min
25 min
50 min
100 pA
50 ms
C
Normalized mEPSC Amplitude
(50 min timepoint)
Normalized mEPSC Amplitude
1.2
1
0.8
0.6
0.4
0.2
0
*
DMSO
(+)Bleb
Bleb
Normalized mEPSC Frequency
(50 min timepoint)
Normalized mEPSC Frequency
1.2
1
0.8
0.6
0.4
0.2
0
*
DMSO
(+)Bleb
Bleb
D
5-8 min
50-53 min
Bleb
(+)Bleb
DMSO
10 pA
5 sec

Figure 6. Inhibition of excitatory synaptic transmission by blebbistatin.

(A) Blebbistatin (50 μM) was administered intracellularly via the recording pipette in CA1 pyramidal neurons of acute hippocampal slices, and AMPA receptor-mediated EPSC's were recorded following Schaffer collateral stimulation (filled squares). Control slices were recorded with normal intracellular solution (open triangles), 0.1% DMSO (open squares), or 50 μM (+)blebbistatin (filled triangles) in the pipette. EPSC amplitude was normalized to baseline.

(B) Representative EPSC traces from neurons treated with normal intracellular solution, DMSO, (+)blebbistatin, or active blebbistatin. Traces were averaged from 5 minutes of uninterrupted recording begun at indicated timepoints.

(C) Blebbistatin (50 μM) was administered intracellularly via the recording pipette into dissociated rat hippocampal neurons (DIV12-14), and mini-EPSC's were recorded over 50 minutes. Control neurons were filled with either DMSO or 50 μM (+)blebbistatin. Mean amplitude and frequency of mEPSCs recorded from 50-53 minutes after patching were normalized to mean mEPSC amplitude and frequency from 5-8 minutes. *$p<0.05$ cf 5 minute timepoint.

(D) Representative mEPSC recordings from dissociated hippocampal neurons filled intracellularly with DMSO, (+)blebbistatin and active blebbistatin. Recordings are from 5-8 minutes after patching, and from 50-53 minutes after patching.

Discussion

Spine morphology and motility are believed to be regulated primarily by dynamic polymerization and depolymerization of the actin cytoskeleton. In support of this, pharmacologic inhibition of actin polymerization with cytochalasin-D inhibits spine motility in both dissociated and slice cultures (Fischer et al., 1998; Dunaevsky et al., 1999). In addition, the F-actin/G-actin ratio and actin turnover in spines are regulated by activity (Star et al., 2002; Okamoto et al., 2004).

A role for actomyosin contraction in spine dynamics was initially excluded, based on pharmacological inhibition using 2,3 butanedione-monoxime (BDM); these experiments showed no effect on morphology or motility of spines after drug treatment (Fischer et al., 1998). BDM, however, was found in subsequent years to be a poor inhibitor for several reasons. First, it has only a low affinity for skeletal myosin II (K_I ~5 mM), and against nonmuscle myosin II, it has no detectable inhibitory activity (Cramer and Mitchison, 1995; Cheung et al., 2002). In addition, BDM nonspecifically affects other proteins in the cell, including myosin II light chain kinase, connexins, potassium channels, and L-type calcium channels (Ostap, 2002). In terms of affinity and specificity for nonmuscle myosin II, the recently discovered inhibitor blebbistatin appears to represent an improvement over BDM. Blebbistatin has a K_I of ~2 μM, and at 50 μM, inhibits both myosin IIA and IIB to ~10% of their maximal ATPase activity. In addition, blebbistatin does not inhibit myosins I, V, or X (Straight et al., 2003).

In light of recent mass spectrometry data showing an abundance of myosin heavy chain IIB in the PSD, we sought to re-examine a potential role for this molecular motor in spine dynamics (Jordan et al., 2004; Peng et al., 2004). The enrichment of myosin IIB in

the PSD fraction and its immunocytochemical localization at synapses is consistent with a role for this molecular motor in shaping the dendritic spine head. In addition to its favorable position at synaptic sites, loss of function experiments – both pharmacologic and genetic – showed that myosin II is in fact essential for spine morphology and normal motility. Both blebbistatin and myosin IIB-RNAi led to depletion of mushroom-type spines and their replacement with irregular filopodia-like processes. The action of blebbistatin is rapid, with time-lapse studies revealing profound alterations in spine morphology and motility occurring within tens of minutes of drug application. Blebbistatin-induced inhibition of myosin II also appears to have functional consequences, resulting in a depression of EPSC's and a decrease in both frequency and amplitude of mini-EPSC's; these effects are more likely secondary to the disruption of synaptic architecture rather than reflecting a direct role of myosin II in synaptic transmission.

Blebbistatin can inhibit both myosin IIA and B, and its neuronal effects could hypothetically be due to inhibition of either or both. We believe that inhibition of myosin IIB most likely underlies the observed phenotype because the IIB isoform is expressed at higher levels in neurons than IIA (Kawamoto et al., 1991; data not shown), and because RNAi of myosin IIB alone increases protrusion length and decreases protrusion width, similarly to blebbistatin. Nevertheless, it should be noted that our study does not rule out a role for myosin IIA in regulation of spine morphology.

In many other cellular contexts, myosin IIB serves to contract or maintain tension in actin filament networks. For example, this contractile function is required for cytokinesis as well as cortical tension in *Dictyostelium* (Knecht and Loomis, 1987;

Pasternak et al., 1989). In *Saccharomyces cerevisiae,* ablation of myosin II results in aberrant cell wall formation at the mother/bud neck, disrupting cell division (Watts et al., 1987). How do these well-conserved functions shed light on the dendritic spine phenotypes caused by myosin IIB loss of function? The volatile projection of filopodia from spine heads could be explained if myosin IIB is required to maintain the integrity of the mushroom surface by generating tangential forces at the spine head membrane. This "surface tension" could counteract the forces of polymerizing actin that act outwardly in a perpendicular direction to the membrane surface to extend filopodia. The unraveling of a mushroom into a filopodium, in turn, could be a more severe consequence of the loss of tangential surface tension in the bulbous spine head. Further studies need to be performed to precisely describe where and how myosin IIB is acting biophysically.

As a regulator of spine morphology and motility, myosin IIB possesses attractive properties. Its actin-binding activity is highly regulated, primarily by phosphorylation of the Ser19 residue on its regulatory light chain, and this light chain has been shown to bind directly to the C-termini of the NR1 and NR2 subunits of NMDA receptors (Suzuki et al., 1978; Amparan et al., 2005). The phosphorylation state of myosin light chain is controlled by signaling pathways that are prominent in neurons and in the PSD in particular. For example, myosin light chain kinase (MLCK), which phosphorylates and thereby activates myosin IIB, is stimulated by Ca^{2+}/calmodulin (Goeckeler and Wysolmerski, 1995). In addition, P21-associated kinase (PAK), and Rho-associated kinase (ROCK) have been shown to directly phosphorylate myosin IIB (Chew et al., 1998; Amano et al., 1998) and to regulate spine morphology (Hayashi et al., 2004).

ROCK is particularly compelling because it is a primary effector of RhoA, a small GTPase with profound consequences on neuronal and spine morphology. Constitutively active RhoA results in marked loss of dendritic spines when transfected into rat hippocampal slices (Nakayama et al., 2000), and this phenotype could perhaps be explained in part by a Rho-ROCK-myosin cascade, culminating in myosin contraction of actin filaments and retraction of spines. Such a model is admittedly simplistic, as Rho and ROCK can influence other proteins as well. In growth cones of retinal ganglion neurons, for example, ROCK regulates filopodial extension via ADF/cofilin rather than myosin IIB, suggesting that the reduction of spines caused by active RhoA could be mediated by inhibition of ADF/cofilin as well as through myosin IIB activation (Gehler et al., 2004).

In conclusion, our findings suggest that spine morphology and motility are not controlled solely by actin polymerization/depolymerization, but are also critically dependent on the molecular motor myosin II. Because it can reversibly bind and contract actin, and because it can be bidirectionally regulated, myosin II appears to be a novel and potent means of controlling the dynamic structure of dendritic spines.

Acknowledgements

We thank A. Straight and T. Mitchison for information and guidance about blebbistatin; J. Jaworski and H. Hering for help with live imaging.

References

Ackermann, M., and Matus, A. (2003). Activity-induced targeting of profilin and stabilization of dendritic spine morphology. Nat. Neurosci. 6, 1194-2000.

Amano, M., Chihara, K., Nakamura, N., Fukata, Y., Yano, T., Shibata, M., Ikebe, M., Kaibuchi, K. (1998). Myosin II activation promotes neurite retraction during the action of Rho and Rho-kinase. Genes Cells 3, 177–188.

Amparan, D., Avram, D., Thomas, C.G., Lindahl, M.G., Yang, J., Bajaj, G., Ishmael, J.E. (2005). Direct interaction of myosin regulatory light chain with the NMDA receptor. J Neurochem. 92, 349-61.

Bertet, C., Sulak, L., Lecuit, T. (2004). Myosin-dependent junction remodelling controls planar cell intercalation and axis elongation. Nature 429, 667-71.

Bonhoffer, T. and Yuste, R. (2002). Spine motility: phenomenology, mechanisms, and function. Neuron 35, 1019-1027.

Cheung, A., Dantzig, J.A., Hollingworth, S., Baylor, S.M., Goldman, Y.E., Mitchison, T.J. and Straight, AF. (2002). A small-molecule inhibitor of skeletal muscle myosin-II. Nature Cell Biol. 4, 83–88.

Chew, T.L., Masaracchia, R.A., Goeckeler, Z.M., Wysolmerski, R.B. (1998). Phosphorylation of non-muscle myosin II regulatory light chain by p21-activated kinase (gamma-PAK). J. Muscle Res. Cell Motil. 19, 839–854.

Cramer, L.P. and Mitchison, T.J. (1995). Myosin is involved in postmitotic cell spreading. J. Cell Biol. 131, 179–189.

Dailey, M.E., Smith, S.J. (1996). The dynamics of dendritic structure in developing hippocampal slices. J. Neurosci. 16, 2983-94.

De Lozanne, A., Spudich, J.A. (1987). Disruption of the Dictyostelium myosin heavy chain gene by homologous recombination. Science 236, 1086-1091.

Dunaevsky, A., Tashiro, A., Majewska, A., Mason, C.A., and Yuste, R. (1999). Developmental regulation of spine motility in mammalian CNS. Proc. Natl. Acad. Sci. USA *96,* 13438-13443.

Engert, F., and Bonhoeffer, T. (1999). Dendritic spine changes associated with hippocampal long-term synaptic plasticity. Nature 399, 66-70.

Fischer, M., Kaech, S., Knutti, D., Matus, A. (1998). Rapid actin-based plasticity in dendritic spines. Neuron. 20, 847-54.

Gehler, S., Shaw, A., Sarmier, P., Bamburg, J., Letourneau, P. (2004). Brain-Derived Neurotrophic Factor Regulation of Retinal Growth Cone Filopodial Dynamics is Mediated through Actin Depolymerizing Factor/Cofilin. J. Neurosci. 24, 10741-10749.

Globus, A. and Scheibel, A. (1967). The effect of visual deprivation on cortical neurons: a Golgi study. Exp. Neurol. 19, 331–45

Goeckeler, Z.M., Wysolmerski, R.B. (1995). Myosin light chain kinase regulated endothelial cell contraction—the relationship between isometric tension, actin polymerization and myosin phosphorylation. J. Cell Biol. 130, 613– 627.

Guo, S. and Kemphues, K.J. (1996). A non-muscle myosin required for embryonic polarity in Caenorhabditis elegans. Nature 382, 455-458.

Harris, K.M. and Kater, S.B. Dendritic spines: cellular specializations imparting both stability and flexibility to synaptic function. (1994). Annu. Rev. Neurosci. 17, 341-371.

Hayashi, M.L., Choi, S.Y., Rao, B.S., Jung, H.Y., Lee, H.K., Zhang, D., Chattarji, S., Kirkwood, A., Tonegawa, S. (2004). Altered cortical synaptic morphology and impaired memory consolidation in forebrain-specific dominant-negative PAK transgenic mice. Neuron. 43, 773-87.

Hering, H., Sheng, M. (2001). Dendritic spines: structure, dynamics and regulation. Nat. Rev. Neurosci. 2, 880-888.

Hering, H., Sheng, M. (2003). Activity-dependent redistribution and essential role of cortactin in dendritic spine morphogenesis. J. Neurosci. 23, 11759-69.

Huttner, W.B., Schiebler, W., Greengard, P. and De Camilli, P., (1983). Synapsin I (Protein I), a nerve terminal-specific phosphoprotein. III. Its association with synaptic vesicles studied in a highly purified synaptic vesicle preparation. J. Cell Biol. 96, 1374–1388.

Jordan, B.A., Fernholz, B.D., Boussac, M., Xu, C., Grigorean, G., Ziff, E.B., Neubert, T.A. (2004). Identification and verification of novel rodent postsynaptic density proteins. Mol. Cell. Proteomics 3, 857-71.

Kawamoto, S., Adelstein, R.S. (1991). Chicken nonmuscle myosin heavy chains: differential expression of two mRNAs and evidence for two different polypeptides. J. Cell Biol. 112, 915-24.

Knecht, D.A. and Loomis, W.F. (1987). Antisense RNA inactivation of myosin heavy chain gene expression in Dictyostelium discoideum. Science 236, 1081-6.

Kovacs, M., Toth, J., Hetenyi, C., Malnasi-Csizmadia, A., Sellers, J.R. (2004). Mechanism of blebbistatin inhibition of myosin II. J. Biol Chem. 279, 35557-63.

Lendvai, B., Stern, E.,Chen, B., and Svoboda, K. (2000). Experience-dependent plasticity of dendritic spines in the developiong rat barrel cortex in vivo. Nature 404, 876-881.

Limouze, J., Straight, A.F., Mitchison, T., Sellers, J.R. (2004). Specificity of blebbistatin, an inhibitor of myosin II. J. Muscle Res. Cell Motil. 25, 337-41.

Maletic-Savatic, M., Malinow, R., and Svoboda, K. (1999). Rapid dendritic morphogenesis in CA1 hippocampal dendrites induced by synaptic activity. Science 283, 123-127.

Matsuzaki, M., Ellis-Davies, G.C., Nemoto, T., Miyashita, Y., Iino, M., Kasai, H. (2001). Dendritic spine geometry is critical for AMPA receptor expression in hippocampal CA1 pyramidal neurons. Nat. Neurosci. 4, 1086-92.

Matsuzaki, M., Honkura, N., Ellis-Davies, G.C., Kasai, H. (2004). Structural basis of long-term potentiation in single dendritic spines. Nature 429, 761-6.

Nagerl, U.V., Eberhorn, N., Cambridge, S., Bonhoeffer, T. (2004). Bidirectional activity-dependent morphological plasticity in hippocampal neurons. Neuron 44, 759-767.

Nakayama, A.Y., Harms, M.B., and Luo, L. (2000). Small GTPases Rac and Rho in the maintenance of dendritic spines and branches in hippocampal pyramidal neurons. J. Neurosci. 20, 5329–38.

Okamoto, K., Nagai, T., Miyawaki, A., Hayashi, Y. (2004). Rapid and persistent modulation of actin dynamics regulates postsynaptic reorganization underlying bidirectional plasticity. Nat Neurosci. 7, 1104-12.

Ostap, E.M. (2002). 2,3-Butanedione monoxime (BDM) as a myosin inhibitor. J. Muscle Res. Cell Motil. 23, 305-8.

Pasternak, C., Spudich, J.A., Elson, E.L. (1989). Capping of surface receptors and concomitant cortical tension are generated by conventional myosin. Nature 341, 549-51.

Peng, J., Kim, M.J., Cheng, D., Duong, D.M., Gygi, S.P., Sheng, M. (2004). Semiquantitative proteomic analysis of rat forebrain postsynaptic density fractions by mass spectrometry. J. Biol. Chem. 279, 21003-11.

Rosenblatt, J., Cramer, L.P., Baum, B., McGee, K.M. (2004). Myosin II-dependent cortical movement is required for centrosome separation and positioning during mitotic spindle assembly. Cell 117, 361-72.

Sala, C., Piech, V., Wilson, N.R., Passafaro, M., Liu, G., Sheng, M. (2001). Regulation of dendritic spine morphology and synaptic function by Shank and Homer. Neuron 31, 115-30.

Sellers, J.R. (2000). Myosins: a diverse superfamily. Biochim. Biophys. Acta. 1496, 3-22.

Star, E.N., Kwiatkowski, D.J., Murthy, V.N. (2002). Rapid turnover of actin in dendritic spines and its regulation by activity. Nat. Neurosci. 5, 239-46.

Straight, A.F., Cheung, A., Limouze, J., Chen, I., Westwood, N.J., Sellers, J.R., Mitchison, T.J. (2003). Dissecting temporal and spatial control of cytokinesis with a myosin II Inhibitor. Science 299, 1743-7.

Suzuki, H., Onishi, K., Takahashi, K., Watanable, S. (1978). Structure and function of chicken gizzard myosin. J. Biochem. (Tokyo) 84, 1529 –1542.

Tullio, A.N., Accili, D., Ferrans, V.J., Yu, Z.X., Takeda, K., Grinberg, A., Westphal, H., Preston, Y.A., Adelstein, R.S. (1997). Nonmuscle myosin II-B is required for normal development of the mouse heart. Proc. Natl. Acad. Sci. USA 94, 12407-12412.

Watts, F.Z., Shiels, G., Orr, E. (1987). The yeast MYO1 gene encoding a myosin-like protein required for cell division. EMBO J. 6, 3499-505.

Young, P.E., Richman, A.M., Ketchum, A.S., Keihart, D.P. (1993). Morphogenesis in Drosophila requires nonmuscle myosin heavy chain function. Genes Dev. 7, 29-41.

Yuste, R. and Bonhoeffer, T. (2001). Morphological changes in dendritic spines associated with long-term synaptic plasticity. Annu. Rev. Neurosci. 24, 1071-89.

Zhou, Q., Homma, K., Poo, M.M. (2004). Shrinkage of dendritic spines associated with long-term depression of hippocampal synapses. Neuron 44, 749-757.

Chapter Three

Constitutively active Rap2 transgenic mice display fewer dendritic spines, reduced ERK signaling, and impaired spatial learning and fear extinction

Jubin Ryu[1], Kensuke Futai[1], Monica Feliu[1], Richard Weinberg[2], Morgan Sheng[1]

[1]The Picower Institute for Learning and Memory, RIKEN-MIT Neuroscience Research Center, Howard Hughes Medical Institute, Massachusetts Institute of Technology, Cambridge, MA 02139 [2]Department of Cell and Developmental Biology, University of North Carolina, CB #7090, Chapel Hill, North Carolina 27599

The majority of work described in this chapter was performed by Jubin Ryu. Kensuke Futai performed the electrophysiological studies. Monica Feliu assisted with the behavior and biochemistry experiments. Richard Weinberg performed the EM studies.

Abstract

Within the Ras superfamily of GTPases, Rap1 and Rap2 are the closest homologs to Ras. In non-neural cells, Rap signaling can antagonize Ras signaling. In neurons, Rap also seems to oppose Ras in terms of synaptic function. While Ras is critical for long term potentiation (LTP), Rap1 has been shown to be required for long term depression (LTD), and Rap2 has been implicated in depotentiation. Moreover, active Rap1 and Rap2 cause loss of surface AMPA receptors and reduced mEPSC amplitude and frequency in cultured neurons. The role of Rap signaling in vivo, however, remains poorly understood. To study Rap2's function in the brain and in behavior, we created transgenic mice expressing either constitutively active (Rap2V12) or dominant negative (Rap2N17) mutants of Rap2 in postnatal forebrain. Multiple lines of Rap2N17 founder mice showed only weak expression of the transgenic protein, and no phenotype was observed. Rap2V12 mice displayed fewer and shorter dendritic spines in CA1 hippocampal neurons and reduced levels of active (phospho-) ERK. These morphological and biochemical changes were associated with altered behavior: hyperactivity, impaired spatial learning, and defective extinction of contextual fear. Finally, Rap2V12 mice displayed reduced ERK signaling at specific timepoints during fear extinction training. Together, these data indicate that Rap2 can oppose Ras-ERK signaling and inhibit dendritic spine development/maintenance in the brain. Our findings also implicate Rap2 signaling in fear extinction mechanisms, which are thought to be aberrant in psychiatric illnesses such as anxiety disorders and post-traumatic stress disorder (PTSD).

Introduction

Multiple lines of evidence support a prominent role for Ras-MAPK signaling in regulation of synaptic structure and function. Ras and its associated GTPase activating proteins (GAPs) and guanine nucleotide exchange factors (GEFs) are present in the postsynaptic density (PSD) of excitatory synapses (Husi et al., 2000; Peng et al., 2004; Sheng and Hoogenraad, 2007). ERK activation is necessary for formation of dendritic spines following depolarization (Wu et al., 2001). Both Ras and ERK are necessary for LTP, and activated Ras is sufficient to induce synaptic strengthening (English and Sweatt, 1996, 1997; Zhu et al., 2002). ERK function is also necessary for several kinds of learning, including spatial learning, fear conditioning, and fear extinction (Atkins et al., 1998; Blum et al., 1999; Fischer et al., 2007).

Other members of the Ras family have also been identified at synapses, but their synaptic functions are less well understood (Husi et al., 2000; Jordan et al., 2004; Peng et al., 2004; Kim et al., 2005). Among these proteins are the Rap GTPases, Rap1 and Rap2. Rap1 and Rap2 share 50% identity with Ras, making them the closest relatives to Ras (Pizon et al., 1988). Moreover, Rap1 and Ras possess identical effector domains, while Rap2's effector domain differs by only one amino acid. Thus Rap GTPases might stimulate the same effectors as Ras, or they might antagonize Ras by competing for common effectors. Consistent with the latter idea, Rap1 was first identified in a screen for suppressors of Ras transforming activity, and Rap2 inhibits Ras-dependent activation of the transcription factor Elk-1 (Kitayama et al., 1989; Ohba et al., 2000).

In neurons, recent data suggest that Rap1 and Rap2 may negatively regulate synaptic strength, thereby opposing Ras action. Constitutively active Rap1 and Rap2

induce loss of surface AMPA receptors, and Rap2 additionally causes shortening of dendrites and axons and loss of synapses (Fu et al., 2007). Spine Associated RapGAP (SPAR) inhibits Rap and enhances spine growth and synaptic strength (Pak et al., 2001; Pak and Sheng, 2003). In hippocampal slices, dominant negative Rap1 blocks long term depression (LTD), while dominant negative Rap2 inhibits depotentiation, the weakening of potentiated synapses (Zhu et al., 2002; Zhu et al., 2005). Therefore, multiple layers of evidence indicate that Rap1 and Rap2 are involved in mechanisms that suppress synaptic strength and synapse growth. Less consistent with this model is a report that transgenic mice expressing dominant negative Rap1 exhibit reduced pERK levels, suggesting that Rap1 can activate neuronal ERK in certain contexts (Morozov et al., 2003).

To date there has been no study of the in vivo function of Rap2 in the nervous system. To address whether Rap2 functions to inhibit synaptic development or transmission *in vivo*, and to determine the behavioral correlates of Rap2 dysfunction, we constructed transgenic mice expressing dominant negative (Rap2N17) or constitutively active (Rap2V12) mutants of Rap2 in postnatal forebrain. We present evidence of reduced ERK signaling and fewer spines in Rap2V12 mice, consistent with an inhibitory role for Rap2 at synapses. These biochemical and morphological abnormalities were associated with spatial learning deficits and impairment of fear extinction, a process that is thought to underlie psychiatric disorders such as posttraumatic stress disorder (PTSD) and anxiety disorders (Fischer et al., 2007; Myers and Davis, 2007).

Materials and Methods

Generation of Rap2V12 and Rap2N17 Transgenic Mice

SV40 intron/polyA sequence from pMSG (Pharmacia) was cloned to the 3' end of pGW1-HA-Rap2V12 or pGW1-HA-Rap2N17 (gifts from D. Pak, Georgetown University). HA-Rap2V12-SV40/polyA or HA-Rap2N17-SV40/polyA were then cloned into pNN19 vector containing the αCaMKII promoter (gift from S. Tonegawa, MIT). This final construct was cut with SalI, releasing a fragment containing αCaMKII promoter, HA-tagged Rap2V12 or Rap2N17, and SV40/polyA. This fragment was purified and microinjected into pronuclei of C57BL/6 zygotes to generate transgenic founders. For genotyping, PCR was performed on tail samples using a primer pair unique to the transgenic construct. All wildtype and transgenic mice in this study are from C57BL/6 background and were bred and maintained under IACUC-approved conditions.

Biochemistry and Antibodies

For expression analysis, cortex, hippocampus, cerebellum and brainstem were dissected from brains of 2 month old littermates and homogenized in buffered sucrose (0.32 M sucrose, 6 mM Tris (pH 8), 1 mM $MgCl_2$, 0.5 mM $CaCl_2$, and protease inhibitors). Homogenates were spun 10 min at 800 x g, and the resulting supernatant was spun 10 min at 10,200 x g. The pellet (P2) was resuspended and 20 μg of protein/lane was loaded for SDS-PAGE. HEK293 cells were transfected with either Rap2V12 or Rap2N17 transgene constructs using Lipofectamine (Invitrogen), and extracts were harvested 48 hours later. For subfractionation analyses, individual forebrains from 2

month old mice were homogenized in buffered sucrose and subjected to differential centrifugation, as previously described (Huttner et al., 1983). 20 μg of protein/lane was loaded for SDS-PAGE.

For phopho-ERK immunoblot analysis during fear extinction, mice were decapitated 1 hour after the indicated training session, and brains were snap-frozen in liquid nitrogen. 1 mm thick coronal sections were cut from frozen brain, and amygdala and hippocampus were dissected from the appropriate section and homogenized in buffered sucrose (0.32 M sucrose, 6 mM Tris (pH 8), 1 mM $MgCl_2$, 0.5 mM $CaCl_2$, 1 mM Na_3VO_4, and protease inhibitors). 20 μg of protein/lane was loaded for SDS-PAGE.

Levels of GTP-bound Rap2 and Rap1 were measured using EZ-Detect Rap Activation Kit (Pierce). Individual forebrains from 2 month old mice were homogenized in lysis buffer (25 mM Tris (pH 7.5), 150 mM NaCl, 5 mM $MgCl_2$, 0.5 mM $CaCl_2$, 1% NP-40, 1 mM DTT, 5% glycerol, and protease inhibitors). The pulldowns were performed according to manufacturer instructions.

Antibodies used in this study include those against Rap1 (Santa Cruz), Rap2 (Santa Cruz), HA (Santa Cruz), tubulin (Sigma), pERK (Cell Signaling), ERK (Cell Signaling), pJNK (Cell Signaling), JNK (Cell Signaling), and phosphorylated MAPK substrates (gift from D. Edbauer, MIT).

Immunohistochemistry

2-month old mice were transcardially perfused with 4% PFA, and brains were removed and fixed in 4% PFA overnight at 4°C. 50 μm sagittal or coronal sections were cut with vibratome, blocked for 1 hour at RT (5% normal horse serum, 0.2% Triton in 1x

PBS), and incubated with either anti-HA or anti-Rap2 primary antibody (diluted in blocking buffer) O/N at 4°C. Sections were then washed in 1x PBS and incubated in Alexa488 conjugated secondary antibody (Invitrogen) for 1 hr at RT. Stained sections were visualized using epifluorescence microscopy at 4x magnification.

Cresyl Violet Staining and DiI Labeling

Brains were fixed in 4% PFA by transcardial perfusion. For cresyl violet, 50 μm sections were cut using vibratome, mounted, and stained. For DiI labeling, 200 μm sections were cut and labeled "diolistically," as previously described (Gan et al., 2000; Hung et al., 2008). 1.7 μm tungsten beads (Bio-Rad) were coated with 1,1'-dioctadecyl-3,3,3',3'-tetramethylindocarbocyanine perchlorate crystals (DiI; Molecular Probes) and shot into fixed sections with a Helios gene gun (BioRad) through a 3 μm pore membrane (Nunc). Sections were postfixed in 4% PFA at RT overnight and mounted.

DiI labeled neurons were imaged using a LSM510 confocal microscope system (Zeiss, Oberkochen, Germany) and an Axioplan microscope (Zeiss), using a 100x oil immersion lens. Each image consisted of a *z*-stack of pictures taken at an interval of 0.5-0.8 μm. Three 50-70 μm segments from CA1 secondary apical dendrites were examined for spine morphological analysis. Metamorph software was used to measure spine length, width and density. Spine length was defined as the distance from the base to the tip of the spine; width was defined as the maximum distance perpendicular to the long axis of the spine. All imaging and quantification were performed blind to genotype.

Electron Microscopy

Mice were anesthetized with avertin (0.5 mg/gm, i.p.) and perfused through the heart with heparinized saline followed by 100 ml of 2% paraformaldehyde/2% glutaraldehyde in phosphate buffer (PB, 0.1 M, pH 7.4). Brains were postfixed for 2 hours in the same fixative and sectioned on a Vibratome at 50 μm. CA1 hippocampus was dissected, and prepared for electron microscopy according to two protocols. For standard procedure, sections were treated for 1 hr at RT in 1% osmium tetroxide in PB, rinsed in maleate buffer pH 6.0, incubated 1 hr in 1% uranyl acetate, dehydrated in graded alcohols, infiltrated and flat-embedded in Epon-Spurr plastic. A second procedure was also used, designed to optimize contrasting of the postsynaptic density; this involved treating in 1% tannic acid in maleate buffer 1 hr, then 1% $CaCl_2$ 30 min. Sections were incubated 1 hr in uranyl acetate; subsequent processing was as described. Chips from stratum radiatum were cut and glued to plastic blocks; 70-80 nm thin sections were cut on an ultramicrotome. collected on 300 mesh copper grids, post-stained with uranyl acetate and Sato's lead. Random images including well-defined synapses were collected at x15,000 on a Philips Tecnai microscope operating at 80 KV; blinded data were analyzed as previously described (Hung et al., 2008).

Electrophysiology

Transverse hippocampal slices (400 μm thickness) were prepared from 3- to 5-week old mice in ice-cold dissection buffer (in mM: 238 sucrose, 2.5 KCl, 1 $CaCl_2$, 5 $MgCl_2$, 26 $NaHCO_3$, 1 NaH_2PO_4, 11 glucose, gassed with 5% CO_2/95% O_2, pH 7.4). Slices were incubated in an interface incubation chamber containing extracellular

artificial cerebrospinal fluid (aCSF; in mM: 119 NaCl, 2.5 KCl, 2.5 $CaCl_2$, 1.3 $MgCl_2$, 26 $NaHCO_3$, 1 NaH_2PO_4, 11 glucose, gassed with 5% CO_2/95% O_2, pH 7.4) for 60 min at 30°C, and maintained at room temperature (24-26°C) at least 2 hours. Slices were then transferred to a submerged recording chamber, and continuously perfused with aCSF. The recording pipettes (1.5-2 MΩ, 3 M NaCl) for field recording were placed in the stratum radiatum. The tungsten bipolar electrode (FHC) was placed in the stratum radiatum and the Schaffer collateral/commissural fibers were stimulated at 0.1 Hz. For LTP or LTD experiments, the stimulus strength was adjusted to evoke an EPSP of slope value between 0.11 and 0.15 mV/ms or 0.13 and 0.17 mV/ms, respectively. All experiments were performed at 28°C, using a temperature controller (TC-324B, Warner Instrument Corporation). Results are reported as mean ± S.E.M. Statistical significance was evaluated by Student-t test. Statistical significance was set at $p<0.05$. All experiments and the analysis of data were performed in a blind manner. Recordings were performed using a MultiClamp 700B amplifier and Digidata 1320B, and the signal was filtered at 1kHz, digitized at 10 kHz, and data was acquired and analyzed using Clampex 9.2 and Clampfit 9.2 (Axon Instruments).

Behavioral analysis

For all behavioral assays, only male littermates between 2-5 months of age were used. Experiments and analyses were performed blind to genotype. Open field test and rotarod were performed as previously described (Crawley, 2007).

Fear conditioning and extinction

Mice were trained in a standard fear conditioning apparatus (Med Associates Inc.). On day 0, they were allowed to explore for 3 min before the onset of a 30s white noise tone (conditioned stimulus [CS]) that coterminated with a 1s, 0.75 mA footshock (unconditioned stimulus [US]). After an additional minute, a second CS-US pair was delivered, and the mice remained in the box for 30s longer before being removed. 24h after training, contextual fear memory was tested by exposing the mice to the original training chamber for 3 minutes. Cued memory was tested 48h post-training by placing the mice in a new context with a different smell, floor, and walls. Mice were allowed to explore for 2 minutes before the onset of a 3 minute white noise tone.

For fear extinction assays, the training protocol remained the same as before. Every 24h after training, mice were exposed to either the same context (contextual fear extinction) or to a novel context with tone (cued fear extinction). Separate cohorts of mice were used for the contextual and cued fear extinction assays.

The percentage of time spent freezing was used as an index of fear and was measured automatically using Video Freeze software (Med Associates Inc), with freezing thresholds set by an observer blind to the genotype.

Morris Water Maze

Mice were trained in the water maze 4 times per day over a period of 14 consecutive days. The intertrial interval for each mouse was ~30 minutes. Each trial ended either when the mouse found the platform or after 60 s had elapsed. A minute-long probe trial in which the platform was removed was conducted on day 15. The swimming traces were digitized and analyzed using HVS Image 2020 Plus Tracking software (HVS Image).

Results

Generation of transgenic mice expressing constitutively active or dominant negative Rap2 in postnatal forebrain

To examine the role of Rap2 *in vivo*, we generated transgenic mice expressing either dominant negative (Rap2N17) or constitutively active Rap2 (Rap2V12). These transgenes were driven by the αCaMKII promoter, which expresses in forebrain from postnatal stages to adult (Figure 1A) (Lerosey et al., 1991; Tsien et al., 1996). The Rap2N17 mutant (Ser to Asn substitution at position 17) has reduced affinity for GTP and should sequester GEFs that normally activate Rap2. The Rap2V12 mutant (Gly to Val substitution at position 12) hydrolyzes GTP more slowly than wildtype and therefore spends more time in the active state. SV40 intron/polyadenylation (polyA) sequence was added at the 3' end, and a hemagglutinin (HA) tag was fused to the N-terminus of each transgene.

At least 10 founder lines were created for both Rap2N17 and Rap2V12 transgenes. Expression in these founder lines was assayed by Western blotting and immunohistochemistry on brains from 2-month old mice. On immunoblots using either HA or Rap2 antibody, Rap2V12 mice showed expression of the transgenic protein in cortex and hippocampus, but not in cerebellum and brainstem (Figure 1B). The transgenic protein (Figure 1B, arrow) was expressed at roughly 4-5-fold higher levels than endogenous Rap2 (arrowhead). The mobility of the Rap2V12 protein from transgenic brain was slightly retarded compared to the endogenous Rap2, but it comigrated with HA-Rap2V12 heterologously expressed in HEK293 cells (Figure 1B). Rap2N17 founder mice showed only weak expression of the transgene in hippocampus

Figure 1

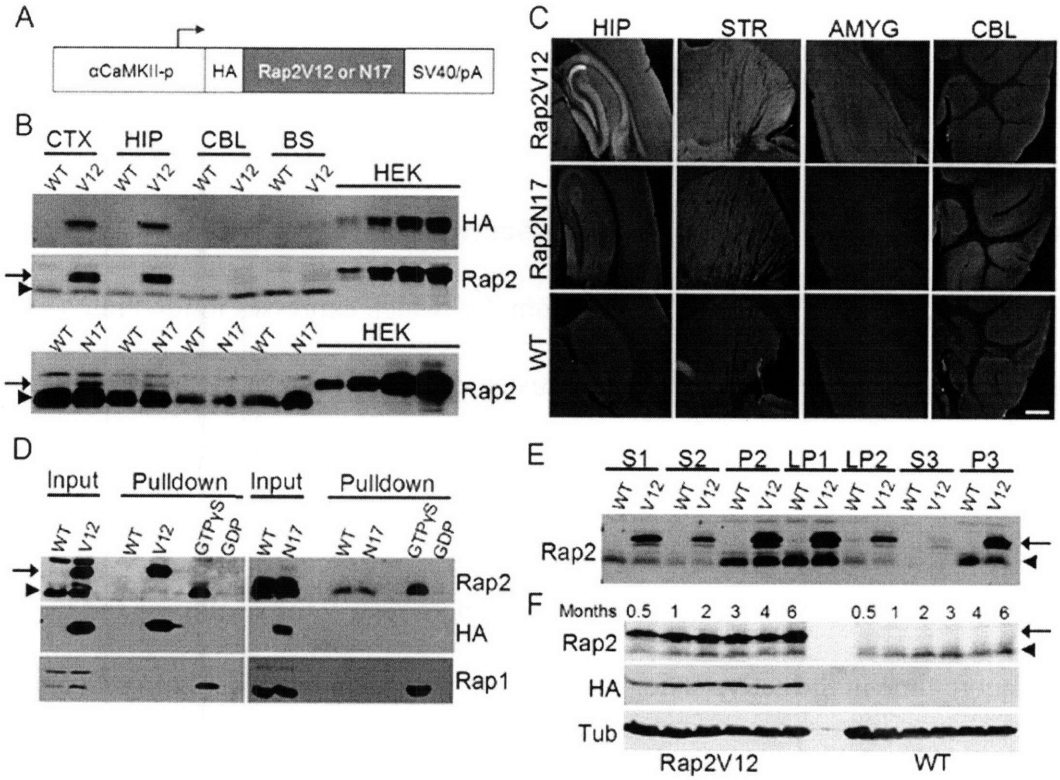
A
αCaMKII-p
HA
Rap2V12 or N17
SV40/pA
B
CTX
HIP
CBL
BS
HEK
WT
V12
N17
HA
Rap2
C
HIP
STR
AMYG
CBL
Rap2V12
Rap2N17
WT
D
Input
Pulldown
GTPγS
GDP
Rap2
HA
Rap1
E
S1
S2
P2
LP1
LP2
S3
P3
Rap2
F
Months
0.5
1
2
3
4
6
Rap2
HA
Tub
Rap2V12
WT

Figure 1. Generation and Characterization of Forebrain Specific Constitutively Active and Dominant Negative Rap2 Transgenic Mice

(A) Schematic of Rap2V12 and Rap2N17 transgene constructs. αCaMKII promoter was used to drive expression. HA, hemagglutinin epitope tag. SV40 intronic sequence and a polyA tail were added to the 3' end of the transgene.

(B) Brain regions from 2-month old Rap2V12, Rap2N17, and wildtype littermate mice were immunoblotted with HA or Rap2 antibodies. Last 4 lanes, extracts from HEK293T cells expressing HA-Rap2V12 or HA-Rap2N17 were titrated and run alongside the brain extracts. Arrows indicate transgenic Rap2 protein; arrowheads indicate endogenous Rap2. CTX, cortex; HIP, hippocampus; CBL, cerebellum; BS, brain stem.

(C) Immunohistochemistry of brain sections from 2-month old Rap2V12, Rap2N17, and wildtype littermate mice using antibody against HA. Hip, hippocampus; Str, striatum; Amyg, amygdala; Cer, cerebellum. Scale bar, 500 μm.

(D) Rap2 activity assay. Forebrains from 2-month old Rap2V12, Rap2N17, or wildtype littermate mice were solubilized and incubated with GST-RalGDS RBD. As positive control, WT lysate was pre-incubated with non-hydrolyzable GTPγS. As negative control, WT lysate was pre-incubated with GDP. Proteins precipitated by GST-RalGDS RBD were immunoblotted for Rap2, HA, and Rap1. Arrows, transgenic Rap2 protein; arrowheads, endogenous Rap2.

(E) Biochemical fractionation of endogenous and transgenic Rap2V12. Forebrains from 2-month old Rap2V12 mice were fractionated by differential centrifugation, and immunoblotted with Rap2 antibody. 20 μg protein loaded for each fraction.

(F) Developmental expression of Rap2V12 transgenic protein. Forebrain extracts from 0.5, 1, 2, 3, 4, and 6 month old mice were immunoblotted using HA, Rap2, and tubulin antibodies.

and cortex by immunoblotting (transgenic protein level <10% of endogenous Rap2) (Figure 1B).

Immunohistochemistry using HA antibody confirmed that Rap2V12 was robustly expressed throughout the forebrain – including hippocampus, cortex, striatum, and amygdala – but not in the cerebellum (Figure 1C). Staining was concentrated in synapse-rich neuropil areas; cell bodies were largely spared of immunoreactivity. We noted particularly intense staining along the hippocampal mossy fiber pathway. A similar Rap2V12 staining pattern was observed by Rap2 antibodies (data not shown). Consistent with its low expression by immunoblotting, Rap2N17 transgenic protein could not be detected above background by immunohistochemistry using either HA or Rap2 antibodies (Figure 1C).

To measure levels of active Rap2 in transgenic brains, we performed a pulldown assay with the Ras binding domain (RBD) of Ral-GDS, which binds specifically to the active (GTP-bound) form of Ras, Rap1, and Rap2 (Hofer et al., 1994; Kikuchi et al., 1994; Urano et al., 1996; Nancy et al., 1999). Immunoblot analysis of precipitated Rap2 from the Ral-GDS pulldown assay showed that forebrain lysates from Rap2V12 mice contained elevated levels of active Rap2 compared to wildtype animals, all of which migrated at the size of the transgenic protein (Figure 1D, arrow). Activated endogenous Rap2 was weakly detected in brain extracts from Rap2V12 or wildtype animals, but could be massively increased by addition of GTPγS to the wildtype lysate (Figure 1D).

Ral-GDS pulldown did not precipitate the transgenic Rap2N17 protein from Rap2N17 lysates, which is not unexpected given that this mutant is inactive (Figure 1D).

However, Rap2N17 mice also did not show any significant decrease in levels of active endogenous Rap2. This negative result could be due to inadequate expression of the dominant negative Rap2N17, or an already very low basal level of active endogenous Rap2. In Rap2N17 as well as Rap2V12 lines, we could not detect basally active endogenous Rap1 in forebrain lysates with the Ral-GDS pulldown assay; however, the presence of Rap1 could be revealed by addition of GTPγS (Figure 1D). Because we could not obtain a Rap2N17 line that expressed the transgene highly and exhibited decreased Rap2 activity, we focused on Rap2V12 transgenic mice in subsequent experiments (in some experiments Rap2N17 mice were used as negative controls).

We further characterized the subcellular distribution of Rap2V12 by immunoblotting biochemical fractions of forebrain extracts. Both the transgenic Rap2V12 and the endogenous Rap2 were enriched in P2 (crude synaptosomes), LP1 (synaptosomal membranes), and P3 (light membrane) fractions (Figure 1E). Rap2V12 and endogenous Rap2 were barely detectable in cytosolic (S3) fractions of the brain. Thus both endogenous Rap2 and overexpressed Rap2V12 appear to be mostly membrane-associated.

We also examined expression of transgenic Rap2V12 protein during postnatal development by immunoblotting of cerebral cortex and hippocampus from mice of different ages (Figure 1F). As expected with the CaMKIIα promoter, transgenic protein expression increased between 0.5 and 1 month and remained relatively constant thereafter. Endogenous Rap2 protein expression showed a similar developmental profile (Figure 1F).

Rap2V12 mice have shorter and fewer dendritic spines in hippocampus

We began phenotyping our Rap2V12 and Rap2N17 mice by examining brain anatomy and spine morphology. By cresyl violet staining, we observed no gross abnormalities in the brain anatomy of 2-month old transgenic mice – cell density, hippocampal size, thickness and laminar organization of cortex, and white matter tracts all appeared normal in Rap2V12 and Rap2N17 mice (Figure 2A). To examine spine morphology, we labeled CA1 pyramidal neurons using the diOlistic method, in which dye coated particles are shot into cells by biolistics (Gan et al., 2000). For quantification, we measured dendritic spines from secondary apical dendrites. Rap2V12 mice showed modest but significant decreases in mean spine length and spine density but no change in mean width of spine heads (Figure 2B and 2C; length, $p<0.01$, unpaired t-test; density, $p<0.01$, unpaired t-test). Neurons from Rap2N17 mice showed no changes in mean spine length, width or density compared to wildtype controls (Figure 2B and 2C). All morphometric analysis was performed blind to the genotype. Our findings are consistent with active Rap2 being a negative regulator of spine morphogenesis *in vivo*.

We also analyzed thin-section electron microscopic (EM) micrographs from 2 month old Rap2V12 and Rap2N17 mice. In the stratum radiatum, PSDs from Rap2V12 or Rap2N17 mice showed no detectable differences from WT in terms of length or thickness of the PSD (Figure 3A and 3B).

Figure 2

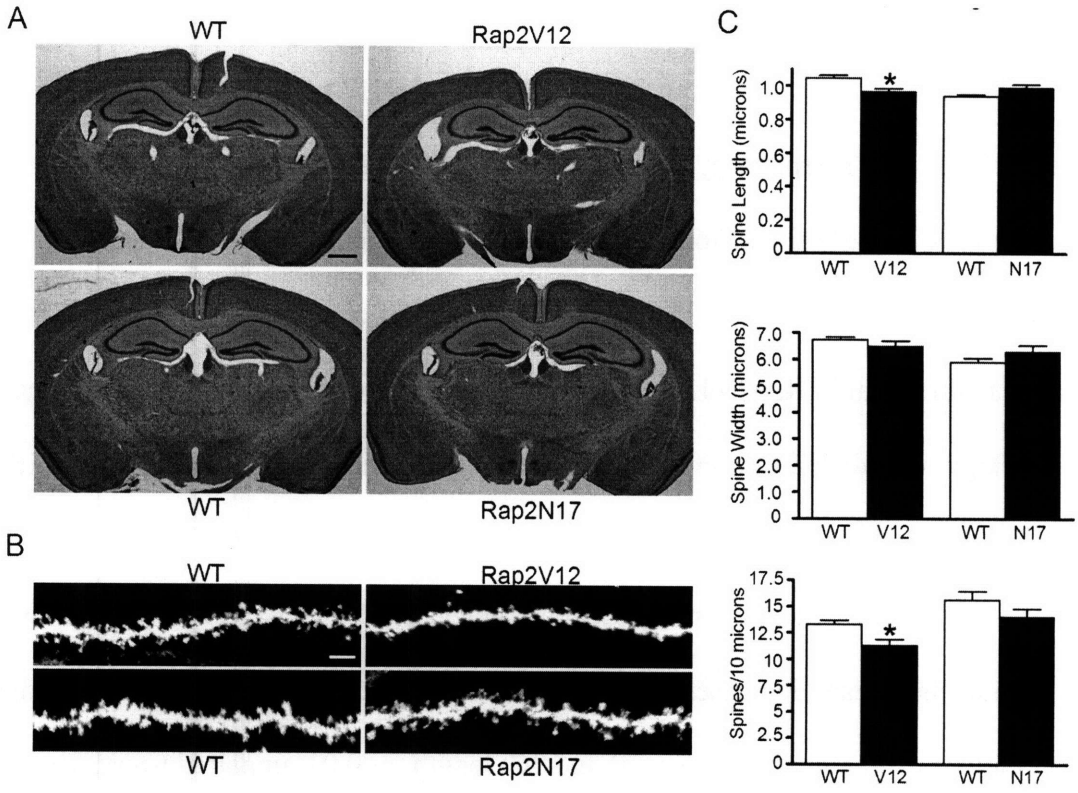
A
WT
Rap2V12
WT
Rap2N17
B
WT
Rap2V12
WT
Rap2N17
C
Spine Length (microns)
1.0
0.8
0.6
0.4
0.2
0
*
WT V12 WT N17
Spine Width (microns)
7.0
6.0
5.0
4.0
3.0
2.0
1.0
0
WT V12 WT N17
Spines/10 microns
17.5
15
12.5
10
7.5
5
2.5
0
*
WT V12 WT N17

Figure 2. Brain anatomy and spine morphology in Rap2V12 transgenic mice.

(A) Coronal sections from 2-month old Rap2V12, Rap2N17, and wildtype littermate mice stained with Cresyl violet. Scale bar, 1 mm.

(B) Spine morphology of CA1 hippocampal neuron apical dendrites in Rap2V12, Rap2N17, and wildtype littermate mice (age 2 months), visualized by DiI staining. Scale bar, 5 μm.

(C) Quantification of CA1 spine length, width, and density in Rap2V12 and Rap2N17 transgenic mice versus wildtype littermates. *$p<0.05$, unpaired t-test.

Figure 3

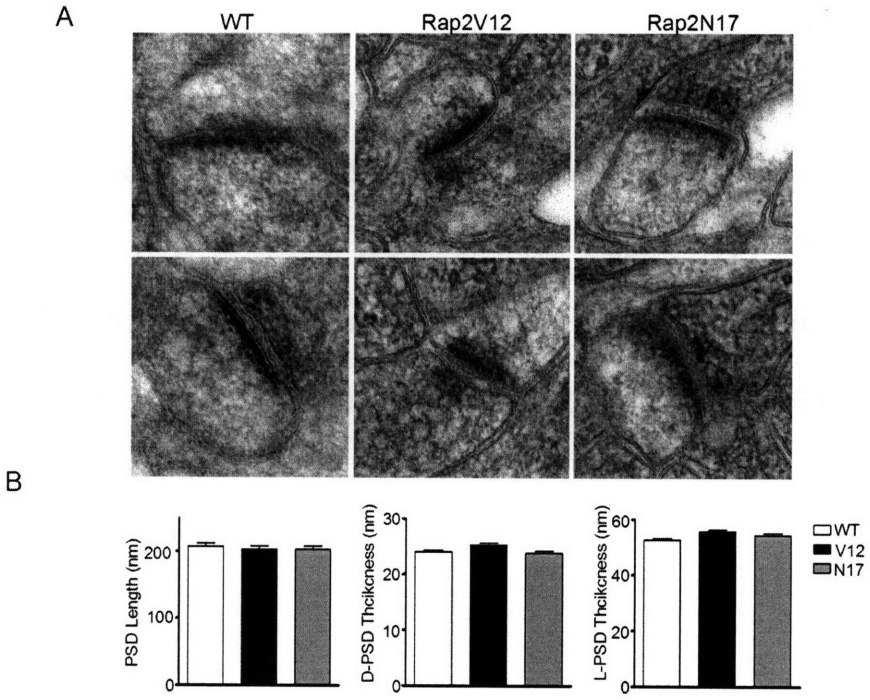
A
WT
Rap2V12
Rap2N17
B
PSD Length (nm)
0
100
200
D-PSD Thickness (nm)
0
10
20
30
L-PSD Thickness (nm)
0
20
40
60
WT
V12
N17

Figure 3. EM analysis of synapses from Rap2V12 and Rap2N17 transgenic mice.

(A) Representative electron micographs of asymmetric synapses in hippocampal CA1 stratum radiatum from Rap2V12, Rap2N17, and WT mice.

(B) Quantification of PSD length and thickness. D-PSD, dense layer of the PSD adjacent to the postsynaptic membrane. L-PSD, light layer of the PSD cytoplasmic to the postsynaptic membrane.

Rap2V12 mice show reduced ERK signaling

In certain contexts, both Rap1 and Rap2 have been shown to inhibit Ras-mediated ERK signaling (Kitayama et al., 1989; Kitayama et al., 1990a, b; Ohba et al., 2000). Rap2 can also activate another MAP kinase, c-Jun N-terminal kinase (JNK), and this Rap2-JNK signaling pathway may be involved in synaptic depotentiation (Machida et al., 2004; Zhu et al., 2005). How does Rap2V12 overexpression affect ERK and JNK activity in transgenic neurons? To measure these signaling pathways, we immunoblotted forebrain fractions from 2-month old mice for activated phosphorylated ERK (pERK) and JNK (pJNK). Two isoforms of ERK, ERK1 and ERK2 (also known as p44 and p42 MAPK, respectively), are known to be activated downstream of Ras (Boulton et al., 1990; Boulton et al., 1991). We quantified pERK1 and pERK2 levels separately, and found that pERK2 (p42) was specifically reduced in LP1 (synaptosomal membrane-enriched) and LP2 (synaptic vesicle-enriched) fractions from Rap2V12 mice (Figure 4A and 4B; p42 LP1 fraction, $p<0.05$, unpaired t-test; p42 LP2 fraction, $p<0.05$, unpaired t-test). In contrast, levels of pERK1 and pJNK did not differ between Rap2V12 and WT brain in all fractions tested (Figure 4A-D).

To test further whether MAPK signaling is dysregulated in Rap2V12 mice, we immunoblotted subcellular fractions with a phospho-antibody raised against a MAP kinase phospho-motif peptide library (biased for P-x-S/T-P sequences) that recognizes a large set of phosphorylated MAPK substrates (Figure 5A) (Edbauer et al., unpublished data). This MAPK phosphomotif antibody also showed reduced intensity by immunoblotting in a subset of bands in the P2 and LP1 fractions of Rap2V12 mice, corroborating that MAPK signaling is partially inhibited in these fractions (Figure 5A-C).

Figure 4

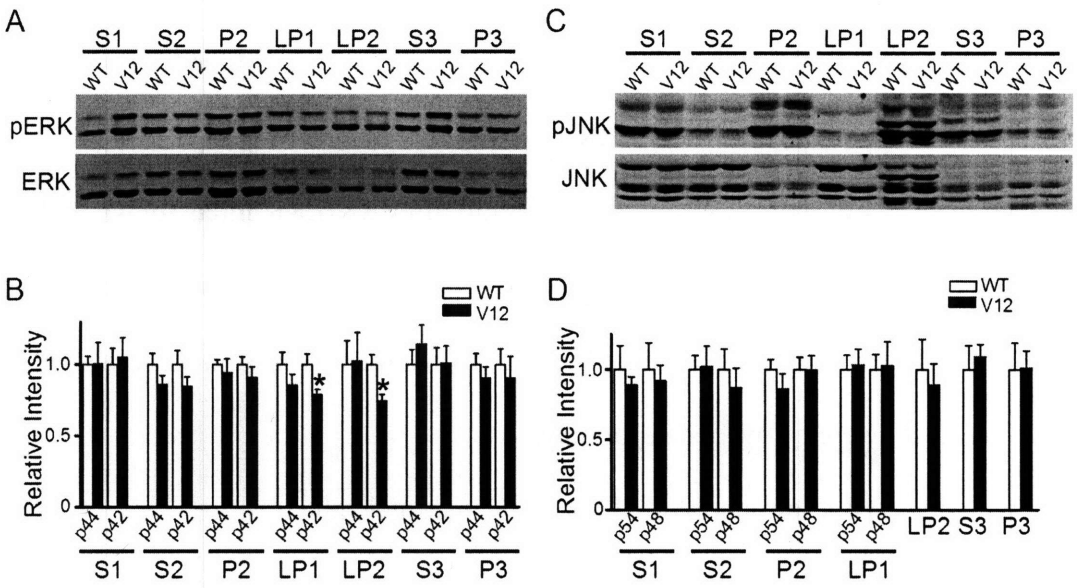
A
S1 S2 P2 LP1 LP2 S3 P3
WT V12 WT V12 WT V12 WT V12 WT V12 WT V12 WT V12
pERK
ERK
C
S1 S2 P2 LP1 LP2 S3 P3
WT V12 WT V12 WT V12 WT V12 WT V12 WT V12 WT V12
pJNK
JNK
B
WT
V12
Relative Intensity
1.0
0.5
0
p44 p42 p44 p42 p44 p42 p44 p42 p44 p42 p44 p42 p44 p42
S1 S2 P2 LP1 LP2 S3 P3
D
WT
V12
Relative Intensity
1.0
0.5
0
p54 p48 p54 p48 p54 p48 p54 p48
LP2 S3 P3
S1 S2 P2 LP1

Figure 4. Reduced pERK levels in Rap2V12 brain fractions.

(A) Forebrains from Rap2V12 and wildtype mice were fractionated and immunoblotted for phospho-ERK (pERK). Blots were stripped and re-probed with antibody against total ERK.

(B) Quantification of pERK levels. The ratio of pERK/ERK intensity was calculated for each fraction and normalized to wildtype (which is shown in white bars). The upper band representing p44 (ERK1) and the lower band representing p42 (ERK2) were quantified separately.

(C) As in (A) but immunoblotted for pJNK and total JNK.

(D) Quantification of pJNK levels. The ratio of pJNK/JNK intensity was calculated for each fraction and normalized to wildtype. For S1, S2, P2, and LP1 fractions, the upper band representing p54 and the lower band representing p48 were quantified separately. For LP2, S3, and P3 fractions, the total intensity in each lane was quantified.

Figure 5

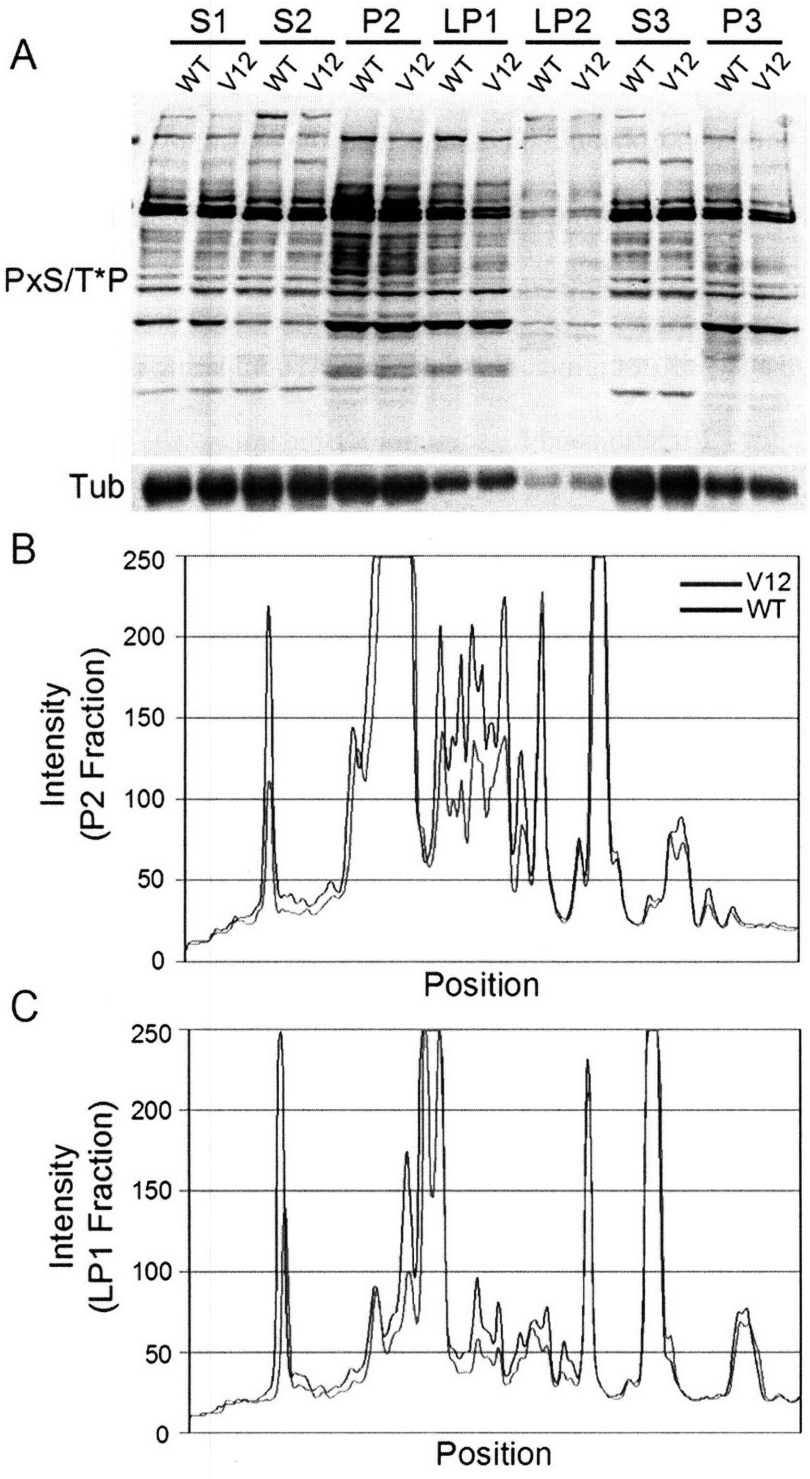
A
S1
S2
P2
LP1
LP2
S3
P3
WT
V12
PxS/T*P
Tub
B
Intensity (P2 Fraction)
250
200
150
100
50
0
V12
WT
Position
C
Intensity (LP1 Fraction)
250
200
150
100
50
0
Position

Figure 5. Reduced phosphorylation of a subset of MAPK substrates in Rap2V12 transgenic mice.

(A) Forebrains from Rap2V12 and wildtype mice were fractionated and immunoblotted with a phosphoantibody that detects the phosphorylated MAPK target motif PxS/T*P. Tubulin was immunoblotted to control for equal loading of wild type versus Rap2V12 extracts.

(B) and (C) Linescan analysis of immunoblot data from A, comparing wildtype versus Rap2V12 for P2 fraction and LP1 fraction. Blue trace, WT; red trace, Rap2V12.

The decreased levels of some phosphorylated MAPK substrates could be due in part to the reduction in ERK2 activity seen in Rap2V12 transgenic brain (see Figure 4).

Rap2V12 mice show normal basal synaptic transmission and synaptic plasticity

To investigate the effects of Rap2 on synaptic function, we measured excitatory synaptic transmission at CA3-CA1 synapses in acute hippocampal slices from 3-5 week old Rap2V12 mice and their wildtype littermates. We first measured AMPA receptor-mediated field excitatory postsynaptic potentials (fEPSPs) in the stratum radiatum (Figure 6A). At all stimulation intensities tested, fEPSPs from Rap2V12 slices were similar to those from WT slices, indicating that basal synaptic transmission is normal in Rap2V12 transgenic mice.

We next investigated bidirectional synaptic plasticity at CA3-CA1 synapses in acute hippocampal slices from 3-5 week old mice. The magnitude of LTP induced by tetanic stimulation (100 Hz, 1 sec) was unaltered in Rap2V12 slices (WT: 1.34 ± 0.05 of baseline at 58 to 60 min, Rap2V12: 1.39 ± 0.11, p=0.717) (Figure 6B). LTD induced by low frequency stimulation (LFS, 1 Hz, 15 min) was slightly but not significantly enhanced in Rap2V12 slices (WT: 0.89 ± 0.03 of baseline at 73 to 75 min, Rap2V12: 0.82 ± 0.03, p=0.100) (Figure 6C) To test if susceptibility to LTD induction was altered by Rap2V12 overexpression, we tried an intermediate frequency of stimulation. 5 Hz stimulation for 3 min also induced slightly but not significantly larger LTD in Rap2V12 slices compared to WT slices (WT: 0.94 ± 0.03 of baseline at 61 to 63 min, n=10 slices/5 mice; Rap2V12: 0.89 ± 0.03, n=7 slices/3 mice, p=0.432). The effects of different conditioning protocols are summarized in frequency-response plots (Figure 6D). Lastly, we tested depotentiation in wildtype and Rap2V12 slices by delivering LFS (1 Hz, 15

Figure 6

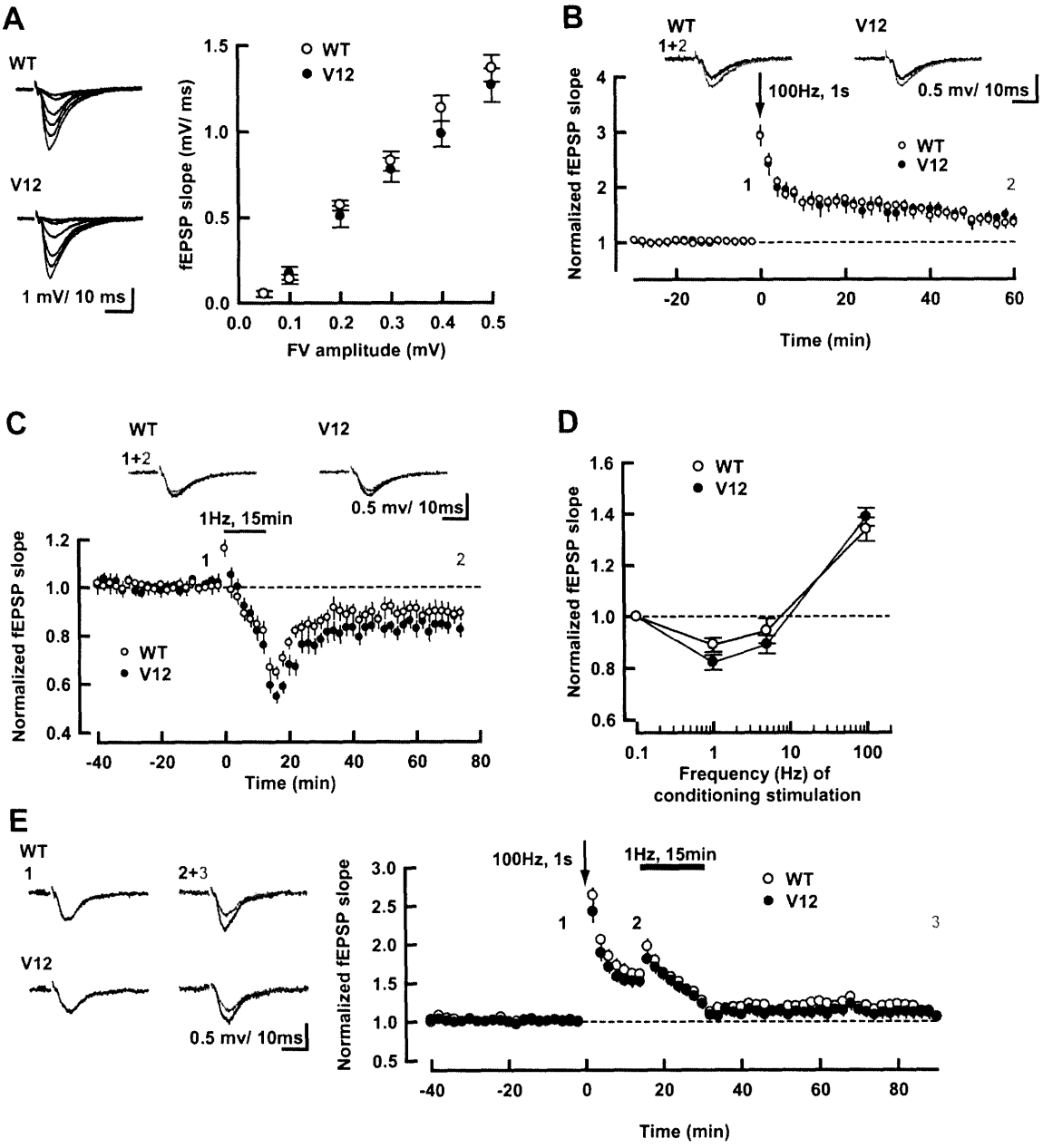
A
WT
V12
1 mV/ 10 ms
WT
V12
fEPSP slope (mV/ ms)
FV amplitude (mV)
B
WT
V12
1+2
100Hz, 1s
0.5 mv/ 10ms
WT
V12
1
2
Normalized fEPSP slope
Time (min)
C
WT
V12
1+2
1Hz, 15min
0.5 mv/ 10ms
1
2
WT
V12
Normalized fEPSP slope
Time (min)
D
WT
V12
Normalized fEPSP slope
Frequency (Hz) of conditioning stimulation
E
WT
1
2+3
V12
0.5 mv/ 10ms
100Hz, 1s
1Hz, 15min
WT
V12
1
2
3
Normalized fEPSP slope
Time (min)

Figure 6. Synaptic transmission and plasticity in Rap2V12 mice

(A) Left: Sample traces (average of ten consecutive responses) represent the responses evoked with six different stimulus intensities from wildtype or Rap2V12 hippocampal slices. Stimulus artifacts were truncated. Right: Summary graph of the input–output relationships of field EPSPs of wildtype (n=9 slices from 5 mice) and Rap2V12 mice (n=9 slices from 5 mice). Symbols indicate the mean ± S.E.M.

(B) Above: Sample traces of field EPSPs of wildtype and Rap2V12 mice recorded at the times indicated in summary graph. Below: Summary graph of the averaged time course of LTP (WT, n=7 slices/4 mice; Rap2V12, n=8 slices/5 mice). Tetanic stimulation (100 Hz, 1 s) was applied at 0 min. Initial EPSP slopes were measured, and the values were normalized to the averaged slope value measured during the baseline period (-30 to 0 min).

(C) Sample traces (above) and summary graph (below) of the averaged time course of LTD (WT, n=11 slices/8 mice; Rap2V12, n=12 slices/8 mice). Low frequency stimulation (1 Hz, 15min) was applied at 0 min.

(D) Summary of the fEPSP changes by three different stimulus frequencies to induce synaptic plasticity. 0.1 Hz was used to monitor synaptic transmission throughout the experiments.

(E) Sample traces (left) and summary graph (right) of the averaged time course of depotentiation (WT, n=11 slices/7 mice; Rap2V12, n=11 slices/8 mice). Following tetanic stimulation (100 Hz, 1 s) at 0 min, low frequency stimulation (1Hz, 15 min) was applied at 15 min to induce depotentiation.

min) 15 min after tetanic stimulation (100 Hz, 1 sec) (Figure 6E). Following LFS, WT and Rap2V12 slices showed similar decreases in synaptic response from their potentiated states (WT: 1.13 ± 0.04 of baseline at 89-90 min, Rap2V12: 1.11 ± 0.08, p=0.932). Thus Rap2V12 transgenic expression does not significantly alter the frequency dependence or the magnitude of bidirectional synaptic plasticity in the CA1 region.

Rap2V12 mice are hyperactive

The Rap2V12 transgenic mice allowed us to investigate Rap2 effects on behavior. We first examined motor coordination and locomotor activity. In the rotarod test (three training trials a day for 4 consecutive days), Rap2V12 mice showed a mild deficit on the first day, but they learned quickly and performed similarly to their WT littermates on subsequent days (Figure 7A).

In the open field test, mice were allowed to explore for 10 minutes and horizontal activity was measured by an infrared grid. Rap2V12 mice were hyperactive, moving a greater total distance and spending a greater percentage of time moving than their WT littermates (Figure 7B and 7C; total distance, $p<0.01$, unpaired t-test; move time, $p<0.001$, unpaired t-test). In contrast, Rap2N17 mice in the open field showed no differences from WT mice in distance moved or time spent moving (Figure 7B and 7C).

Rap2V12 mice exhibit impaired spatial learning

We next tested spatial learning in Rap2V12 mice using the hidden-platform version of the Morris water maze. Rap2V12 mice and their WT littermates were trained

Figure 7

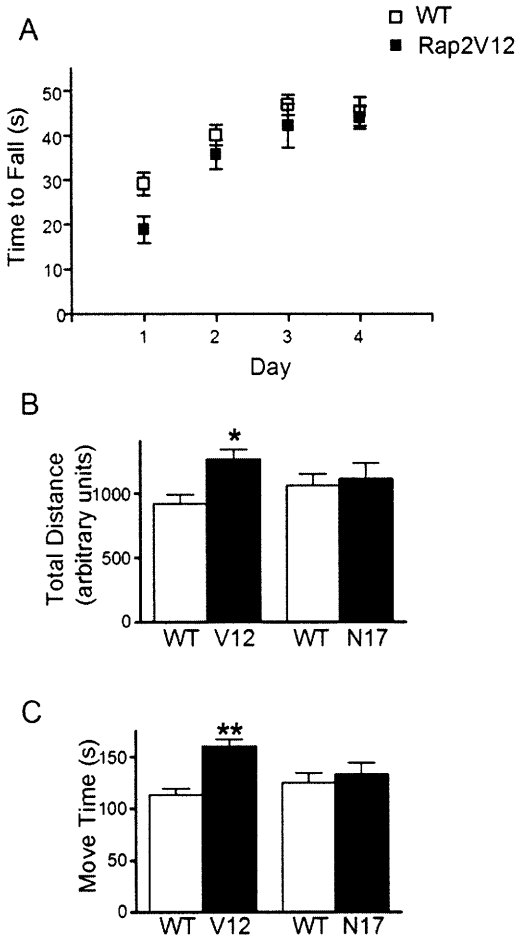
A
WT
Rap2V12
Time to Fall (s)
0
10
20
30
40
50
1
2
3
4
Day
B
Total Distance (arbitrary units)
0
500
1000
*
WT
V12
WT
N17
C
Move Time (s)
0
50
100
150
**
WT
V12
WT
N17

Figure 7. Rotarod performance and open field behavior.

(A) Rotarod performance (latency to fall) was measured for Rap2V12 and WT littermate mice on 4 consecutive days, with 3 trials per day. Each daily block represents the average of 3 trials.

(B) and (C) Open Field Test. 2-4 month old Rap2V12, Rap2N17, or wildtype mice were placed in an open arena for 10 minutes. Total distance traveled and time spent moving were quantified. *$p<0.05$; **$p<0.001$, unpaired t-test.

over 14 consecutive days, with each mouse receiving four training sessions per day. Over the course of training, Rap2V12 mice took significantly longer times than WT littermates to find the hidden platform (Figure 8A; $p<0.01$, repeated measures 2-way ANOVA).

At the end of the 14-day training session, the platform was removed, and the mice were placed in the maze for a minute-long probe trial. During the probe trial, Rap2V12 mice spent a similar amount of time in the target quadrant as their WT littermates (Figure 8B; $p=0.46$, t-test). However, the Rap2V12 mice crossed the exact platform position ~50% less often than their WT littermates (Figure 8C; $p<0.05$, t-test). Together these results indicate that Rap2V12 mice are impaired in spatial learning; however, the defect is modest and only picked up by measuring their spatial memory at finer resolution (time to reach platform during training and platform crossings in the probe trial, as opposed to time spent in correct quadrant). .

Normal acquisition but impaired extinction of fear memory in Rap2V12 mice

Fear conditioning represents another form of long-term memory, and is thought to involve both the hippocampus and amygdala. Rap2V12 protein is expressed in both these regions (Figure 1C). For contextual and cued fear conditioning, mice were trained by exposing them to 2 tone-shock pairings, spaced one minute apart in a defined environment. Baseline freezing (before training) was similar in Rap2V12 and WT mice (<5%; Figure 9A). 24 hours after fear conditioning, freezing behavior was measured in the same context in which training occurred. Rap2V12 and WT mice froze for similar amounts of time (~50%), indicating that Rap2V12 overexpression does not affect

Figure 8

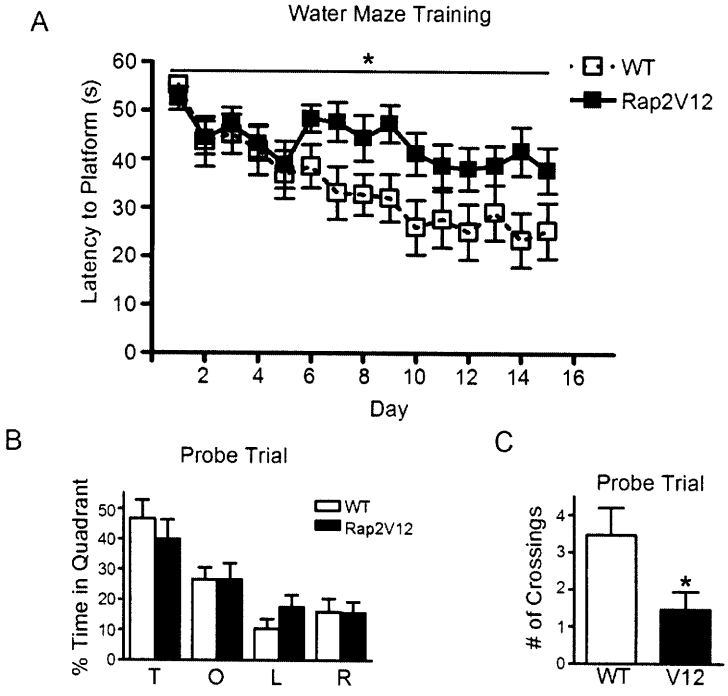
A
Water Maze Training
*
WT
Rap2V12
Latency to Platform (s)
60
50
40
30
20
10
0
2
4
6
8
10
12
14
16
Day
B
Probe Trial
WT
Rap2V12
% Time in Quadrant
50
40
30
20
10
0
T
O
L
R
C
Probe Trial
# of Crossings
4
3
2
1
0
*
WT
V12

Figure 8. Rap2V12 transgenic mice exhibit impaired spatial learning.

(A) Hidden Platform Morris Water Maze. Latency to find hidden platform is plotted for 2-4 month old Rap2V12 or wildtype mice receiving 4 trials a day for 14 days (each daily block is average of 4 trials). *$p<0.05$, repeated measures 2-way ANOVA.

(B) and (C) Probe trial. After 14 day training, the platform was removed. Fraction of time spent in each quadrant (B), or the number of crossings over the position of removed platform (C) were measured. T, target quadrant; O, opposite quadrant; L, left adjacent quadrant; R, right adjacent quadrant.

Figure 9

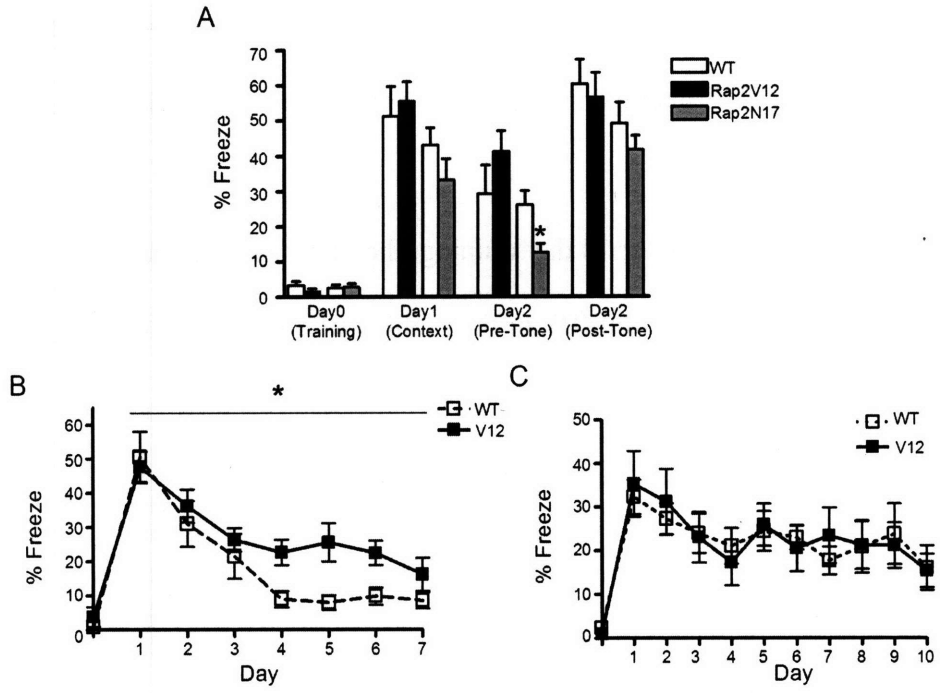
A
% Freeze
70
60
50
40
30
20
10
0
WT
Rap2V12
Rap2N17
*
Day0 (Training)
Day1 (Context)
Day2 (Pre-Tone)
Day2 (Post-Tone)
B
*
WT
V12
% Freeze
Day
C
WT
V12
% Freeze
Day

Figure 9. Normal fear acquisition but impaired extinction of contextual fear in Rap2V12 transgenic mice.

(A) Contextual and cued fear learning. 2-4 month old Rap2V12, Rap2N17, or wildtype littermate mice were subjected to fear conditioning on Day 0 and were tested for contextual fear at 24 h and cued fear at 48 h. *$p<0.05$, unpaired t-test. Percent of time spent immobile (% Freeze) was measured as index of fear.

(B) Time course of contextual fear extinction. 2-4 month old Rap2V12 or wildtype mice were trained on Day 0 and re-exposed to the training context once a day for the following 7 days. *$p<0.05$, repeated measures 2-way ANOVA.

(C) Time course of cued fear extinction. 2-4 month old Rap2V12 or wildtype mice were trained on Day 0 and re-exposed to the tone in a novel context once a day for the following 10 days.

contextual fear learning (Figure 9A; p=0.67, unpaired t-test). 48 hrs after training, cued fear memory was tested by exposing the mice to the tone in a novel context. Again, the WT and Rap2V12 mice froze for similar amounts of time, both before the tone and in response to the tone (Figure 9A; pre-tone freezing, p=0.23, unpaired t-test; freezing during tone, p=0.71, unpaired t-test). Like Rap2V12 mice, Rap2N17 mice showed no significant abnormalities in either contextual or cued fear conditioning, though we noted a decrease in pre-tone freezing at 48 hours after training (Figure 9A; $p<0.05$, unpaired t-test).

Fear memory is extinguished following repeated exposure to the context or the tone in the absence of foot shock. We performed contextual and cued fear extinction in separate cohorts of animals. The training protocol for these extinction experiments was identical to that used for fear conditioning. Starting 24 hr after the training session, these mice were exposed to either the training context (contextual fear extinction) or a novel context with tone (cued fear extinction) once a day for three minutes. During both types of extinction training, WT mice eventually reduced their freezing responses (Figure 9B and 9C). However, Rap2V12 mice showed a significantly slower timecourse of contextual fear extinction (Figure 9B; $p<0.05$, repeated measures 2-way ANOVA). Cued fear extinction was normal in Rap2V12 mice (Figure 9C; p=0.96, repeated measures 2-way ANOVA). Therefore, Rap2V12 mice can acquire contextual and cued fear memories normally, but are specifically impaired in the extinction of contextual fear.

Rap2V12 mice display reduced ERK signaling during fear extinction

MEK inhibitors have previously been shown to impair the extinction of fear memories. Since Rap2V12 mice showed reduced basal levels of pERK, we hypothesized that reduced ERK signaling might underlie the fear extinction deficit we observed. To test this idea, we isolated hippocampal and amygdalar extracts from Rap2V12 mice and their wildtype littermates at multiple stages of fear extinction training: from naïve, untrained mice; after fear conditioning; and after the 2^{nd}, 3^{rd}, and 4^{th} fear extinction trials (Figure 10A). We then immunoblotted for pERK and ERK at each of these timepoints.

In hippocampal extracts, we observed a decrease in phosphorylation of p42 MAPK (ERK2) in naïve Rap2V12 mice relative to wildtype controls (Figure 10B and 10C; $p<0.05$; unpaired t-test). We also saw decreased p42 activity later in the timecourse, occurring at the E3 timepoint ($p<0.05$; unpaired t-test). In addition to these changes in p42, we observed a decrease in p44 (ERK1) phosphorylation occurring at the E2 timepoint in Rap2V12 mice ($p<0.05$; unpaired t-test).

In amygdalar extracts, we again observed a decrease in p42 phosphorylation in naïve Rap2V12 mice relative to wildtype mice (Figure 10B and 10D; $p<0.05$; unpaired t-test). Unlike our results from hippocampus, we observed no changes in p42 phosphorylation at any of the subsequent timepoints, nor did we find any abnormalities in p44 phosphorylation in Rap2V12 mice. Taken together, these data suggest that Rap2V12 mice have deficits in both ERK1 and ERK2 activity at specific times during fear extinction.

Figure 10

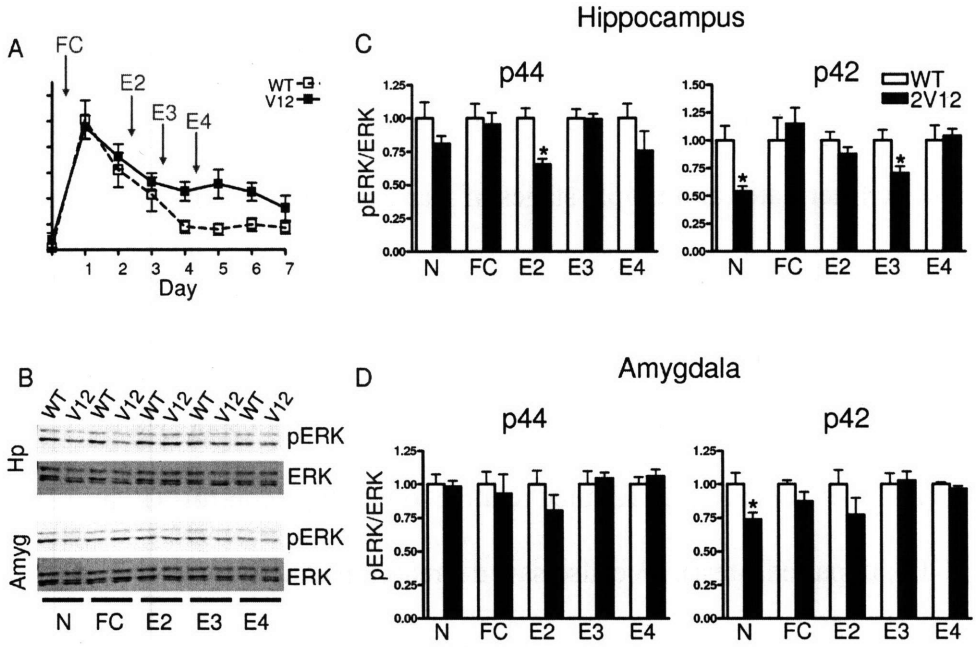
A
FC
E2
E3
E4
WT
V12
1 2 3 4 5 6 7
Day
B
WT V12 WT V12 WT V12 WT V12 WT V12
Hp
pERK
ERK
Amyg
pERK
ERK
N FC E2 E3 E4
C
Hippocampus
p44
p42
WT
2V12
pERK/ERK
N FC E2 E3 E4
D
Amygdala
p44
p42
pERK/ERK
N FC E2 E3 E4

Figure 10. Rap2V12 mice show reduced pERK activity during contextual fear extinction.

(A) Schematic of experiment. Hippocampal and amygdalar extracts were isolated from Rap2V12 mice and wildtype littermates (WT) at the following timepoints: naïve (N), 1 hr after fear conditioning (FC); 1 hr after 2nd extinction trial (E2); 1 hr after 3rd extinction trail (E3); 1 hr after 4th extinction trial (E4).

(B) Hippocampal and amygdalar extracts were immunoblotted with pERK antibody., and the blots were stripped and reprobed with ERK antibody (Hp: hippocampus; Amyg: amygdala).

(C) and (D) The ratio of pERK/ERK intensity was calculated for each sample and normalized to wildtype (which is shown in white bars). The upper band representing p44 (ERK1) and the lower band representing p42 (ERK2) were quantified separately.

Discussion

To investigate Rap2 neuronal function *in vivo*, we constructed transgenic mice expressing either constitutively active or dominant negative Rap2 in postnatal forebrain. Unfortunately, we were unable to generate a highly expressing Rap2N17 line, perhaps because excessive inhibition of Rap2 function in the brain is lethal. Presumably because of inadequate expression of the dominant negative construct (<10% of endogenous Rap2 levels), our Rap2N17 lines showed no detectable phenotype in several morphological, biochemical, and behavioral assays. In contrast, Rap2V12 mice expressed the transgene at high levels and displayed significant defects in neuron structure, biochemistry and behavior.

Rap2 and MAPK signaling

Rap2V12 transgenic mice showed lower pERK levels and reduced phosphorylation of a subset of MAPK substrates, suggesting that Rap2 suppresses the ERK signaling pathway in the brain. Activated ERK (pERK) was specifically reduced in LP1 and LP2 biochemical fractions from Rap2V12 forebrains. These fractions roughly correspond to synaptosomal membranes and synaptic vesicles, respectively, and thus the data suggest that activated Rap2 can suppress ERK signaling in synaptic compartments. Overexpression of constitutively active Rap2 can have both presynaptic and postsynaptic effects in neurons, as evidenced by pruning of dendrites and axons in dissociated cultures (Fu et al., 2007).

How might Rap2 dampen ERK signaling in the brain? Rap2 has a very similar effector domain sequence to Ras, and therefore might inhibit Ras signaling by competing for common effectors (Lerosey et al., 1991). Consistent with this hypothesis, Rap2 has been shown to interact with several canonical Ras effectors and thereby inhibit Ras signaling. In HEK293 cells, Rap2 can bind to the Ras binding domain (RBD) of Raf-1 and inhibit Ras-dependent activation of the transcription factor Elk1, a direct downstream target of ERK (Ohba et al., 2000). In COS7 cells, Rap2 can interact with RalGDS but fails to activate Ral, the downstream target of RalGDS (Nancy et al., 1999). In B-cell lymphoma cells, Rap2 can bind to PI3K and inhibit activation of Akt, a direct target of PI3K (Christian et al., 2003). In Rap2V12 transgenic mice, it is possible that Rap2 inhibits ERK signaling by sequestering B-Raf and/or Raf1, thereby preventing Ras from activating ERK.

In addition to binding known Ras effectors, Rap2 has also been shown to bind specifically to Traf2- and Nck-interacting kinase (TNIK) (Machida et al., 2004; Taira et al., 2004; Zhu et al., 2005). TNIK, in turn, can activate the MAP kinase JNK, and in hippocampal slices, Rap2 has been proposed to signal through TNIK and JNK to mediate depotentiation of synaptic strength (Zhu et al., 2005). However, we found no evidence of increased pJNK in Rap2V12 mice and no abnormality in synaptic transmission and plasticity. It is possible that compensatory mechanisms restore normal synaptic function and modifiability in the face of chronically elevated Rap2 activity. For example, the function of PSD-95 in promoting synaptic strength is revealed with acute molecular knockdown in vitro but not in the knockout mouse (Elias et al., 2006).

Rap2 and Dendritic Spines

Overexpression of Rap2V12 causes loss of spines and depletion of PSD-95 clusters in dissociated hippocampal neurons (Fu et al., 2007). Consistent with this, we found that Rap2V12 mice have fewer and shorter spines in CA1 hippocampal neurons, though the effect is much smaller than in culture. How might Rap2 negatively affect spine number and size? Activation of the ERK pathway is necessary for the formation of new spines/filopodia in neurons stimulated by depolarization or NMDAR stimulation (Wu et al., 2001; Goldin and Segal, 2003). By antagonizing the positive role of Ras-ERK signaling in spine morphogenesis, Rap2V12 could suppress spine number and length, as observed in our transgenic mice.

Another pathway that Rap2 might utilize to regulate dendritic spines is via its effector protein kinase TNIK. *In vitro,* TNIK can phosphorylate and activate the F-actin fragmenting enzyme gelsolin, and in cultured cells, TNIK induces actin fiber disassembly (Fu et al., 1999). Actin is one of the most enriched proteins in the PSD and is thought to be the primary cytoskeletal component regulating spine shape and size (Fischer et al., 1998; Okamoto et al., 2004; Sheng and Hoogenraad, 2007). Therefore, constitutively active Rap2 could lead to increased actin disassembly via TNIK, ultimately causing spine shrinkage or loss.

Rap GTPases are increasingly recognized as regulators of cell adhesion (Caron, 2003; Bos, 2005). Rap2 could also alter spine structure via integrins and cadherins, two classes of cell adhesion molecules found at synapses. Several subunits of heterodimeric integrins, including β1, α3, and α5, are critical for proper spine morphology, synaptic

plasticity, and some forms of learning and memory (Chan et al., 2003; Chan et al., 2006; Shi and Ethell, 2006; Chan et al., 2007; Webb et al., 2007). Rap1 regulates inside-out signaling to several integrin heterodimers, including α4β1, α5β1, αLβ2, αMβ2, and αIIbβ3 (Caron et al., 2000; Katagiri et al., 2000; Reedquist et al., 2000). Neuronal (N)-cadherins form calcium-dependent homophilic associations across the synapse (Dalva et al., 2007) and together with their cytoplasmic binding proteins (αN, β, and p120 catenins) are involved in adherens junction formation and spine morphogenesis (Togashi et al., 2002; Elste and Benson, 2006; Nuriya and Huganir, 2006; Saglietti et al., 2007). Loss of Rap1 or several of its GEFs has been shown to disrupt cadherin localization and formation of adherens junctions (Bos, 2005). Although less well characterized in cell adhesion, Rap2 has recently been shown to be necessary for integrin-dependent adhesion in B lymphocytes (McLeod et al., 2004). Thus it is possible that Rap2 shares similar functions with Rap1 in the regulation of integrin and/or cadherin function, thereby influencing the structure of synapses and spines.

Rap2's Role in Spatial Memory and Contextual Fear Extinction

Rap2V12 mice showed impaired spatial learning in the Morris water maze test, as well as impaired extinction of contextual fear. The ERK signaling pathway has been implicated in several different types of learning and memory. Training in the Morris water maze leads to ERK activation in the hippocampus, and pharmacological inhibition of the ERK pathway impairs learning in this assay (Blum et al., 1999; Selcher et al., 1999). Similarly, hippocampal pERK levels are induced by, and are necessary for, contextual fear extinction training in mice (Fischer et al., 2007). It is therefore possible

that the impaired spatial learning and defective fear extinction seen in Rap2V12 transgenic mice is due to repressed ERK signaling by active Rap2.

To explore this model, we examined pERK levels in Rap2V12 mice during fear extinction training. We found that in hippocampus, Rap2V12 mice showed reduced p42 phosphorylation in the naïve state and also after the third day of extinction training (E3). In addition, p44 phosphorylation was reduced after the second day of extinction training (E2). In amygdala, we observed relatively fewer changes, with only a reduction in p42 phosphorylation in naïve Rap2V12 mice. One question these data pose is why pERK levels seem to be inhibited in Rap2V12 mice only at specific timepoints over fear extinction. One explanation is that distinct signaling pathways may mediate fear acquisition and different stages of fear extinction. For example, Rap2V12 protein may inhibit an ERK activation pathway that is critical following E2 and E3 (where reductions in phosphorylated p42 and p44, respectively, were observed), but this inhibition could be countered by separate ERK pathways that predominate during other stages, such as FC and E4 (where no changes were seen).

Spatial learning in the Morris water maze requires the hippocampus (Morris et al., 1982). Fear extinction is thought to be mediated primarily by the amygdala and the prefrontal cortex (PFC) (Lu et al., 2001; Milad and Quirk, 2002; Myers and Davis, 2002; Lebron et al., 2004; Milad et al., 2006; Milad et al., 2007; Myers and Davis, 2007). In addition, the hippocampus seems to be important specifically for contextual modulation of fear extinction (Schimanski et al., 2002; Fischer et al., 2004; Fischer et al., 2007; Sananbenesi et al., 2007). The Rap2V12 transgenic protein is highly expressed throughout the forebrain – including the hippocampus, cortex, and amygdala – so it could

interfere with biochemical mechanisms of learning in one or all these critical regions. Because the Rap2V12 mice show normal extinction of cue-dependent fear, we speculate that the amygdala and PFC are working normally in this process. Therefore, although a more targeted genetic approach is needed to know with certainty, the hippocampus appears to be a major site of Rap2 action underlying the learning and extinction disabilities.

Several psychiatric disorders, including major depressive disorder and PTSD, are thought to occur in part from a failure to extinguish fearful or aversive memories (Rothbaum and Davis, 2003; Bremner et al., 2005; Gillespie and Ressler, 2005). In addition, patients suffering from these diseases have been reported to display deficits in spatial memory as well (Gurvits et al., 2002; Gurvits et al., 2006). Rap2V12 mice, which are impaired in spatial learning and contextual fear extinction but show few other behavioral deficits, could potentially be developed as an animal model for these disorders. In addition, the fact that activated Rap2 impairs fear extinction raises the possibility that useful therapeutic targets for PTSD could be found in Rap2 signaling pathways.

Acknowledgments

We thank A. Hung for experimental advice and guidance; M. Hayashi, T. McHugh, and A. Govindarajan for assistance with behavioral experiments; K. Phend and S. Grand for EM processing and analysis; D. Rooney and X. Zhou for microinjections.

References

Atkins CM, Selcher JC, Petraitis JJ, Trzaskos JM, Sweatt JD (1998) The MAPK cascade is required for mammalian associative learning. Nat Neurosci 1:602-609.

Blum S, Moore AN, Adams F, Dash PK (1999) A mitogen-activated protein kinase cascade in the CA1/CA2 subfield of the dorsal hippocampus is essential for long-term spatial memory. J Neurosci 19:3535-3544.

Bos JL (2005) Linking Rap to cell adhesion. Curr Opin Cell Biol 17:123-128.

Boulton TG, Yancopoulos GD, Gregory JS, Slaughter C, Moomaw C, Hsu J, Cobb MH (1990) An insulin-stimulated protein kinase similar to yeast kinases involved in cell cycle control. Science 249:64-67.

Boulton TG, Nye SH, Robbins DJ, Ip NY, Radziejewska E, Morgenbesser SD, DePinho RA, Panayotatos N, Cobb MH, Yancopoulos GD (1991) ERKs: a family of protein-serine/threonine kinases that are activated and tyrosine phosphorylated in response to insulin and NGF. Cell 65:663-675.

Bremner JD, Vermetten E, Schmahl C, Vaccarino V, Vythilingam M, Afzal N, Grillon C, Charney DS (2005) Positron emission tomographic imaging of neural correlates of a fear acquisition and extinction paradigm in women with childhood sexual-abuse-related post-traumatic stress disorder. Psychol Med 35:791-806.

Caron E (2003) Cellular functions of the Rap1 GTP-binding protein: a pattern emerges. J Cell Sci 116:435-440.

Caron E, Self AJ, Hall A (2000) The GTPase Rap1 controls functional activation of macrophage integrin alphaMbeta2 by LPS and other inflammatory mediators. Curr Biol 10:974-978.

Chan CS, Weeber EJ, Kurup S, Sweatt JD, Davis RL (2003) Integrin requirement for hippocampal synaptic plasticity and spatial memory. J Neurosci 23:7107-7116.

Chan CS, Weeber EJ, Zong L, Fuchs E, Sweatt JD, Davis RL (2006) Beta 1-integrins are required for hippocampal AMPA receptor-dependent synaptic transmission, synaptic plasticity, and working memory. J Neurosci 26:223-232.

Chan CS, Levenson JM, Mukhopadhyay PS, Zong L, Bradley A, Sweatt JD, Davis RL (2007) Alpha3-integrins are required for hippocampal long-term potentiation and working memory. Learn Mem 14:606-615.

Christian SL, Lee RL, McLeod SJ, Burgess AE, Li AH, Dang-Lawson M, Lin KB, Gold MR (2003) Activation of the Rap GTPases in B lymphocytes modulates B cell antigen receptor-induced activation of Akt but has no effect on MAPK activation. J Biol Chem 278:41756-41767.

Crawley JN (2007) What's wrong with my mouse? : behavioral phenotyping of transgenic and knockout mice, 2nd Edition. Hoboken, N.J.: Wiley-Interscience.

Dalva MB, McClelland AC, Kayser MS (2007) Cell adhesion molecules: signalling functions at the synapse. Nat Rev Neurosci 8:206-220.

Elias GM, Funke L, Stein V, Grant SG, Bredt DS, Nicoll RA (2006) Synapse-specific and developmentally regulated targeting of AMPA receptors by a family of MAGUK scaffolding proteins. Neuron 52:307-320.

Elste AM, Benson DL (2006) Structural basis for developmentally regulated changes in cadherin function at synapses. J Comp Neurol 495:324-335.

English JD, Sweatt JD (1996) Activation of p42 mitogen-activated protein kinase in hippocampal long term potentiation. J Biol Chem 271:24329-24332.
English JD, Sweatt JD (1997) A requirement for the mitogen-activated protein kinase cascade in hippocampal long term potentiation. J Biol Chem 272:19103-19106.
Fischer A, Sananbenesi F, Schrick C, Spiess J, Radulovic J (2004) Distinct roles of hippocampal de novo protein synthesis and actin rearrangement in extinction of contextual fear. J Neurosci 24:1962-1966.
Fischer A, Radulovic M, Schrick C, Sananbenesi F, Godovac-Zimmermann J, Radulovic J (2007) Hippocampal Mek/Erk signaling mediates extinction of contextual freezing behavior. Neurobiol Learn Mem 87:149-158.
Fischer M, Kaech S, Knutti D, Matus A (1998) Rapid actin-based plasticity in dendritic spines. Neuron 20:847-854.
Fu CA, Shen M, Huang BC, Lasaga J, Payan DG, Luo Y (1999) TNIK, a novel member of the germinal center kinase family that activates the c-Jun N-terminal kinase pathway and regulates the cytoskeleton. J Biol Chem 274:30729-30737.
Fu Z, Lee SH, Simonetta A, Hansen J, Sheng M, Pak DT (2007) Differential roles of Rap1 and Rap2 small GTPases in neurite retraction and synapse elimination in hippocampal spiny neurons. J Neurochem 100:118-131.
Gan WB, Grutzendler J, Wong WT, Wong RO, Lichtman JW (2000) Multicolor "DiOlistic" labeling of the nervous system using lipophilic dye combinations. Neuron 27:219-225.
Gillespie CF, Ressler KJ (2005) Emotional learning and glutamate: translational perspectives. CNS Spectr 10:831-839.
Goldin M, Segal M (2003) Protein kinase C and ERK involvement in dendritic spine plasticity in cultured rodent hippocampal neurons. Eur J Neurosci 17:2529-2539.
Gurvits TV, Lasko NB, Repak AL, Metzger LJ, Orr SP, Pitman RK (2002) Performance on visuospatial copying tasks in individuals with chronic posttraumatic stress disorder. Psychiatry Res 112:263-268.
Gurvits TV, Metzger LJ, Lasko NB, Cannistraro PA, Tarhan AS, Gilbertson MW, Orr SP, Charbonneau AM, Wedig MM, Pitman RK (2006) Subtle neurologic compromise as a vulnerability factor for combat-related posttraumatic stress disorder: results of a twin study. Arch Gen Psychiatry 63:571-576.
Hofer F, Fields S, Schneider C, Martin GS (1994) Activated Ras interacts with the Ral guanine nucleotide dissociation stimulator. Proc Natl Acad Sci U S A 91:11089-11093.
Hung A, Futai K, Sala C, Valtschanoff J, Ryu J, Burgoon M, Kidd F, Sung C, Miyakawa T, Bear MF, Weinberg RJ, Sheng M (2008) Smaller Dendritic Spines, Weaker Synaptic Transmission but Enhanced Spatial Learning in Mice Lacking Shank1. J Neurosci.
Husi H, Ward MA, Choudhary JS, Blackstock WP, Grant SG (2000) Proteomic analysis of NMDA receptor-adhesion protein signaling complexes. Nat Neurosci 3:661-669.
Huttner WB, Schiebler W, Greengard P, De Camilli P (1983) Synapsin I (protein I), a nerve terminal-specific phosphoprotein. III. Its association with synaptic vesicles studied in a highly purified synaptic vesicle preparation. J Cell Biol 96:1374-1388.

Jordan BA, Fernholz BD, Boussac M, Xu C, Grigorean G, Ziff EB, Neubert TA (2004) Identification and verification of novel rodent postsynaptic density proteins. Mol Cell Proteomics 3:857-871.

Katagiri K, Hattori M, Minato N, Irie S, Takatsu K, Kinashi T (2000) Rap1 is a potent activation signal for leukocyte function-associated antigen 1 distinct from protein kinase C and phosphatidylinositol-3-OH kinase. Mol Cell Biol 20:1956-1969.

Kikuchi A, Demo SD, Ye ZH, Chen YW, Williams LT (1994) ralGDS family members interact with the effector loop of ras p21. Mol Cell Biol 14:7483-7491.

Kim MJ, Dunah AW, Wang YT, Sheng M (2005) Differential roles of NR2A- and NR2B-containing NMDA receptors in Ras-ERK signaling and AMPA receptor trafficking. Neuron 46:745-760.

Kitayama H, Matsuzaki T, Ikawa Y, Noda M (1990a) A domain responsible for the transformation suppressor activity in Krev-1 protein. Jpn J Cancer Res 81:445-448.

Kitayama H, Matsuzaki T, Ikawa Y, Noda M (1990b) Genetic analysis of the Kirsten-ras-revertant 1 gene: potentiation of its tumor suppressor activity by specific point mutations. Proc Natl Acad Sci U S A 87:4284-4288.

Kitayama H, Sugimoto Y, Matsuzaki T, Ikawa Y, Noda M (1989) A ras-related gene with transformation suppressor activity. Cell 56:77-84.

Lebron K, Milad MR, Quirk GJ (2004) Delayed recall of fear extinction in rats with lesions of ventral medial prefrontal cortex. Learn Mem 11:544-548.

Lerosey I, Chardin P, de Gunzburg J, Tavitian A (1991) The product of the rap2 gene, member of the ras superfamily. Biochemical characterization and site-directed mutagenesis. J Biol Chem 266:4315-4321.

Lu KT, Walker DL, Davis M (2001) Mitogen-activated protein kinase cascade in the basolateral nucleus of amygdala is involved in extinction of fear-potentiated startle. J Neurosci 21:RC162.

Machida N, Umikawa M, Takei K, Sakima N, Myagmar BE, Taira K, Uezato H, Ogawa Y, Kariya K (2004) Mitogen-activated protein kinase kinase kinase kinase 4 as a putative effector of Rap2 to activate the c-Jun N-terminal kinase. J Biol Chem 279:15711-15714.

McLeod SJ, Shum AJ, Lee RL, Takei F, Gold MR (2004) The Rap GTPases regulate integrin-mediated adhesion, cell spreading, actin polymerization, and Pyk2 tyrosine phosphorylation in B lymphocytes. J Biol Chem 279:12009-12019.

Milad MR, Quirk GJ (2002) Neurons in medial prefrontal cortex signal memory for fear extinction. Nature 420:70-74.

Milad MR, Rauch SL, Pitman RK, Quirk GJ (2006) Fear extinction in rats: implications for human brain imaging and anxiety disorders. Biol Psychol 73:61-71.

Milad MR, Wright CI, Orr SP, Pitman RK, Quirk GJ, Rauch SL (2007) Recall of fear extinction in humans activates the ventromedial prefrontal cortex and hippocampus in concert. Biol Psychiatry 62:446-454.

Morozov A, Muzzio IA, Bourtchouladze R, Van-Strien N, Lapidus K, Yin D, Winder DG, Adams JP, Sweatt JD, Kandel ER (2003) Rap1 couples cAMP signaling to a distinct pool of p42/44MAPK regulating excitability, synaptic plasticity, learning, and memory. Neuron 39:309-325.

Morris RG, Garrud P, Rawlins JN, O'Keefe J (1982) Place navigation impaired in rats with hippocampal lesions. Nature 297:681-683.
Myers KM, Davis M (2002) Behavioral and neural analysis of extinction. Neuron 36:567-584.
Myers KM, Davis M (2007) Mechanisms of fear extinction. Mol Psychiatry 12:120-150.
Nancy V, Wolthuis RM, de Tand MF, Janoueix-Lerosey I, Bos JL, de Gunzburg J (1999) Identification and characterization of potential effector molecules of the Ras-related GTPase Rap2. J Biol Chem 274:8737-8745.
Nuriya M, Huganir RL (2006) Regulation of AMPA receptor trafficking by N-cadherin. J Neurochem 97:652-661.
Ohba Y, Mochizuki N, Matsuo K, Yamashita S, Nakaya M, Hashimoto Y, Hamaguchi M, Kurata T, Nagashima K, Matsuda M (2000) Rap2 as a slowly responding molecular switch in the Rap1 signaling cascade. Mol Cell Biol 20:6074-6083.
Okamoto K, Nagai T, Miyawaki A, Hayashi Y (2004) Rapid and persistent modulation of actin dynamics regulates postsynaptic reorganization underlying bidirectional plasticity. Nat Neurosci 7:1104-1112.
Pak DT, Sheng M (2003) Targeted protein degradation and synapse remodeling by an inducible protein kinase. Science 302:1368-1373.
Pak DT, Yang S, Rudolph-Correia S, Kim E, Sheng M (2001) Regulation of dendritic spine morphology by SPAR, a PSD-95-associated RapGAP. Neuron 31:289-303.
Peng J, Kim MJ, Cheng D, Duong DM, Gygi SP, Sheng M (2004) Semiquantitative proteomic analysis of rat forebrain postsynaptic density fractions by mass spectrometry. J Biol Chem 279:21003-21011.
Pizon V, Chardin P, Lerosey I, Olofsson B, Tavitian A (1988) Human cDNAs rap1 and rap2 homologous to the Drosophila gene Dras3 encode proteins closely related to ras in the 'effector' region. Oncogene 3:201-204.
Reedquist KA, Ross E, Koop EA, Wolthuis RM, Zwartkruis FJ, van Kooyk Y, Salmon M, Buckley CD, Bos JL (2000) The small GTPase, Rap1, mediates CD31-induced integrin adhesion. J Cell Biol 148:1151-1158.
Rothbaum BO, Davis M (2003) Applying learning principles to the treatment of post-trauma reactions. Ann N Y Acad Sci 1008:112-121.
Saglietti L, Dequidt C, Kamieniarz K, Rousset MC, Valnegri P, Thoumine O, Beretta F, Fagni L, Choquet D, Sala C, Sheng M, Passafaro M (2007) Extracellular interactions between GluR2 and N-cadherin in spine regulation. Neuron 54:461-477.
Sananbenesi F, Fischer A, Wang X, Schrick C, Neve R, Radulovic J, Tsai LH (2007) A hippocampal Cdk5 pathway regulates extinction of contextual fear. Nat Neurosci 10:1012-1019.
Schimanski LA, Wahlsten D, Nguyen PV (2002) Selective modification of short-term hippocampal synaptic plasticity and impaired memory extinction in mice with a congenitally reduced hippocampal commissure. J Neurosci 22:8277-8286.
Selcher JC, Atkins CM, Trzaskos JM, Paylor R, Sweatt JD (1999) A necessity for MAP kinase activation in mammalian spatial learning. Learn Mem 6:478-490.
Sheng M, Hoogenraad CC (2007) The postsynaptic architecture of excitatory synapses: a more quantitative view. Annu Rev Biochem 76:823-847.

Shi Y, Ethell IM (2006) Integrins control dendritic spine plasticity in hippocampal neurons through NMDA receptor and Ca2+/calmodulin-dependent protein kinase II-mediated actin reorganization. J Neurosci 26:1813-1822.

Taira K, Umikawa M, Takei K, Myagmar BE, Shinzato M, Machida N, Uezato H, Nonaka S, Kariya K (2004) The Traf2- and Nck-interacting kinase as a putative effector of Rap2 to regulate actin cytoskeleton. J Biol Chem 279:49488-49496.

Togashi H, Abe K, Mizoguchi A, Takaoka K, Chisaka O, Takeichi M (2002) Cadherin regulates dendritic spine morphogenesis. Neuron 35:77-89.

Tsien JZ, Chen DF, Gerber D, Tom C, Mercer EH, Anderson DJ, Mayford M, Kandel ER, Tonegawa S (1996) Subregion- and cell type-restricted gene knockout in mouse brain. Cell 87:1317-1326.

Urano T, Emkey R, Feig LA (1996) Ral-GTPases mediate a distinct downstream signaling pathway from Ras that facilitates cellular transformation. Embo J 15:810-816.

Webb DJ, Zhang H, Majumdar D, Horwitz AF (2007) alpha5 integrin signaling regulates the formation of spines and synapses in hippocampal neurons. J Biol Chem 282:6929-6935.

Wu GY, Deisseroth K, Tsien RW (2001) Spaced stimuli stabilize MAPK pathway activation and its effects on dendritic morphology. Nat Neurosci 4:151-158.

Zhu JJ, Qin Y, Zhao M, Van Aelst L, Malinow R (2002) Ras and Rap control AMPA receptor trafficking during synaptic plasticity. Cell 110:443-455.

Zhu Y, Pak D, Qin Y, McCormack SG, Kim MJ, Baumgart JP, Velamoor V, Auberson YP, Osten P, van Aelst L, Sheng M, Zhu JJ (2005) Rap2-JNK removes synaptic AMPA receptors during depotentiation. Neuron 46:905-916.

Chapter Four

Conclusions and Perspectives

Jubin Ryu

Myosin II is critical for dendritic spine morphology and synaptic function

In Chapter 2, we present data showing that the molecular motor myosin II is necessary for proper spine morphology and basal synaptic transmission. When myosin II activity is inhibited either genetically or pharmacologically with blebbistatin, mature spines lose their classic mushroom-head morphology and transform into filopodia-like protrusions. Live imaging showed that this change can occur within 30-60 minutes of blebbistatin treatment. These structural changes are correlated with functional deficits; mEPSC frequency and amplitude both decreased after application of blebbistatin, indicating that the number of synapses and the number of receptors at each synapse both decreased.

Which myosin II isoform is critical?

Currently, there exist three known isoforms of myosin II – myosins IIA, IIB, and IIC. Both myosin IIA and IIB have been detected in neurons, with the IIB isoform reported to be expressed at higher levels in neuronal tissue than IIA (Sellers, 2000). Little expression data exists for myosin IIC, but it has been observed in embryonic peripheral nerves (Brown and Bridgman, 2004). Blebbistatin has been shown to inhibit myosin IIA and B, and could presumably inhibit the IIC isoform as well (Straight et al., 2003; Limouze et al., 2004). Therefore, the structural and electrophysiological phenotypes displayed by blebbistatin-treated neurons could be due to loss of activity of any of the three isoforms, or of some combination of the three. Like blebbistatin treatment, short hairpin RNA directed against myosin IIB causes an increase in dendritic protrusion length and a decrease in protrusion width, suggesting that myosin IIB could be

the critical isoform in dendritic spines. However, myosin IIB RNAi does not lead to the density increase observed after blebbistatin, suggesting that either IIA or IIC could also have roles in dendritic spine morphology. The three myosin II isoforms have different rates of ATP hydrolysis and actin turnover, and each one may therefore fulfill a specific function within dendritic spine structure (Kelley et al., 1996). To address this issue and assign roles to each myosin II isoform, RNAi interference specific for IIA and IIC, respectively, could be performed in neurons.

Possible mechanisms behind myosin II neuronal function

How might myosin II work biophysically to maintain proper spine morphology, and what signaling pathways might regulate its function? Myosin II molecules can associate with each other via their α-helical tails to form filaments (Sellers, 2000) (Figure 1). Two types of myosin filaments have been observed: bipolar filaments and side polar filaments (Xu et al., 1996). In bipolar filaments, myosin molecules at the center of the filament associate in an antiparallel orientation, and those at the ends of the filament associate parallel to each other. This produces a filament with actin-binding motor domains clustered at the ends and a central bare zone consisting of tail domains. Such myosin filaments can bind actin filaments at either end and pull them inwards towards the central bare zone, producing a contraction of the actin cytoskeleton. Side polar myosin filaments are produced by purely antiparallel interactions and possess no central bare zone. Like bipolar filaments, side polar filaments can also contract actin and are thought to allow for extreme shortening of actin filaments, as is observed in smooth muscle cells.

Figure 1

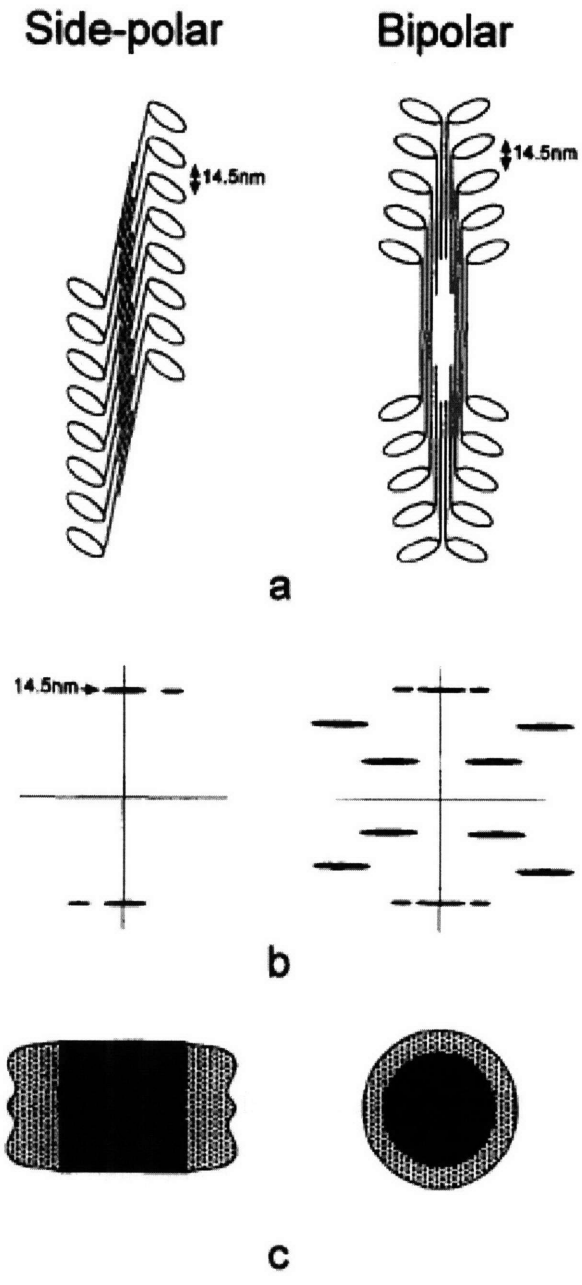

Figure 1. Side-polar and bipolar arrangements of myosin filaments. Myosin molecules can self-assemble into filaments that can contract actin filaments. Bipolar filaments contain a central bare zone without any motor domains, and side polar filaments are though to allow for extreme shortening of actin cytoskeleton. (A) Longitudinal view (B) Fourier transforms of longitudinal views (C) Transverse views (reproduced from Xu et al., 1996).

Our experiments suggest that myosin II filaments may be required to cross-link and maintain tension on the actin cytoskeleton within dendritic spines. This tension may be necessary to produce the classical mushroom-headed spine, and without it, actin filaments may become haphazardly organized, resulting in the filopodia-like projections seen after blebbistatin or myosin II RNAi. Such contraction of the actin cytoskeleton could also be regulated in response to activity, much like polymerization/depolymerization of actin. For example, stimuli causing spines to shrink in size could activate myosin and cause it to "ratchet" actin filaments further. Conversely, increases in spine size could be produced by an inhibition of myosin activity and subsequent reduction in actin filament contraction. These hypotheses could be tested by transfecting fluorescently labeled actin and myosin and observing their distribution under a variety of conditions – over development, during blebbistatin treatment, and after electrical or pharmacological activity.

One way of regulating myosin II is by phosphorylation of the myosin light chain (MLC) (Figure 2). This modification activates actin-binding and permits bipolar filament formation (Suzuki et al., 1978). Several signaling pathways regulating MLC phosphorylation have been identified. In the first, Ca^{2+}/calmodulin activates myosin light chain kinase (MLCK), which in turn can phosphorylate MLC at Ser19 and Thr18 (Goeckeler and Wysolmerski, 1995). In a second pathway, Cdc42 and Rac GTPases activate PAK, which directly phosphorylates MLC at Ser19 (Chew et al., 1998). Rho kinase (ROCK), a serine/threonine kinase activated by the Rho GTPase, can also directly

Figure 2

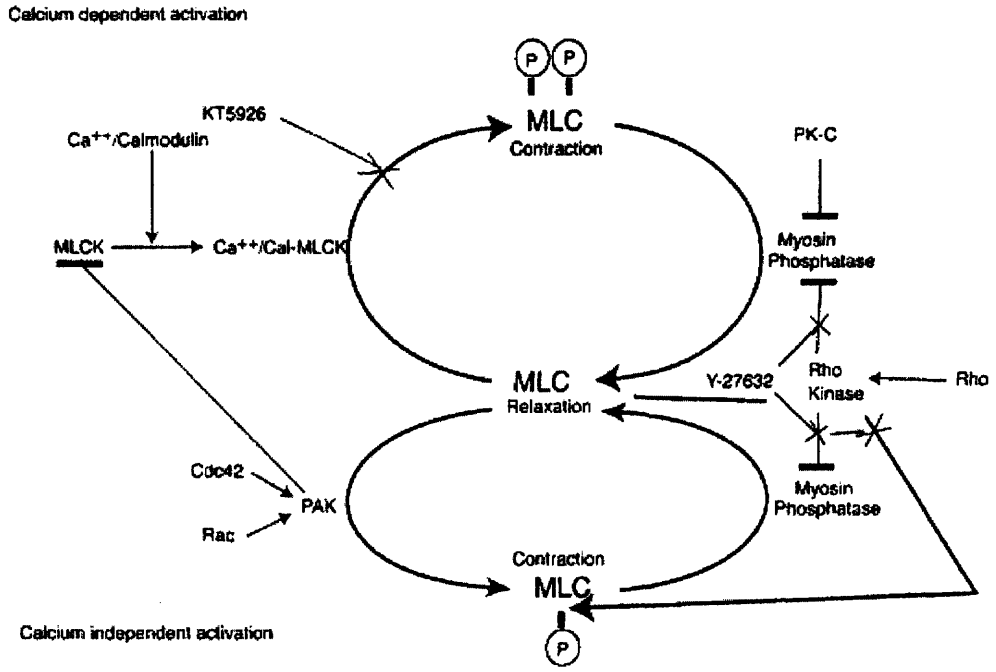

Figure 2. Myosin II regulation. Myosin light chains (MLC) can be phosphorylated at two distinct sites: Ser-19 and Thr-18. Phosphorylation at these sites increases actin binding activity and myosin filament assembly (reproduced from Brown and Bridgman, 2003).

phosphorylate MLC, and it also inhibits MLC phosphatase (Amano et al., 1998; Hirose et al., 1998; Feng et al., 1999). MLC phosphatase is also inhibited by CPI-17, which is activated by PKC (Murakami et al., 1998; Kitazawa et al., 2003).

Many of these myosin regulatory proteins have been identified at synapses and have been implicated in regulation of spine structure and number. Inhibition of Rac1 causes a decrease in spine density, while RhoA inhibition increases spine density and length (Nakayama et al., 2000; Tashiro et al., 2000). In addition, these two GTPases seem to regulate different types of spine motility. Rac1 inhibition blocks spine head morphing, while RhoA inhibition prevents protrusive spine motility (Tashiro and Yuste, 2004). PKC appears to have a positive effect on spine development and growth. In rats subjected to spatial training, an increase in dendritic spines was observed relative to controls, and this increase was augmented by PKC activators and blocked by PKC inhibitors (Hongpaisan and Alkon, 2007). Though these proteins have many direct and indirect targets, part of their effect on spine development and structure may be mediated by myosin II. In support of this, Zhang et al. have reported a GIT1/PIX/Rac/Pak pathway that culminates with MLC phosphorylation to regulate spine morphogenesis (Zhang et al., 2005). Further studies could look at the timecourse and spatial distribution of MLC phosphorylation following activation/downregulation of other signaling pathways involved in spine morphogenesis. More functionally, genetic epistatis experiments could be performed using myosin RNAi and constitutively active mutants of other signaling molecules to determine if they function within the same signaling pathways.

Myosin II and behavior

Since myosin II appears to be critical for synaptic structure and function, it may be involved in learning and memory as well. Lamprecht et al. injected ML-7, in inhibitor of MLCK, into the lateral amygdala of rats and found that ML-7 injected rats showed enhanced short-term and long-term fear learning (Lamprecht et al., 2006). The authors concluded that MLCK was specifically regulating acquisition – and not consolidation or retrieval – of fear memories because ML-7 injection after training or before testing caused no changes from control animals. Consistent with these behavioral results, they found that bath application of ML-7 enhanced LTP in the auditory thalamic pathway to the lateral nucleus of the amygdala. One explanation for these findings may be that acute loss of myosin activity allows spines to be more plastic, therefore leading to enhanced LTP and learning. Consistent with this idea, mice missing the postsynaptic scaffold Shank1 displayed smaller dendritic spines but enhanced working memory relative to wildtype controls (Hung et al., 2008). Future experiments could study fear learning in ML-7 injected mice at later timepoints to see if their memories were less stable than controls. In addition, different learning paradigms could be used, and blebbistatin could be utilized as a second myosin inhibitor to confirm specificity of the results.

Rap2V12 mice show reduced pERK, fewer spines, and impaired spatial learning and fear extinction

In Chapter 3, we presented data from a novel transgenic mouse expressing constitutively active Rap2 (Rap2V12) in the postnatal forebrain. In vitro evidence suggested that Rap2 could inhibit neuronal and synaptic growth and could mediate

depotentiation. Consistent with this data, Rap2V12 mice displayed fewer and shorter dendritic spines and reduced levels of pERK, a signaling molecule that generally promotes synaptic growth and strength. However, we could not detect any abnormalities in synaptic plasticity at CA3-CA1 synapses of the hippocampus. Behaviorally, these mice exhibited hyperactivity and impaired spatial learning and contextual fear extinction.

Caveats with Rap2V12 mice

Before discussing the phenotype observed in Rap2V12 mice, it is worthwhile to delve into some overarching caveats regarding this experimental approach. Most obviously, the Rap2V12 mice represent a gain-of-function genetic model. While such models can reveal useful insights into a protein's potential function, it is nonetheless impossible to know that any phenotype that the Rap2V12 mice display reflects endogenous Rap2 function. While we sought to create transgenic mice expressing the dominant negative Rap2N17 mutant, we unfortunately could not obtain founder lines that expressed this transgene robustly. One possibility for this lack of expression is that the Rap2N17 protein is toxic to the organism, and high levels of it are lethal. Such a scenario seems plausible, especially if the Rap2N17 protein sequesters GEFs not only for Rap2, but also for Rap1 and Ras as well (Nancy et al., 1999).

A second cause for caution is the possibility that the Rap2V12 protein might actually have dominant negative effects in the brain. This could occur because the Rap2V12 protein could localize to different regions of the cell than endogenous Rap2 and sequester downstream effectors away from sites of physiological Rap2 signaling. This rationale has in fact been employed to create dominant negative mutants of Ras by

deleting the membrane localization sequence of constitutively active Ras mutants (Stacey et al., 1991). Therefore the phenotype of Rap2V12 mice may reflect a loss of Rap2 function rather than an increase in it. To examine the localization of endogenous and overexpressed Rap2, we immunoblotted brain extracts from Rap2V12 mice with Rap2 antibody (Chapter 3, Figure 1). These data revealed that Rap2V12 protein is distributed similarly to endogenous Rap2, suggesting that Rap2V12 protein may activate Rap2 effectors in physiological locations. However, the possibility of dominant negative effects has certainly not been ruled out and should be kept in consideration.

A third caveat is the substantial increase in active GTP-bound Rap2 in the forebrains of Rap2V12 mice, and the chronic nature of this manipulation. Immunoblot data showed that Rap2V12 protein is expressed 4-5 fold over endogenous Rap2, and the transgenic protein could be detected as early as 2 weeks after birth (Chapter 3, Figure 1). In light of these conditions, one must consider that the phenotype observed in Rap2V12 mice may not be directly caused by an increase in Rap2 activity, but by compensatory mechanisms several degrees removed from the actual physiological role of Rap2.

Remaining Questions and Future Directions

A need for tighter genetic manipulation

In light of both the positive and negative data from Rap2V12 mice, a useful reagent would be transgenic mice that express Rap2V12 or Rap2N17 in a spatially-restricted and temporally inducible manner. Such mice could be constructed using Tet-On or Tet-Off systems in combination with region-specific promoters. If the Rap2N17 protein is in fact toxic, turning it on acutely after development to adulthood could bypass

this problem. This in vivo loss-of-function data would be critical to proving that endogenous Rap2 has a functional role at synapses. In addition, such temporal control could minimize the possibility that phenotypes are produced by compensatory mechanisms, while also revealing new phenotypes that were otherwise compensated for in a chronically altered state. Finally, this system could allow one to more precisely determine when and where Rap2 function is necessary during various behavioral assays. In addition to creating more tightly regulated transgenic mice, we could also perform future experiments on the existing Rap2V12 mice to address several interesting questions and speculations that arise from the data. These ideas will be discussed below.

Does Rap2 mediate depotentiation?

One of the more pressing points arising from the data is whether Rap2 truly does activate JNK and mediate depotentiation, as suggested by experiments performed in organotypic hippocampal slices (Zhu et al., 2005). Our Rap2V12 mice show no changes in pJNK levels or in synaptic plasticity, and one explanation for this result is that Rap2 simply is not critical for these processes. However, several alternate interpretations can be made. First, as mentioned earlier in this chapter, compensatory mechanisms could have developed to rescue JNK signaling and depotentiation. A second, and not mutually exclusive, explanation is that the assays we performed may not have been sensitive enough. Perhaps the biochemical fractions isolated for immunoblot analysis were too crude and mixed several distinct pJNK pools, thereby obscuring subtle differences. Alternatively, baseline levels of pJNK were normal in Rap2V12 mice, but synaptic activity might have revealed a difference from wildtype littermates. Similar to the

biochemistry, we may not have been looking in the right place or time in our electrophysiology assays. Zhu et al. performed their experiments in organotypic slices that had been dissected from 6-7 day old pups and incubated for 6-8 days in vitro (Zhu et al., 2005). In contrast, our experiments on Rap2V12 mice were performed in acute slices taken from 3-5 week old animals. This difference in timepoints might therefore account for some or all of the discrepancy in results.

Rap2 and ERK signaling in the brain

Rap2V12 mice displayed reduced pERK2 levels in LP1 and LP2 biochemical fractions, which roughly correspond to synaptosomes and synaptic vesicles, respectively. Therefore, Rap2V12 protein appears to suppress certain pools of ERK in the brain, either by directly antagonizing the ERK pathway or by causing compensatory signaling that in turns reduces ERK activity. In addition to this finding, the P2 and LP1 fractions from Rap2V12 mice have decreased levels of phosphorylated MAPK substrates, as revealed by an antibody raised against peptides containing phosphorylated MAPK target motifs. One question that arises from these data is why different fractions show abnormalities in the two assays. That is, why is there no reduction in phosphorylated MAPK substrates in LP2 fractions, and why is there no reduction in ERK2 activity in P2 fractions? One possibility is that the decrease in pERK2 in LP2 fractions is not significant enough to cause a detectable decrease in phosphorylation of downstream effectors. However, the decrease in pERK2 in LP2 fraction is greater than that seen in LP1, making this scenario unlikely. Alternatively, ERK2 effectors may not make up a significant portion of the MAPK effectors in the LP2 fractions. In addition, the phosphoantibody may not detect

all MAPK substrates with equal sensitivity and may fail to recognize key ERK2 effectors. Regarding the P2 fraction, one explanation is that a MAPK besides ERK or JNK is impaired in this fraction in Rap2V12 mice, leading to the observed reduction in phosphorylation.

Rap2 and fear extinction

In recent years, several molecules have been shown to regulate fear extinction (Figure 3). Bilateral infusion of PI3K inhibitor in the hippocampus prevents contextual fear extinction but not reconsolidation, showing that PI3K is specifically required for extinction (Chen et al., 2005). Conversely, transgenic mice expressing dominant negative PKA show facilitated fear extinction, indicating that endogenous PKA normally suppresses extinction learning (Isiegas et al., 2006). A third study delineated a Rac-1/Cdk5/PAK-1 signaling pathway that regulates fear extinction (Sananbenesi et al., 2007). In this model, PAK-1 activity is necessary for fear extinction, but Rac-1 and Cdk5 suppress PAK-1. Therefore, Rac-1 and Cdk5 must be suppressed in order to disinhibit PAK-1 and facilitate fear extinction. Hippocampal MEK/ERK signaling has also been shown to be necessary for fear extinction (Fischer et al., 2007). pERK levels increased following four days of fear extinction, and hippocampal infusion of MEK or ERK inhibitors prevented fear extinction.

Rap2V12 mice exhibit impaired fear extinction, raising the possibility that endogenous Rap2 might suppress this process. Although a loss-of-function animal model is necessary to prove this, it is interesting to speculate which of the known fear extinction

Figure 3

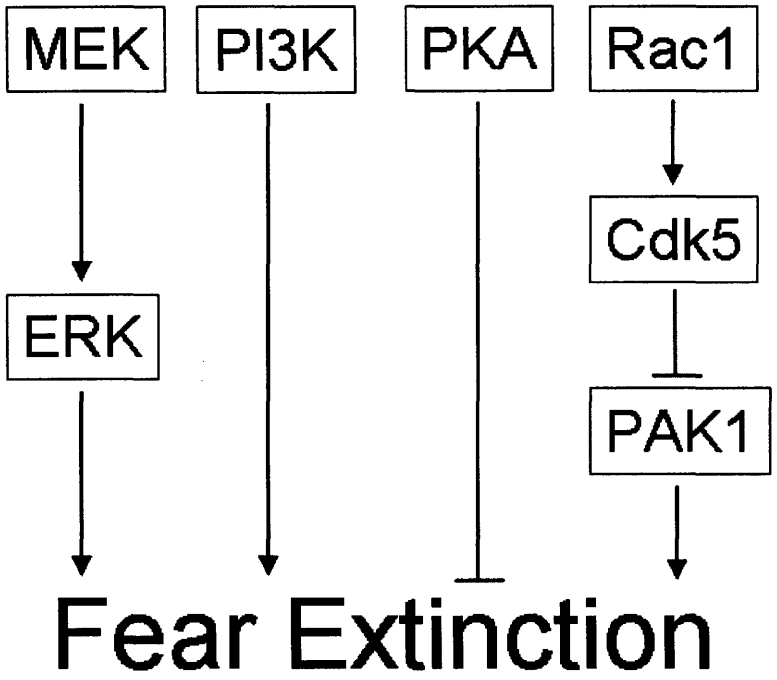

Figure 3. Signaling molecules regulating contextual fear extinction. Several different pathways have been shown to facilitate or constrain contextual fear extinction. Rap2 could potentially interact with one or more of these pathways to impair the learning required for fear extinction (Chen et al., 2005; Isiegas et al., 2006; Fischer et al., 2007; Sananbenesi et al., 2007).

pathways Rap2 might participate in. In B-cell lymphoma cells, Rap2 has been shown to bind to PI3K and inhibit activation of Akt, a downstream target of PI3K (Christian et al., 2003). The impaired fear extinction seen in Rap2V12 mice would be consistent with Rap2 mediated inhibition of PI3K signaling, which is necessary for fear extinction. Two possible links between Rap2 and the Rac-1/Cdk5/PAK-1 pathway are the RacGEFs TIAM1 and VAV2. In HeLa cells, active Rap1 can bind to both of these RacGEFs and is necessary for their proper localization within the cell (Arthur et al., 2004). Both TIAM1 and VAV2 have been shown to play functional roles in neurons. TIAM1 is necessary for dendritic spine morphogenesis following EphrinB1 stimulation, and VAV2 mediates receptor-ligand endocytosis during axon guidance (Cowan et al., 2005; Tolias et al., 2005; Tolias et al., 2007). Based on data reported by Tsai et al., Rap2-mediated enhancement of Rac-1 signaling would be expected to suppress PAK-1 and impair fear extinction, which is the phenotype observed for Rap2V12 mice. Rap2 might also suppress fear extinction by inhibiting ERK signaling. In HEK293 cells, Rap2 can bind to the Ras effector Raf-1 and sequester it, thereby preventing downstream ERK signaling. In addition, Rap2V12 mice exhibit decreased levels of pERK, which is consistent with – though not conclusive of – Rap2 inhibiting ERK to impair fear extinction. To explore Rap2's involvement in the other fear extinction pathways, we could immunoblot for the activities of different signaling candidates, as we did for ERK.

Rap2 and dendritic spines

Consistent with earlier in vitro results, Rap2V12 mice displayed a reduction in length and number of hippocampal dendritic spines (Fu et al., 2007). The molecular

mechanism behind this phenotype needs to be elucidated. One way in which Rap2 could affect spine morphology is through the regulation of integrins. Integrins exist as heterodimers of transmembrane proteins and can mediate cellular adhesion to the extracellular matrix or to other cells. In several immune cell lines, agonists of integrin activity have been shown to increase levels of endogenous GTP-Rap1, and active Rap1 is sufficient to increase integrin affinity and/or avidity (Caron, 2003). Conversely, dominant negative Rap1 blocks integrin activation by extracellular agonists. In total, several different classes of integrin heterodimers appear to be regulated by Rap1: α4β1, α5β1, αLβ2, αMβ2, and αIIbβ3. Fewer studies have explored the relationship between Rap2 and integrins, but in B lymphocytes, Rap2 has recently been shown to be necessary and sufficient for the activation of αL and α4-containing integrins (McLeod et al., 2004).

In neurons, multiple integrin subunits are expressed in the mammalian brain and have been shown to be important for dendritic spine structure and synaptic plasticity. In cultured hippocampal neurons, integrin activation using the tripeptide integrin ligand RGD induced elongation of extant dendritic spines as well as formation of new filopodia (Shi and Ethell, 2006). In addition, this treatment caused actin reorganization and synapse remodeling. Function blocking antibodies against β1 and β3 subunits blocked these effects. In mice, deletion of the α3 subunit led to loss of LTP maintenance, and α3/α5 double KO mice show a defect in paired pulse facilitation (Chan et al., 2003; Chan et al., 2007). Triple KO mice missing α3, α5, and α8 show impaired LTP and hippocampus-dependent spatial memory (Chan et al., 2003). Mice lacking the β1 subunit exhibit decreased AMPAR-mediated synaptic transmission, defective LTP, and impaired nonmatching-to-place working memory(Chan et al., 2006). Because Rap GTPases are

known to regulate integrins and integrins play functional roles at synapses, integrins are a promising downstream candidate to mediate the loss of dendritic spines observed in Rap2V12 mice. To test this model, one could immunostain for different integrin subunits in Rap2V12 neurons. A more functional approach would be to treat cultured transgenic neurons with RGD and assay for known readouts of integrin activation, such as actin reorganization or spine morphological changes.

Constitutively active Rap2 might also inhibit spine growth via its effector Traf2- and Nck-interacting kinase (TNIK). TNIK can bind to GTP-bound Rap2, but not to GDP-bound Rap2 or any forms of Ras or Rap1 (Taira et al., 2004). Active Rap2 also causes translocation of TNIK from a soluble fraction to a detergent-insoluble cytoskeletal fraction. One of TNIK's identified functions is regulation of the actin cytoskeleton. It induces actin fiber disassembly and causes loss of cell spreading. In vitro, TNIK can phosphorylate and thereby activate gelsolin, an F-actin fragmenting and capping enzyme. This mechanism might underlie TNIK's observed effects on adherent cells. In Rap2V12 mice, constitutively active Rap2 may recruit TNIK, leading to actin fiber disassembly and loss of spines. TNIK distribution could be examined in brain fractions from the Rap2V12 mice, and antibodies specific for phosphorylated gelsolin could also be used to immunostain neurons from Rap2V12 mice.

In reflection, Rap2V12 mice exhibited an array of interesting phenotypes that suggest that Rap2 is a protein of significance within the synapse. However, there remain many unanswered questions regarding the mechanisms behind the observed phenotypes and about the exact role of endogenous Rap2. Loss-of-function genetic models that can be controlled temporally and spatially are the most critical tool to address these questions.

These more targeted approaches can hopefully confirm or rule out a potential role for Rap2 in several compelling neuronal and synaptic processes – dendritic spine structure, depotentiation of synapses, and extinction of fear memories.

References

Amano M, Chihara K, Nakamura N, Fukata Y, Yano T, Shibata M, Ikebe M, Kaibuchi K (1998) Myosin II activation promotes neurite retraction during the action of Rho and Rho-kinase. Genes Cells 3:177-188.

Arthur WT, Quilliam LA, Cooper JA (2004) Rap1 promotes cell spreading by localizing Rac guanine nucleotide exchange factors. J Cell Biol 167:111-122.

Brown ME, Bridgman PC (2004) Myosin function in nervous and sensory systems. J Neurobiol 58:118-130.

Caron E (2003) Cellular functions of the Rap1 GTP-binding protein: a pattern emerges. J Cell Sci 116:435-440.

Chan CS, Weeber EJ, Kurup S, Sweatt JD, Davis RL (2003) Integrin requirement for hippocampal synaptic plasticity and spatial memory. J Neurosci 23:7107-7116.

Chan CS, Weeber EJ, Zong L, Fuchs E, Sweatt JD, Davis RL (2006) Beta 1-integrins are required for hippocampal AMPA receptor-dependent synaptic transmission, synaptic plasticity, and working memory. J Neurosci 26:223-232.

Chan CS, Levenson JM, Mukhopadhyay PS, Zong L, Bradley A, Sweatt JD, Davis RL (2007) Alpha3-integrins are required for hippocampal long-term potentiation and working memory. Learn Mem 14:606-615.

Chen X, Garelick MG, Wang H, Lil V, Athos J, Storm DR (2005) PI3 kinase signaling is required for retrieval and extinction of contextual memory. Nat Neurosci 8:925-931.

Chew TL, Masaracchia RA, Goeckeler ZM, Wysolmerski RB (1998) Phosphorylation of non-muscle myosin II regulatory light chain by p21-activated kinase (gamma-PAK). J Muscle Res Cell Motil 19:839-854.

Christian SL, Lee RL, McLeod SJ, Burgess AE, Li AH, Dang-Lawson M, Lin KB, Gold MR (2003) Activation of the Rap GTPases in B lymphocytes modulates B cell antigen receptor-induced activation of Akt but has no effect on MAPK activation. J Biol Chem 278:41756-41767.

Cowan CW, Shao YR, Sahin M, Shamah SM, Lin MZ, Greer PL, Gao S, Griffith EC, Brugge JS, Greenberg ME (2005) Vav family GEFs link activated Ephs to endocytosis and axon guidance. Neuron 46:205-217.

Feng J, Ito M, Ichikawa K, Isaka N, Nishikawa M, Hartshorne DJ, Nakano T (1999) Inhibitory phosphorylation site for Rho-associated kinase on smooth muscle myosin phosphatase. J Biol Chem 274:37385-37390.

Fischer A, Radulovic M, Schrick C, Sananbenesi F, Godovac-Zimmermann J, Radulovic J (2007) Hippocampal Mek/Erk signaling mediates extinction of contextual freezing behavior. Neurobiol Learn Mem 87:149-158.

Fu Z, Lee SH, Simonetta A, Hansen J, Sheng M, Pak DT (2007) Differential roles of Rap1 and Rap2 small GTPases in neurite retraction and synapse elimination in hippocampal spiny neurons. J Neurochem 100:118-131.

Goeckeler ZM, Wysolmerski RB (1995) Myosin light chain kinase-regulated endothelial cell contraction: the relationship between isometric tension, actin polymerization, and myosin phosphorylation. J Cell Biol 130:613-627.

Hirose M, Ishizaki T, Watanabe N, Uehata M, Kranenburg O, Moolenaar WH, Matsumura F, Maekawa M, Bito H, Narumiya S (1998) Molecular dissection of the Rho-associated protein kinase (p160ROCK)-regulated neurite remodeling in neuroblastoma N1E-115 cells. J Cell Biol 141:1625-1636.

Hongpaisan J, Alkon DL (2007) A structural basis for enhancement of long-term associative memory in single dendritic spines regulated by PKC. Proc Natl Acad Sci U S A 104:19571-19576.

Hung A, Futai K, Sala C, Valtschanoff J, Ryu J, Burgoon M, Kidd F, Sung C, Miyakawa T, Bear MF, Weinberg RJ, Sheng M (2008) Smaller Dendritic Spines, Weaker Synaptic Transmission but Enhanced Spatial Learning in Mice Lacking Shank1. J Neurosci.

Isiegas C, Park A, Kandel ER, Abel T, Lattal KM (2006) Transgenic inhibition of neuronal protein kinase A activity facilitates fear extinction. J Neurosci 26:12700-12707.

Kelley CA, Sellers JR, Gard DL, Bui D, Adelstein RS, Baines IC (1996) Xenopus nonmuscle myosin heavy chain isoforms have different subcellular localizations and enzymatic activities. J Cell Biol 134:675-687.

Kitazawa T, Eto M, Woodsome TP, Khalequzzaman M (2003) Phosphorylation of the myosin phosphatase targeting subunit and CPI-17 during Ca2+ sensitization in rabbit smooth muscle. J Physiol 546:879-889.

Lamprecht R, Margulies DS, Farb CR, Hou M, Johnson LR, LeDoux JE (2006) Myosin light chain kinase regulates synaptic plasticity and fear learning in the lateral amygdala. Neuroscience 139:821-829.

Limouze J, Straight AF, Mitchison T, Sellers JR (2004) Specificity of blebbistatin, an inhibitor of myosin II. J Muscle Res Cell Motil 25:337-341.

McLeod SJ, Shum AJ, Lee RL, Takei F, Gold MR (2004) The Rap GTPases regulate integrin-mediated adhesion, cell spreading, actin polymerization, and Pyk2 tyrosine phosphorylation in B lymphocytes. J Biol Chem 279:12009-12019.

Murakami N, Chauhan VP, Elzinga M (1998) Two nonmuscle myosin II heavy chain isoforms expressed in rabbit brains: filament forming properties, the effects of phosphorylation by protein kinase C and casein kinase II, and location of the phosphorylation sites. Biochemistry 37:1989-2003.

Nakayama AY, Harms MB, Luo L (2000) Small GTPases Rac and Rho in the maintenance of dendritic spines and branches in hippocampal pyramidal neurons. J Neurosci 20:5329-5338.

Nancy V, Wolthuis RM, de Tand MF, Janoueix-Lerosey I, Bos JL, de Gunzburg J (1999) Identification and characterization of potential effector molecules of the Ras-related GTPase Rap2. J Biol Chem 274:8737-8745.

Sananbenesi F, Fischer A, Wang X, Schrick C, Neve R, Radulovic J, Tsai LH (2007) A hippocampal Cdk5 pathway regulates extinction of contextual fear. Nat Neurosci 10:1012-1019.

Sellers JR (2000) Myosins: a diverse superfamily. Biochim Biophys Acta 1496:3-22.

Shi Y, Ethell IM (2006) Integrins control dendritic spine plasticity in hippocampal neurons through NMDA receptor and Ca2+/calmodulin-dependent protein kinase II-mediated actin reorganization. J Neurosci 26:1813-1822.

Stacey DW, Feig LA, Gibbs JB (1991) Dominant inhibitory Ras mutants selectively inhibit the activity of either cellular or oncogenic Ras. Mol Cell Biol 11:4053-4064.

Straight AF, Cheung A, Limouze J, Chen I, Westwood NJ, Sellers JR, Mitchison TJ (2003) Dissecting temporal and spatial control of cytokinesis with a myosin II Inhibitor. Science 299:1743-1747.

Suzuki H, Onishi H, Takahashi K, Watanabe S (1978) Structure and function of chicken gizzard myosin. J Biochem 84:1529-1542.

Taira K, Umikawa M, Takei K, Myagmar BE, Shinzato M, Machida N, Uezato H, Nonaka S, Kariya K (2004) The Traf2- and Nck-interacting kinase as a putative effector of Rap2 to regulate actin cytoskeleton. J Biol Chem 279:49488-49496.

Tashiro A, Yuste R (2004) Regulation of dendritic spine motility and stability by Rac1 and Rho kinase: evidence for two forms of spine motility. Mol Cell Neurosci 26:429-440.

Tashiro A, Minden A, Yuste R (2000) Regulation of dendritic spine morphology by the rho family of small GTPases: antagonistic roles of Rac and Rho. Cereb Cortex 10:927-938.

Tolias KF, Bikoff JB, Kane CG, Tolias CS, Hu L, Greenberg ME (2007) The Rac1 guanine nucleotide exchange factor Tiam1 mediates EphB receptor-dependent dendritic spine development. Proc Natl Acad Sci U S A 104:7265-7270.

Tolias KF, Bikoff JB, Burette A, Paradis S, Harrar D, Tavazoie S, Weinberg RJ, Greenberg ME (2005) The Rac1-GEF Tiam1 couples the NMDA receptor to the activity-dependent development of dendritic arbors and spines. Neuron 45:525-538.

Xu JQ, Harder BA, Uman P, Craig R (1996) Myosin filament structure in vertebrate smooth muscle. J Cell Biol 134:53-66.

Zhang H, Webb DJ, Asmussen H, Niu S, Horwitz AF (2005) A GIT1/PIX/Rac/PAK signaling module regulates spine morphogenesis and synapse formation through MLC. J Neurosci 25:3379-3388.

Zhu Y, Pak D, Qin Y, McCormack SG, Kim MJ, Baumgart JP, Velamoor V, Auberson YP, Osten P, van Aelst L, Sheng M, Zhu JJ (2005) Rap2-JNK removes synaptic AMPA receptors during depotentiation. Neuron 46:905-916.